7-1-2010

Characterization of subspecies B1 human adenovirus ORF E3-10.9K

Kathryn Marie Frietze

Follow this and additional works at: https://digitalrepository.unm.edu/biom_etds
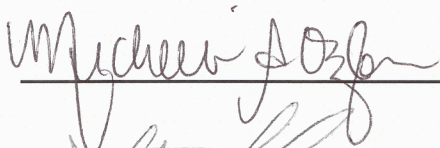
Kathryn M. Frietze

Candidate

Biomedical Sciences
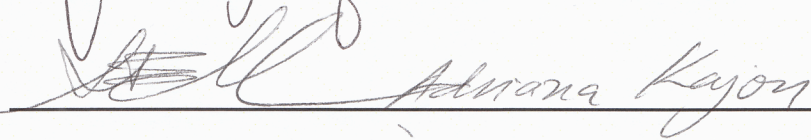
Department
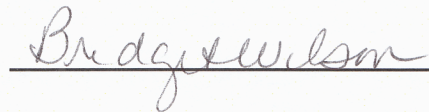
This dissertation is approved, and it is acceptable in quality
and form for publication:
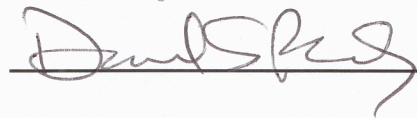
Approved by the Dissertation Committee:

_____, Chairperson

_____ Adriana Kajon

_____

_____

_____

_____

_____

_____

CHARACTERIZATION OF SUBSPECIES B1 HUMAN ADENOVIRUS ORF E3-10.9K

BY

KATHRYN M. FRIETZE

B.S., Biological Sciences, Central Washington University, 2004

DISSERTATION

Submitted in Partial Fulfillment of the
Requirements for the Degree of

**Doctor of Philosophy
Biomedical Sciences**

The University of New Mexico
Albuquerque, New Mexico

July, 2010

DEDICATION

This dissertation is dedicated to my husband, Luke, and my soon to arrive daughter, Cornelia Theone Frietze.

ACKNOWLEDGEMENTS

**CHARACTERIZATION OF SUBSPECIES B1 HUMAN
ADENOVIRUS ORF E3-10.9K**

BY

KATHRYN M. FRIETZE

ABSTRACT OF DISSERTATION

Submitted in Partial Fulfillment of the
Requirements for the Degree of

**Doctor of Philosophy
Biomedical Sciences**

The University of New Mexico
Albuquerque, New Mexico

July, 2010

CHARACTERIZATION OF SUBSPECIES B1 HUMAN ADENOVIRUS

ORF E3-10.9K

by

Kathryn M. Frietze

B.S., BIOLOGICAL SCIENCES, CENTRAL WASHINGTON UNIVERSITY, 2004

DOCTOR OF PHILOSOPHY, BIOMEDICAL SCIENCES

ABSTRACT

Subspecies B1 human adenoviruses (HAdVs) are important causes of acute respiratory disease in pediatric and military recruit populations. Although extensive epidemiological data document the genetic diversity of these human pathogens, little is known about the relevance of this genetic diversity on the pathogenesis and fitness of subspecies B1 HAdVs. Additionally, the unique molecular biology of these pathogens is understudied compared to the species C HAdV serotypes 2 and 5. One of the uniquely diverse regions of the HAdV genomes is the early region 3 (E3) transcription unit. These genes are implicated in pathogenesis, host-species specificity, and the modulation of the host immune response to infection. Subspecies B1 HAdVs encode a set of novel open reading frames (ORFs) within the E3 region, including E3-20.1K, E3-20.5K, and E3-10.9K. ORF E3-10.9K is highly polymorphic among subspecies B1 HAdVs, and it

displays extensive variation among strains of serotypes 3 and 7. In an effort to understand the role ORF E3-10.9K plays in the context of subspecies B1 HAdV infectious cycle and fitness in nature and the biological implications of the observed polymorphism, a biochemical characterization of ORF E3-10.9K-encoded proteins, the investigation of membrane permeabilizing acitivity of these proteins, and the examination of growth phenotypes of virus mutants lacking ORF E3-10.9K was undertaken. This research showed that ORF E3-10.9K was expressed late in infection from the HAdV major late promoter and that its products were N- and O-glycosylated, similar to E3-11.6K/adenovirus death protein (ADP) of species C HAdV. However, ORF E3-10.9K-encoded protein orthologs showed a subcellular localization distinct from the nuclear envelope localization of the E3-11.6K/ADP. Proteins with a hydrophobic domain were capable of permeabilizing membranes in an *E. coli* expression system, but not in a mammalian expression system. Subspecies B1 HAdV mutants lacking ORF E3-10.9K displayed similar virus growth and egress kinetics as control subspecies B1 HAdVs containing ORF E3-10.9K. These data suggested that ORF E3-10.9K is not the subspecies B1 HAdV equivalent of species C HAdV E3-11.6K/ADP.

Table of Contents

List of Figures

List of Tables

Chapter 1: Introduction

Human adenoviruses (HAdV) are recognized etiological agents of acute respiratory, gastrointestinal, and conjunctival infections in pediatric, military recruit, and immunocompromised populations. The HAdV serotypes classified within subspecies B1 (HAdV-3, HAdV-7, HAdV-16, HAdV-21, and HAdV-50) are particularly important causes of acute respiratory infections, which can result in severe clinical manifestations or fatal outcome (Carballal et al., 2002; Kim et al., 2003; Lang et al., 1969; Videla et al., 1999). Subspecies B1 HAdV infection is linked to the development of long-term respiratory sequelae in patients (Becroft, 1971; Herbert et al., 1977; Similä et al., 1981). Although a vaccine to protect against HAdV-7 and the species E HAdV serotype 4 infections is licensed for use in military recruits, there is currently no vaccine available to the civilian population.

Despite the importance of subspecies B1 HAdVs in the etiology of severe, acute respiratory infections, little is known about their unique molecular biology. Most characterizations of adenoviruses (AdV) and their gene products have focused almost exclusively on HAdV-2 and HAdV-5, both members of species C HAdV. However, a wide range of associated clinical disease and viral genomic content exists among HAdV. The limited study of non-species C HAdV molecular biology has hindered our ability to address questions regarding the molecular basis of HAdV pathogenesis, specifically with regards to subspecies B1 HAdV infections.

Extensive intraserotypic genetic diversity within subspecies B1 HAdVs is well documented (Golovina et al., 1991; Kajon and Wadell, 1994; Li and Wadell, 1986; Li and Wadell, 1988). The existence of genomic variants (also known as genome types) of subspecies B1 HAdV serotypes is well-established and detected primarily by restriction enzyme analysis of the viral genomes. The circulation of these genomic variants in human populations is often geographically restricted. Over time, these genomic variants can spread to new geographic areas and take over as the predominant circulating genomic variant (Erdman et al., 2002; Golovina et al., 1991; Wadell et al., 1980). These shifts are correlated with an apparent increased severity of associated disease (Erdman et al., 2002; Kajon and Wadell, 1994; Kajon et al., 1996; Larranaga et al., 2000; Wadell et al., 1980; Wadell et al., 1985). However, the selective pressures driving these shifts and the emergence of new genomic variants are poorly understood. The molecular basis of the apparent increase in severity associated with these shifts is also unclear. Our limited knowledge of subspecies B1 HAdV molecular biology has hindered our ability to understand the impact genetic diversity plays in the evolution of these diverse viruses.

The early region 3 (E3) transcription unit has attracted intense interest within the adenovirology field. This transcription unit encodes non-structural protein products primarily involved in modulating the host response to infection. The E3 transcription unit is present only in the genomes of members of the genus *Mastadenovirus* and in the genomes of some members of the genus *Siadenovirus* (Davison et al., 2003), and is highly diverse in its coding capability. For HAdV, the E3 transcription unit is a hot spot of genetic diversity, with species-specific arrays of open reading frames (ORFs) (Burgert and Blusch, 2000). Previous work on the E3 transcription unit supports its role in

pathogenesis, host species specificity, tropism, and immune evasion (Belak et al., 1986; Ginsberg et al., 1989; Linne, 1992; Sparer et al., 1996). Because of the important role the E3 transcription unit plays in virus-host interactions, natural variation among HAdV in the E3 transcription unit could account for differences in the manifestation of clinical disease caused by HAdV. However, experimental work on the E3 ORFs has focused almost exclusively on species C HAdVs. This leaves a significant gap in our understanding of the role species-specific E3 ORFs play in the pathogenesis of non-species C HAdV infections, including subspecies B1 HAdV infections.

Three subspecies B1 HAdV-specific E3 ORFs are currently recognized: E3-20.1K, E3-20.5K, and E3-10.9K. The functions of the products of these ORFs for the subspecies B1 HAdV life cycle are unknown. ORF E3-20.5K-encoded protein is expressed throughout infection and is N- and O-glycosylated (Hawkins and Wold, 1995a; Hawkins and Wold, 1995b). ORF E3-20.1K and ORF E3-10.9K have not been extensively characterized. However, transcripts containing ORF E3-10.9K and ORF E3-20.1K are detected in infected cells (Kajon et al., 2005; Signäs et al., 1986). These three E3 ORFs unique to subspecies B1 HAdV are attractive candidates for study to understand the molecular basis of subspecies B1 HAdV pathogenesis.

For this dissertation, I focused on the functional and structural characterization of ORF E3-10.9K and its encoded polypeptide products. Although transcripts containing ORF E3-10.9K are detected in cells infected with subspecies B1 HAdVs (Kajon et al., 2005), a more extensive analysis of the expression of this coding region and the protein products has not been carried out. Previous work has shown that ORF E3-10.9K is highly polymorphic among subspecies B1 HAdVs (Kajon et al., 2005). As will be

discussed in Chapter 2, this ORF encodes polypeptide products that range in predicted size from 4.8 kDa to 10.9 kDa. Some genomic variants of HAdV-7 and HAdV-3 are predicted not to encode a polypeptide from this ORF due to a mutated ATG start codon (Kajon et al., 2005). The ORF E3-10.9K polymorphism is striking in the variety of mutations that exist within an individual subspecies B1 HAdV serotype, particularly in HAdV-7 and HAdV-3. This naturally occurring intraserotypic diversity has not been described for any other coding region of the HAdV genome, and offers the unique opportunity to investigate genetic diversity of HAdV in the context of virus fitness and pathogenesis.

We hypothesized that the ORF E3-10.9K-encoded products function in the efficient release of progeny virions from the host cell by permeabilization of host cell membranes. Several observations led us to this hypothesis. First, ORF E3-10.9K is in an analogous location in the E3 transcription unit to the previously characterized species C HAdV E3-11.6K/adenovirus death protein (ADP) (Tollefson et al., 1992). E3-11.6K/ADP is a late, glycosylated and palmitoylated non-structural viral protein involved in the efficient release of virus progeny from the host cell at the end of infection, although the mechanism by which E3-11.6K/ADP carries out this function is currently unknown (Hausmann et al., 1998; Scaria et al., 1992; Tollefson et al., 1996a; Tollefson et al., 1996b). ORF E3-10.9K predicted products and E3-11.6K/ADP are similar in size and contain a hydrophobic domain. However, ORF E3-10.9K-encoded protein products and E3-11.6K/ADP share little sequence similarity. Second, ORF E3-10.9K-encoded protein products share similarities with a class of viral proteins known as viroporins. The term viroporin is used to describe a group of virus-encoded proteins that share similar

4

structural characteristics and function (Carrasco, 1995; Gonzalez and Carrasco, 2003). These characteristics are small size (60-120 amino acids), one or more hydrophobic domains, polybasic regions, and aromatic residues in or near the hydrophobic domain(s) (Gonzalez and Carrasco, 2003). Additionally, viroporins play a role in the efficient release of virus progeny at the end of infection, and are thought to carry out this function through a mechanism that involves the permeabilization or disruption of host cell membranes (Gonzalez and Carrasco, 2003). ORF E3-10.9K predicted protein products meet the structural criteria to be considered candidate viroporins.

Because of the observed similarities between ORF E3-10.9K predicted protein products, species C HAdV E3-11.6K/ADP, and viroporins, we hypothesized that ORF E3-10.9K-encoded products function in the efficient release of progeny virions from the host cell by permeabilization of host cell membranes. In accordance with this hypothesis, we predicted that ORF E3-10.9K and its protein products would be expressed at late times post infection (pi). Additionally, we predicted that the proteins would localize to host cell membranes and permeabilize membranes to small molecules. Finally, if ORF E3-10.9K-encoded protein products functioned as we hypothesized, mutant subspecies B1 HAdVs that lacked the ability to express these proteins would be predicted to exit the host cell less efficiently than viruses that did express the proteins.

The main goal of this work was to carry out a characterization of ORF E3-10.9K-encoded protein products to understand their role in the subspecies B1 HAdV life cycle. Additionally, by examining this polymorphic ORF we strove to gain an understanding of the role ORF E3-10.9K-encoded protein products would play in subspecies B1 HAdV fitness and evolution. This work was a first step toward determining the implications of

naturally occurring genetic diversity among subspecies B1 HAdV for viral fitness, evolution, and pathogenesis.

The specific aims of the research described in this dissertation were to:

(1)   Carry out a biochemical characterization of ORF E3-10.9K and its predicted protein products

(2)   Investigate the membrane permeabilizing activity of ORF E3-10.9K-encoded proteins

(3)   Examine the role of ORF E3-10.9K in B1 HAdV growth and progeny virion egress

Adenoviruses

Structure. Viruses of the Family *Adenoviridae* have non-enveloped, icosahedral capsids surrounding an approximately 36 kbp-long double-stranded DNA genome. The genome is covalently attached at the 5' and 3' ends to the terminal protein, which is involved in viral genome replication. The icosahedral virus particles are approximately 90 nm in diameter and are composed of several structural proteins. Hexons (240 capsomers) and pentons (12 capsomers) constitute the majority of the surface structure of the AdV capsid. Hexon capsomers are composed of a trimer of the hexon polypeptide, and penton capsomers are composed of the penton base and an associated, projecting fiber protein (Ginsberg et al., 1966) (Fig. 1). The fiber proteins are involved in primary
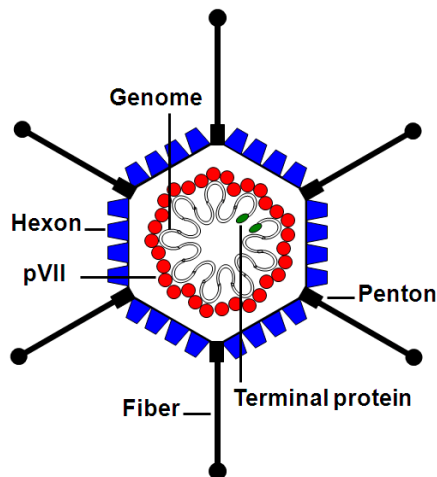
Figure 1. Adenovirus virion. Important structural components of the adenovirus virion are indicated, including capsid proteins (hexon, fiber, and penton base) and the viral dsDNA genome associated with the terminal protein and surrounded by pVII. Adapted from ICTVdb, 2002.

receptor binding (Lonberg-Holm et al., 1969). Minor capsid proteins include proteins VIII, IX, VI, and IIIa. These proteins are involved in stabilizing the capsid structure, endosomal membrane disruption during viral entry into the host cell, and assembly. Virion core proteins are located on the interior of the viral capsid and include proteins V, VII, μ, and the terminal protein. Proteins V, VII, and μ are thought to condense the viral DNA within the core of the capsid (Russell, 2009).

Classification and taxonomy. The Family *Adenoviridae* currently includes four genera: *Atadenovirus*, *Aviadenovirus*, *Mastadenovirus*, and *Siadenovirus*. A fifth unassigned genus containing sturgeon AdV is currently under review by the International Committee on the Taxonomy of Viruses (ICTV) (ICTVdB, 2002). HAdV belong to the genus *Mastadenovirus*, along with many of the other AdV that have mammals as their host species. AdV genera are further divided into species (designated with a capital letter) and subspecies (designated with a capital letter followed by a number). Species and subspecies classification of the *Mastadenovirus* genus is based on a number of characteristics including calculated phylogenetic distance, relative DNA homology, restriction fragment profiles, percentage of GC content in the viral genome, oncogenicity in rodents, growth phenotypes, host range, cross-neutralization, possibility of recombination with other members, and genetic organization of the E3 transcription unit. Species of AdV contain serotypes (given an Arabic number in the order they are discovered), distinguishable by horse or rabbit reference sera. The serotypes are further differentiated into genome types (or genomic variants) by restriction fragment length polymorphism analysis (ICTVdB, 2002). Genome types are designated by a lower case letter, and sometimes by a lower case letter followed by a number, following the serotype

(for instance HAdV-7h, HAdV-7b, HAdV-3a2) (Li and Wadell, 1986). This naming system is established within the field and is particularly useful for subspecies B1 HAdV, and so has been chosen for use in this dissertation.

Several controversies and inconsistencies have arisen for the classification of AdV. First, because HAdV have historically been studied more extensively than other AdV, detailed classification criteria have been developed for HAdV. Serology to define a new AdV "type" is the standard, and is reflected in the use of the term "serotype". However, this has led to questions regarding the classification of new AdV, including many non-mammalian AdV for which infectious virus cannot be isolated. Additionally, technological advances in the isolation and sequencing of AdV DNA have prompted a reevaluation of the criteria by which AdV are classified. Use of nomenclature has been inconsistent and incorrect (Jones et al., 2007; Walsh et al., 2009; Walsh et al., 2010), despite clear guidelines from ICTV and established norms within the field.

Second, classification of AdV has historically placed emphasis on the host species. For instance, previously all HAdV were classified separately from all simian AdV, bovine AdV, etc. However, the emergence of new molecular and bioinformatics tools has shown this classification scheme to be inappropriate. A greater emphasis is now placed on genome sequence analysis, such that some simian AdV and bovine AdV are classified with HAdV species (ICTVdB, 2002). However, the natural host species remains important for the designation of AdV, as is obvious with "simian adenovirus", "bovine adenovirus", "human adenovirus", etc.

The dynamic field of AdV taxonomy likely will incorporate technological advances in future classification and nomenclature. But, for the purpose of this

dissertation, AdV will be designated utilizing the most current ICTV guidelines and established norms for the *Adenoviridae* Family.

Genome organization and transcription. The size and organization of the genomes of viruses in the Family *Adenoviridae* vary among genera and species. For instance, the E3 transcription unit is only present among the members of the genus *Mastadenovirus* and some members of the genus *Siadenovirus* (Davison et al., 2003). The smallest reported genome for a member of the Family *Adenoviridae* is 26,163 bp for frog AdV 1 and the largest is 45,063 bp for fowl AdV D. HAdV genomes are consistently around 36,000 bp in size (ICTVdB, 2002).

AdV genomes contain inverted terminal repeats (ITR), which are important in viral DNA replication (Davison et al., 2003). AdV genes are transcribed from both the l and r strands and are organized into transcription units (Fig. 2). HAdV genomes, which serve as the prototype for study, contain five early transcription units—E1A, E1B, E2, E3, and E4—which are transcribed prior to the onset of viral DNA replication. Three delayed early transcription units—IX, IVa2, and E2 late—are transcribed from promoters separate from the early transcription units. One late transcription unit—major late (ML)—is efficiently transcribed from the major late promoter (MLP) after the onset of viral DNA replication and primarily encodes structural genes. In addition to the transcription units, some AdV genomes encode virus associated RNA (VA RNA) genes. In general, the AdV transcription units encode genes that serve related functions (Table 1). The organization and content of these transcription units varies among the members of the *Adenoviridae* Family members (Davison et al., 2003).
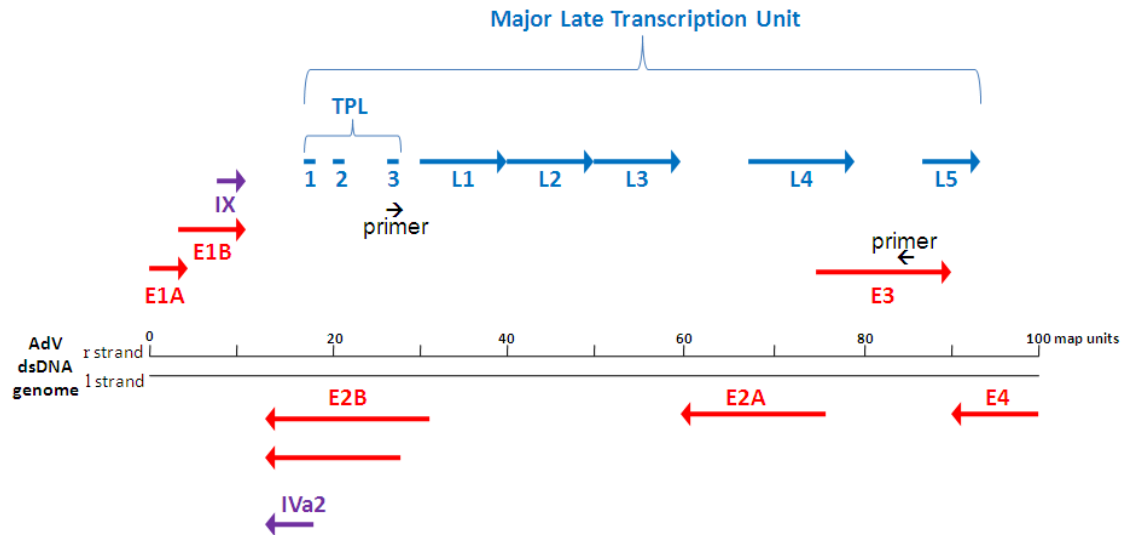
Figure 2. Genetic organization of the adenovirus transcription units. Early (red arrows), delayed early (purple arrows), and late (blue arrows) adenovirus transcription units are shown at their approximate location in the dsDNA genome. Forward arrows (above) indicate transcription units encoded by the r strand, and reverse arrows (below) indicate transcription units encoded by the l strand. Approximate locations corresponding to primers used for detection of major late promoter expression of ORF E3-10.9K are indicated by black arrows (see Table 5 for more details). Adapted from Akusjarvi, 2008.

Much of what is currently known regarding transcription of AdV genes comes from work carried out on species C HAdV serotypes 2 and 5. Viral gene transcription is temporally regulated. By definition, early genes are expressed prior to the onset of viral DNA replication and late genes are expressed after viral DNA replication begins. Host cell RNA polymerase II transcribes the viral genome transcription units while RNA polymerase III transcribes the VA RNA genes (Pettersson and Roberts, 1986; Weinmann et al., 1976). Alternative splicing produces multiple mRNA products from the AdV transcription units (Fig. 2).

Expression of AdV transcription units is activated by the E1A viral proteins (Berk et al., 1979; Nevins, 1981). E1A genes are the first genes transcribed once the viral genome reaches the host cell nucleus upon infection (Nevins et al., 1979). Activation of

11

Table 1. Adenovirus transcription units and encoded protein functions.

Transcription unit	# of protein products	Temporal expression	General function of protein products
E1A	2	Early	Activation of transcription and host cell induction of S phase
E1B	2	Early	Inhibition of apoptosis
E2 early	3	Early	DNA replication
E3	Varies	Early	Modulation of host response to infection
E4	6	Early	Diverse, unrelated functions (including induction of host cellular S-phase)
IX	1	Delayed early	Transcriptional activation, nuclear reorganization, progeny virion stability
IVa2	1	Delayed early	Virion structural protein / MLP activation
E2 late	3	Delayed early	DNA replication
Major late	13	Late	Production and assembly of progeny virions

early transcription unit promoters is largely driven by the large E1A protein (Berk, 1986) and is carried out through interaction of large E1A protein with host cellular transcription factors (Berk, 2005; Liu and Green, 1994). The small E1A protein is responsible for activation of transcription of the E2 early promoter (Bagchi et al., 1990; Phelps et al., 1991). The MLP is the major controller of late mRNA expression for AdV. Although it is active at early stages of infection, the MLP is over a hundred times more active after viral DNA replication begins (Shaw et al., 1980). The MLP is activated by viral E1A proteins along with host cellular transcription factors (Parks and Shenk, 1997), but the mechanism by which the MLP activity depends on viral DNA replication is unknown. However, there is evidence to suggest that changes in the viral chromatin that occur upon

viral DNA replication could play a role (Toth et al., 1992) as well as induction of a viral transcription factor, protein IVa2, which is also involved in viral DNA packaging (Pardo-Mateos and Young, 2004; Tribouley et al., 1994). Late coding regions are transcribed as a single, large transcript of approximately 28 kb (Evans et al., 1977; Nevins et al., 1978). The late transcript is spliced into distinct mRNAs that contain poly-A tails and a 201 nucleotide untranslated region referred to as the tripartite leader (TPL) (Berget et al., 1977; Chow et al., 1977). The TPL is generated by the splicing of three short exons (leader 1, 2, and 3) to the 5' end of a larger ORF (Berget et al., 1977). The TPL is important for enhancing the translation of the ORFs to which it is spliced (Logan and Shenk, 1984). While most products encoded in the ML transcription unit are structural proteins, a region of the E3 transcription unit is expressed late for species C HAdVs (Bhat and Wold, 1986).

Single cell replication cycle. Like other DNA viruses, the AdV replication cycle is divided into two stages: early and late. By definition, the early stage occurs prior to viral genome replication and the late stage after DNA replication begins. The early stage of infection encompasses attachment, entry, uncoating, transport of the viral DNA to the nucleus, and early viral gene expression. Upon viral genome replication, the late stage of infection begins. At this stage, the viral late genes are expressed and progeny virions are assembled and released from the host cell.

Attachment of the virion to the host cell is the first step in the AdV replication cycle. This step is primarily mediated by the fiber protein on the surface of the AdV virion (Lonberg-Holm et al., 1969). The host cell attachment receptor differs among HAdV. In general, HAdV of species A, C, E and F interact with the coxsackievirus B

13

and adenovirus receptor (CAR), a protein involved in the formation of cellular tight junctions in polarized epithelial cells (Philipson and Pettersson, 2004). Species D HAdV use sialic acid moieties as receptors (Arnberg et al., 2002). For species B HAdV, the attachment receptor appears to vary with the serotype. Most of species B HAdVs use complement regulatory molecule CD46 as an attachment receptor (Marttila et al., 2005), but species B HAdV serotypes 3 and 7 bind to CD80 or CD86 (Short et al., 2004; Short et al., 2006).

Concomitant with attachment of the AdV virion to the primary receptor via interaction with the fiber protein, the penton base can also interact with host cellular $\alpha_v\beta_3/\alpha_v\beta_5$ integrins. This interaction facilitates the internalization of the virions into clathrin-coated vesicles and then into the host cell endosomal pathway (Mathias et al., 1994; Patterson and Russell, 1983). The interaction of the virion with $\alpha_v\beta_3/\alpha_v\beta_5$ integrins also induces the activation of PI3 kinases and Rho GTPases, leading to the alteration of the host cytoskeleton (Li et al., 1998a; Li et al., 1998b). After entry of the virion into the host cell endosomal pathway, the AdV particle is disrupted and releases peripentonal hexons, protein IIIa, and protein VI from the virion, leaving a subviral particle consisting of a hexon shell and associated viral core containing the viral genome and associated proteins (Russell, 2009). The infected endosome/lysosome is then ruptured, allowing the release of the hexon shell and virion core into the cytoplasm of the host cell. The hexon shell is transported to the nuclear pore complex by way of microtubules (Dales and Chardonnet, 1973; Greber and Way, 2006; Leopold et al., 2000; Mabit et al., 2002; Suomalainen et al., 1999). Viral genome uncoating occurs at the nuclear pore complex, where viral DNA and protein VII enter the nucleus (Greber et al., 1997).

Early gene expression begins upon entry of the viral DNA into the host cell nucleus. The early genes (encoded in the E1A, E1B, E2, E3, and E4 transcription units) prepare the host cell for the production of viral progeny. This function is accomplished by (1) inducing the host cell to enter S phase, (2) protecting the host cell from antiviral defenses while the virus replicates, and (3) synthesizing viral gene products necessary for viral genome replication. As discussed in the "Genome organization and transcription" section, the large and small E1A proteins activate the transcription of early genes. Induction of the host cell to enter S phase is accomplished primarily by the E1A and E4 gene products. E1B, E3, and the VA RNA gene products are involved in protecting the host cell from antiviral defenses. Viral gene products necessary for viral genome replication are encoded by the E2 transcription unit.

AdV genome replication requires three virus-encoded products—preterminal protein (pTP), DNA polymerase (AdPol), and DNA binding protein (DBP)—and is enhanced by three host-cell encoded products—transcription factor NFI, transcription factor Oct-1, and type I topoisomerase NFII (de Jong et al., 2003). The first step of viral genome replication is the formation of a heterodimer of pTP and the AdPol. This heterodimer binds to the origin of DNA replication in the viral genome, located within the ITR at the ends of the viral genome. DNA replication is then initiated by AdPol using a strand-displacement mechanism that requires DBP. Synthesis of viral DNA is initiated at one of the DNA termini and proceeds to the other end of the genome, with only one strand serving as template. The complement to the second strand (the displaced strand) is then synthesized. The displaced strand forms a panhandle structure consisting of the self-complementing ITR at either ends of the strand. This panhandle structure is recognized

by the pTP/AdPol heterodimer and DNA synthesis proceeds (Lechner and Kelly, 1977; Liu et al., 2003).

Late gene expression begins upon the initiation of viral genome replication. Late genes (expressed from the ML transcription unit) encode products whose function is to assemble progeny virions. The production of structural proteins that will encapsidate the newly synthesized viral DNA and associated proteins that will aid in the assembly of the progeny virions begins at this stage. Also during this time, the E3-11.6K/ADP encoded in the E3 transcription unit of species C HAdVs is produced in large quantities (Tollefson et al., 1992).

The assembly of progeny virions proceeds through a maturation process that involves structural viral proteins as well as viral proteins that serve as scaffolds for the newly assembled capsids. Progeny virions are assembled in the nucleus of the host cell and have historically been thought to egress through lysis of the host cell. However, evidence from species C HAdV suggests that egress is a more controlled process that is mediated by viral factors. For species C HAdVs, the E3-11.6K/ADP is involved in the efficient release of newly assembled viral particles from infected cells (Tollefson et al., 1996b). It is unknown whether all members of the *Adenoviridae* Family use a similar mechanism for egress.

Human adenoviruses

Discovery. HAdV were first discovered in 1953 by two separate research groups (Hilleman and Werner, 1954; Rowe et al., 1953). The isolation of cells from adenoids of young children led to the observation of a cytopathic agent that was capable of being

passed to new cells. The agent was determined to be a virus, and was called "adenoid degeneration agent" (Rowe et al., 1953).   The same agent was isolated from respiratory secretions of military recruits collected during an outbreak of pneumonitis at Fort Leonard Wood, MO (Hilleman and Werner, 1954). The original isolation of AdV from adenoid tissue led to their name (Enders et al., 1956).

Classification and taxonomy. All 51 recognized HAdV serotypes are currently classified into six species (A-F) (Table 2) (ICTVdB, 2002). Species B is further divided into subspecies B1 and B2 primarily on the basis of genomic DNA homology (Wadell, 1984).   A new HAdV, tentatively designated HAdV-52, was recently described and proposed to belong to an entirely new species G (Jones et al., 2007). The classification of HAdV-52 along with the recognition of recently proposed new "types" remain tentative until a review by the ICTV is complete (Jones et al., 2007).

Table 2. Classification of 51 recognized human adenovirus serotypes.[1]   Adapted from ICTVdb, 2002.

Species	Subspecies	Serotypes
A		12, 18, 31
B	1	3, 7, 16, 21, 50
	2	11, 14, 34, 35
C		1, 2, 5, 6
D		8, 9, 10, 13, 15, 17, 19, 20, 23, 30, 32, 33, 36, 37, 38, 39, 42, 43, 44, 45, 46, 47, 48, 49, 51
E		4
F		40, 41

[1]Candidate species G and its associated serotype 52 are not shown because of current controversy regarding the use of this designation.

Remarkable intraserotypic genetic diversity exists among HAdV. This diversity has historically been documented through the use of restriction endonuclease digestion of HAdV genomic DNA, but PCR and sequence analysis have also been important for revealing this genetic variability. While essential viral proteins (including structural proteins and proteins involved in viral replication and assembly) are largely conserved among HAdV, the E1, E3, and E4 transcription units are not well conserved. Additionally, "hotspots" of variability exist within the hexon and fiber genes and are associated with major neutralizing epitopes on the virion (Bailey and Mautner, 1994; Crawford-Miksza and Schnurr, 1996; Pichla-Gollan et al., 2006; Xia et al., 1994). Homologous recombination among closely related HAdV serotypes is a recognized mechanism contributing to AdV genetic diversity (Sambrook et al., 1980) and can lead to the emergence of intermediate variants (Adrian and Wigand, 1986; Hierholzer et al., 1980; Hierholzer and Rodriguez, 1981; Kajon and Wadell, 1996; Li and Wadell, 1988; Wigand and Adrian, 1989).

Associated disease. HAdV are associated with upper respiratory tract infections, lower respiratory tract infections, epidemic keratoconjunctivitis, conjunctivitis, acute hemorrhagic cystitis, hepatitis, gastroenteritis, and myocarditis. The unambiguous association of HAdV serotypes with disease cannot be made, since route of infection and immunocompetence of the host play a large role in the resulting clinical manifestation. Some generalizations can be made about the different species, however. Species A serotypes are associated with cryptic infections, although HAdV-31 is associated with infant gastroenteritis and encephalitis (Adrian & Wigand, 1989; Schnurr et al., 1995). Species B serotypes are associated with respiratory disease in children and adults,

conjunctivitis, and urinary tract infections. Species C serotypes are associated with respiratory disease in children under 5 years of age. Species D serotypes are associated with epidemic keratoconjunctivitis and infections of immunocompromised individuals. The only species E serotype, HAdV-4, is associated with respiratory infections and conjunctivitis. Species F serotypes are associated with gastrointestinal infections.

Although some AdV induce tumors in rodent models, there is little evidence to indicate a role for AdV in human tumor formation. Evidence suggestive of a role for HAdV in the etiology of cancer comes from a recent study, which shows an association between the detection of AdV DNA in neonatal blood and the development of acute lymphoblastic leukemia, suggesting that prenatal AdV infection correlates with the development of acute lymphoblastic leukemia (Gustafsson et al., 2007). However, a more comprehensive study carried out by the same group shows no correlation between the presence of AdV DNA in neonatal blood and acute lymphoblastic leukemia (Honkaniemi et al., 2010). These conflicting findings leave the role of AdV in the etiology of acute lymphoblastic leukemia currently unclear.

Treatment and vaccine. The lack of specific antivirals against AdV necessitates the treatment of most infected individuals by symptomatic care. However, in immunocompromised patients, the risk of disseminated infection often requires pharmaceutical interventions. No formally approved anti-adenoviral drugs are currently available. However, small clinical studies of cidofovir and ribavirin show conflicting results (Lenaerts et al., 2008). A vaccine against HAdV-4 and HAdV-7 was routinely administered to U.S. military recruits from 1973 to 1996 (Gray et al., 2000; Top, 1975),

and was effective at protecting this population from AdV outbreaks. No vaccine is currently licensed for use in civilian populations.

Subspecies B1 human adenoviruses

Species B HAdVs are divided into two clusters of homology: subspecies B1 and subspecies B2. Subspecies B1 includes the serotypes HAdV-3, -7, -16, -21, and -50 and their genomic variants. Of these, HAdV-3 and HAdV-7 are most frequently isolated in association with disease, while HAdV-16 and HAdV-21 are less frequently detected. HAdV-50 was isolated from a 34-year old male with diarrhea who was hospitalized because of AIDS (De Jong et al., 1999). HAdV-50 has not been isolated in association with respiratory disease to date. Subspecies B2 includes the serotypes HAdV-11, -14, -34, and -35. Subspecies B2 HAdVs are isolated in association with conjunctivitis, urinary tract infections, and respiratory disease. Until the recent emergence of HAdV-14 into North America, the association of subspecies B2 HAdVs with severe respiratory infections has been infrequent (Louie et al., 2008). Because the focus of this dissertation is on the characterization of a subspecies B1 HAdV-specific ORF, the next sections focus exclusively on the associated respiratory disease, epidemiology, and genetic diversity of this subspecies.

Associated respiratory disease. HAdV-3, -7, -16, and -21 are associated with acute lower respiratory infections of variable severity in pediatric and military recruit populations. Symptoms range from mild to severe, and include sore throat, coughing, rhinorrhea, wheezing, dyspnea, sinus tenderness, vomiting, abdominal pain, and diarrhea. HAdV-3, -7, and -21 are associated with long-term pulmonary sequelae, including

bronchiolitis obliterans and bronchiectasis in young children up to ten years after acute infection and HAdV-associated pneumonia (Becroft, 1971; Herbert et al., 1977; Similä et al., 1981). The viral factors contributing to the clinical manifestations of subspecies B1 HAdV acute lower respiratory infections are unknown.

Epidemiology and genetic diversity. Subspecies B1 HAdVs have long been recognized as important causative agents of epidemic outbreaks of respiratory tract infections and pharyngoconjunctival fever (Becroft, 1971; Dudding et al., 1972; Gerber et al., 2001; Herbert et al., 1977; Ryan et al., 2002; Spigelblatt and Rosenfeld, 1983; Wadell et al., 1980). These outbreaks are most common in pediatric populations and military recruits, and most frequently involve HAdV-7 and HAdV-3 and their genomic variants.

Military recruit populations are highly susceptible to HAdV respiratory infection. Since soon after its discovery, HAdV has been recognized as the causative agent of the majority of acute respiratory disease outbreaks among military recruits in the U.S. (Grayston et al., 1959; Hilleman, 1957; McNamara et al., 1962). HAdV-7 and HAdV-4 (Species E) were the major causes of respiratory infections, and were chosen for use in the vaccine administered to military recruits in the U.S. (Top, 1975). Since the cessation of the vaccination protocols in 1996, HAdV infections re-emerged in the U.S. military recruit populations (Gray et al., 2000; Metzgar et al., 2007; Ryan et al., 2002). The extensive genetic diversity for some of the re-emerging HAdV serotypes, including HAdV-3, HAdV-7, and HAdV-4 (Species E) has been described (Dickson, 2009; Kajon et al., 2007).

In contrast to military recruit populations, surveillance of HAdV infections in civilian populations is limited. Most available typing data are restricted to outbreaks of

severe disease and fatal case reports. HAdV-3 and HAdV-7 and their genomic variants are important causes of severe disease in pediatric populations. HAdV-3 respiratory illness is associated with fatalities in pediatric patients (Hon et al., 2008; Kajon et al., 1990; Kim et al., 2003). HAdV-7 is associated more frequently than HAdV-3 with severe respiratory infections and fatal outcome (de Silva et al., 1989; Gerber et al., 2001; Kajon et al., 1996; Kim et al., 2003).

Subspecies B1 HAdVs, in particular HAdV-7 and HAdV-3, show extensive intraserotypic genetic diversity (Golovina et al., 1991; Kajon and Wadell, 1994; Li and Wadell, 1986; Li and Wadell, 1988). Genomic variants of HAdV-7 and HAdV-3 are often geographically restricted, but can spread to new geographic areas and take over as the predominant circulating genomic variant (Erdman et al., 2002; Golovina et al., 1991; Wadell et al., 1980). This phenomenon is called a genome type shift, and is correlated with an apparent increased severity of associated disease (Erdman et al., 2002; Kajon and Wadell, 1994; Kajon et al., 1996; Larranaga et al., 2000; Wadell et al., 1980; Wadell et al., 1985). The reason for this apparent increase in associated disease severity is currently unknown.

Early region 3 transcription unit

The size and coding content of the E3 transcription unit varies considerably among the AdV (Davison et al., 2003). The E3 transcriptin unit encodes non-structural products that are dispensable for growth in cell culture, hamster lungs, or cotton rats (Ginsberg et al., 1989; Morin et al., 1987). The E3 transcription unit is transcribed from the r strand of the double-stranded DNA viral genome, and is the only region of the

HAdV genome that encodes integral membrane proteins (Wold et al., 1995). The E3 transcription unit is only present in the genomes of members of the genus *Mastadenovirus* and some members of the genus *Siadenovirus* (Davison et al., 2003). This transcription unit is thought to have arisen independently within these two genera, or to represent an ancient locus of rapid gene evolution that has been subsequently lost in the *Atadenovirus* and *Aviadenovirus* genera (Davison et al., 2003). The flanking ORFs present within the HAdV E3 (E3-12.5K and E3-14.7K) are distantly related and are hypothesized to have arisen by a gene duplication event early in *Mastadenovirus* evolution (Davison et al., 2003).

The analysis of the E3 transcription unit has been undertaken for mouse AdV (Beard et al., 1990; Beard and Spindler, 1995; Beard and Spindler, 1996; Cauthen et al., 1999; Cauthen and Spindler, 1999), canine AdV (Dragulev et al., 1991; Linné, 1992), bovine AdV (Belák et al., 1986; Esford and Haj-Ahmad, 1994; Evans et al., 1998; Idamakanti et al., 1999; Mittal et al., 1993), porcine AdV (Kleiboeker, 1994; Reddy et al., 1995; Tuboly and Nagy, 2000), and ovine AdV (Vrati et al., 1995). However, functional roles for E3-encoded protein products have only been determined for HAdV. The remainder of this section will focus on the HAdV E3 transcription unit.

Diversity of E3 among human adenoviruses. No other HAdV transcription unit is as heterogeneous as E3 (Chroboczek et al., 1992). ORFs E3-12.5K, E3-19K, E3-10.4K, E3-14.5K, and E3-14.7K are highly conserved among HAdV species A-F (Fig. 3). Species F is the only HAdV species that does not encode ORF E3-12.5K. Species A and F do not encode ORF E3-19K. Between the highly conserved ORFs E3-19K and E3-10.4K, species-specific E3 ORFs are encoded. For species C HAdVs, this region

23

contains ORF E3-11.6K. For species B HAdV, ORFs E3-20.1K and E3-20.5K are encoded. Subspecies B1 HAdVs, but not subspecies B2 HAdVs, additionally encode ORF E3-10.9K in the species-specific region.
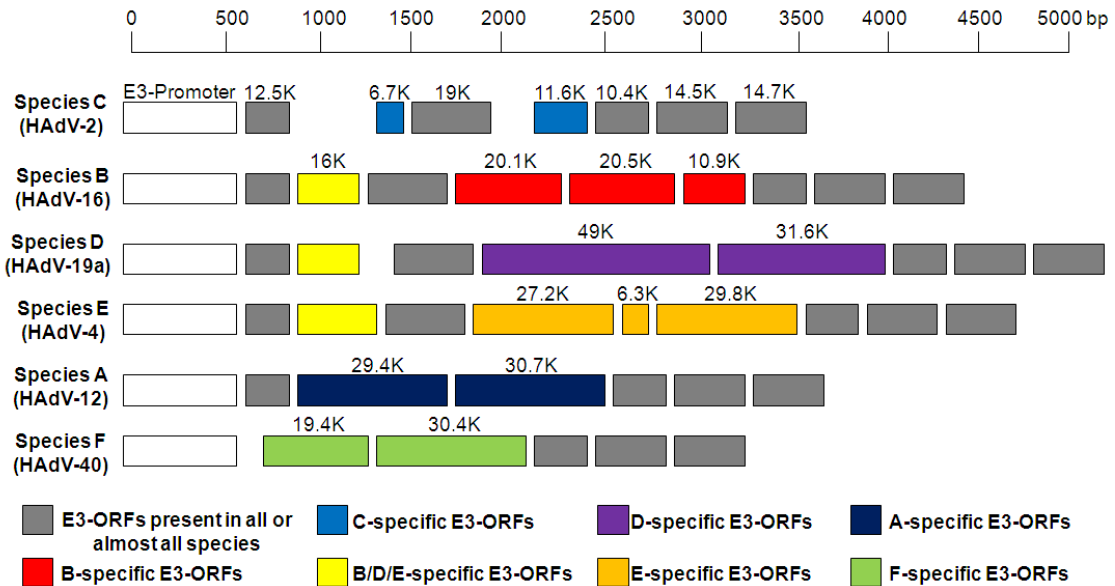
Figure 3. Comparison of the E3 transcription unit coding capability for human adenoviruses of species A-F. E3 ORFs are indicated for a representative member of each HAdV species A-F. Adapted from Burgert and Blusch, 2000.

Transcription and splicing. Our knowledge of the transcription and splicing of the E3 transcription unit has come from studies of HAdV-2 and HAdV-5. The E3 promoter is activated by AdV E1A protein and tumor necrosis factor α (TNFα) (Deryckere and Burgert, 1996; Korner et al., 1992; Kornuc et al., 1990). The E3 mRNAs and splicing for HAdV-2 and HAdV-5 have been characterized extensively, but E3 mRNAs for other serotypes belonging to other species of HAdV have been neglected (Wold et al., 1995). For HAdV-2 and HAdV-5, nine mRNAs are produced from the E3 transcription unit. These are alternatively spliced and polyadenylated at either the E3A or

24

E3B polyadenylation sites (Wold et al., 1995). Limited analysis of HAdV-3 E3 mRNAs show that exact RNA splice junctions are not conserved between HAdV-2 and HAdV-3, although mRNAs corresponding to most HAdV-3 E3 ORFs can be detected (Signäs et al., 1986).

Conserved E3 proteins encoded by HAdV genomes. The characterization of HAdV E3 proteins has largely focused on species C HAdV-encoded proteins. The E3 proteins that are highly conserved among HAdV and are expressed in infected cells include E3-12.5K (Hawkins and Wold, 1992), E3-19K (Persson et al., 1980; Ross and Levine, 1979), E3-10.4K (Tollefson et al., 1990), E3-14.5K (Tollefson et al., 1990), and E3-14.7K (Persson et al., 1978; Tollefson and Wold 1988; Wang et al., 1988). Functions are assigned to all these proteins except E3-12.5K.

The E3-19K protein blocks MHC class I transport to the plasma membrane, interfering with antigen presentation and T-cell recognition of infected cells (Andersson et al., 1985; Andersson et al., 1987; Burgert and Kvist, 1985; Burgert et al., 1987). In animal models, the immunomodulatory role for E3-19K has been confirmed; cotton rats infected with wild type HAdV-5 show less immunopathology than those infected with HAdV-5 mutants lacking the E3-19K (Ginsberg et al., 1989). HAdV serotypes from species B, D, and E but not A or F express the conserved E3-19K, and the protein modulates the expression of MHC class I like its counterpart for species C HAdV (Pääbo et al., 1986)

E3-10.4K/RIDα and E3-14.5K/RIDβ are referred to collectively as the receptor internalization and degradation (RID) complex, and are involved in the inhibition of host cell apoptosis through several mechanisms. First, RID down-regulates proapoptotic cell

25

surface receptors, including Fas, TRAILR1, and TRAILR2. Downregulation of these receptors protects HAdV infected cells from apoptosis (Benedict et al., 2001; Elsing and Burgert, 1998; Shisler et al., 1997; Tollefson et al., 1998; Tollefson et al., 2001). Second, RID inhibits TNF-α-induced arachidonic acid release by blocking the translocation of cytosolic phospholipase A_2 to host cell membranes, which prevents TNF-α-mediated apoptosis (Dimitrov et al., 1997; Krajcsi et al., 1996). Third, RID inhibits NF-κB activation induced by interleukin-1 and TNF-α by inhibiting NF-κB translocation to the nucleus (Friedman and Horwitz, 2002).

E3-14.7K, unlike other E3 proteins, is not an integral membrane protein. E3-14.7K is a cytoplasmic and nucleoplasmic protein that functions primarily in the inhibition of TNF-α-induced apoptosis of host cells (Gooding et al., 1990). However, E3-14.7K accomplishes this function through a mechanism independent of RID (Horton et al., 1991).

Species-specific E3 proteins. Several species-specific E3 ORFs have been shown to be expressed in infected cells. These include species C HAdV E3-11.6K, species C HAdV E3-6.7K, species B HAdV E3-20.5K, species D HAdV E3-49K, and speices E HAdV E3-30K (Fig. 3). Of these, functions have been assigned only to E3-11.6K and E3-6.7K.

E3-6.7K localizes primarily to the ER and interacts with the RID complex to down-regulate TRAIL2 receptors (Benedict et al., 2001). Additionally, E3-6.7K represses apoptosis of host cells by maintaining cytosolic Ca^{2+}, similar to host cellular protein Bcl-2 (Moise et al., 2002).

E3-11.6K is the most extensively characterized species-specific E3 ORF. This ORF encodes the ADP. E3-11.6K/ADP is expressed at early stages of infection like other E3 proteins, but expression is greatly amplified at late stages of infection, primarily as a result of increased transcription from the AdV MLP (Tollefson et al., 1992). The protein is both N- and O-glycosylated (Scaria et al., 1992; Tollefson et al., 2003), palmitoylated at the cytoplasmic tail (Hausmann et al., 1998), and localizes primarily to the nuclear envelope (Scaria et al., 1992). HAdV-2 and HAdV-5 E3-11.6K/ADP deletion mutants have a small plaque phenotype, kill cells more slowly, and retain progeny virions in the nucleus compared to wild-type viruses that produce virions that exit the host cell efficiently (Tollefson et al., 1996a). Furthermore, the E3-11.6K/ADP is required for the efficient release of progeny virions from infected cells (Tollefson et al., 1996b). Directed mutation of the E3-11.6K/ADP shows that, in general, (1) the lumenal domain is important for the efficient transit of E3-11.6K/ADP through the trans-Golgi network and into the nuclear envelope, (2) glycosylation seems to stabilize E3-11.6K/ADP, (3) deletion of the transmembrane domain results in aggregation of E3-11.6K/ADP in the cytoplasm and loss of function, and (4) the cytoplasmic-nucleoplasmic domain is important for localization (Tollefson et al., 2003). The mechanism of action for E3-11.6K/ADP is unknown. However, in yeast two-hybrid screens and glutathione-S-transferase (GST)-pull down assays, the C-terminus (cytoplasmic-nucleoplasmic domain) of E3-11.6K/ADP interacts with the human protein MAD2B, a protein implicated in mitosis control, error-prone DNA synthesis promotion, and cell-cell interactions (Ying and Wold, 2003). However, the importance or functional significance of this interaction is unknown.

The E3-20.5K protein is expressed in HAdV-3 and HAdV-7 infected KB cells (Hawkins and Wold, 1995a). The protein is synthesized throughout the viral replication cycle (Hawkins and Wold, 1995a). Treatment with glycosidases shows that the protein is both N- and O-glycosylated (Hawkins and Wold, 1995b). Although E3-20.5K protein was hypothesized to cause MHC class I retention in the ER because of its structural similarities to E3-19K, no evidence thus far supports this hypothesis (Hawkins and Wold, 1995b), and a function for this protein is currently unknown.

A549 cells infected with species D HAdV serotypes 8, 9, 15, 19a, and 37 express E3-49K   (Blusch et al., 2002). The E3-49K protein is detected at early stages of infection, and expression continues throughout the viral replication cycle. The E3-49K protein contains N- and O-linked glycans, and the protein localizes primarily to the trans-Golgi network and early endosomes. However, some plasma membrane localization is detected in infected cells expressing high levels of the E3-49K protein. The function of the E3-49K protein is currently unknown (Windheim and Burgert, 2002).

HAdV-4, the sole member of the species E HAdV, encodes ORF E3-30K. The E3-30K protein is expressed at early stages of infection but is amplified at late stages of infection, similar to species C HAdV E3-11.6K/ADP. The protein is N-glycosylated and localizes primarily to the nuclear membrane and endoplasmic reticulum. A function has not been assigned to the E3-30K protein (Li and Wold, 2000).

Role of E3 in adenovirus pathogenesis. The E3 transcription unit is dispensable for virus growth in cell culture (Lewis et al., 1974). However, the E3 transcription unit plays an important role in AdV pathogenesis. Both cotton rats (*Sigmodon hispidus*) and mice are used in studies investigating the role of E3 in the pathogenesis of respiratory

infections. Intranasal inoculation of cotton rats or mice with HAdV-5 E3 deletion mutant viruses results in more extensive pathology compared to wild-type viruses (Ginsberg et al., 1989; Sparer et al., 1996). Additionally, E3-deleted AdV vectors administered to cystic fibrosis patients induce a major inflammatory response (Crystal et al., 1994), further supporting the role of the E3 transcription unit in AdV-pathogenesis.

ORF E3-10.9K of subspecies B1 human adenoviruses

ORF E3-10.9K is encoded only in subspecies B1 HAdV genomes. This ORF is absent in subspecies B2 HAdV genomes. In HAdV-11 and HAdV-35, of subspecies B2 HAdV, the lack of ORF E3-10.9K is postulated to account for their unique association with persistent infection of the renal epithelia (Flomenberg et al., 1988; Mei and Wadell, 1992). ORF E3-10.9K shows extensive intraserotypic diversity. Predicted protein products range in size from 4.8 kDa to 10.9 kDa, with some genomic variants of HAdV-7 and HAdV-3 lacking the ability to encode a protein because of a mutated start codon. For ease of discussion herein, the ORF will be referred to as ORF E3-10.9K regardless of the size of the encoded product. For instance, ORF E3-10.9K of HAdV-3p is predicted to encode a polypeptide of 9 kDa, ORF E3-10.9K of HAdV-7p is predicted to encode a polypeptide of 7.7 kDa, and ORF E3-10.9K of HAdV-7h is predicted to encode no polypeptide.

Intraserotypic diversity. The intraserotypic polymorphism of ORF E3-10.9K was first noted when examining an Argentinean isolate of HAdV-7h (Kajon and Wadell, 1996). HAdV-7h was the predominant circulating genome type of HAdV-7 in South America, and was the sole genomic variant circulating after replacing HAdV-7c in 1986

(Kajon and Wadell, 1994). Genome type HAdV-7h attracted intense interest because of its association with severe acute respiratory infections of children (Kajon et al., 1994; Murtagh et al., 1993). In a search for a molecular basis for the apparent increased severity of disease associated with HAdV-7h infection, sequencing of the E3 transcription unit revealed the absence of an E3 ORF found in HAdV-7p, referred to as ORF E3-7.7K. This difference was because of an ATG→ATT mutation, eliminating the putative start codon (Kajon and Wadell, 1996).

A more thorough sequence examination of this ORF was carried out on 55 laboratory strains and field isolates representing all subspecies B1 HAdV serotypes and many HAdV-3 and HAdV-7 genome types (Kajon et al., 2005). This study documented extensive intraserotypic variation of ORF E3-10.9K for subspecies B1 HAdVs, and identified eight sequence profiles (SP1-SP8) for this coding region (Fig. 4). Additionally, RT-PCR showed the expression of mRNAs corresponding to ORF E3-10.9K in cells infected with HAdV-16p, HAdV-3p, HAdV-7p, HAdV-7b, and HAdV-7h (Kajon et al., 2005).

Illegitimate recombination as a mechanism generating variability in ORF E3-10.9K. Because the striking variation of ORF E3-10.9K among genomic variants of the same serotype is unique among HAdV, it is referred to as a "hot spot" of mutations (Kajon et al., 2005). Sequence analysis suggests a slippage/misalignment model for the generation of the ORF E3-10.9K polymorphism. In the slippage/misalignment model, a transient dissociation of the DNA duplex during replication results in a slipped-strand mispairing between two regions having short homologies (Kunkel, 1990). One of these repeats is deleted along with the intervening sequences in the daughter strand.
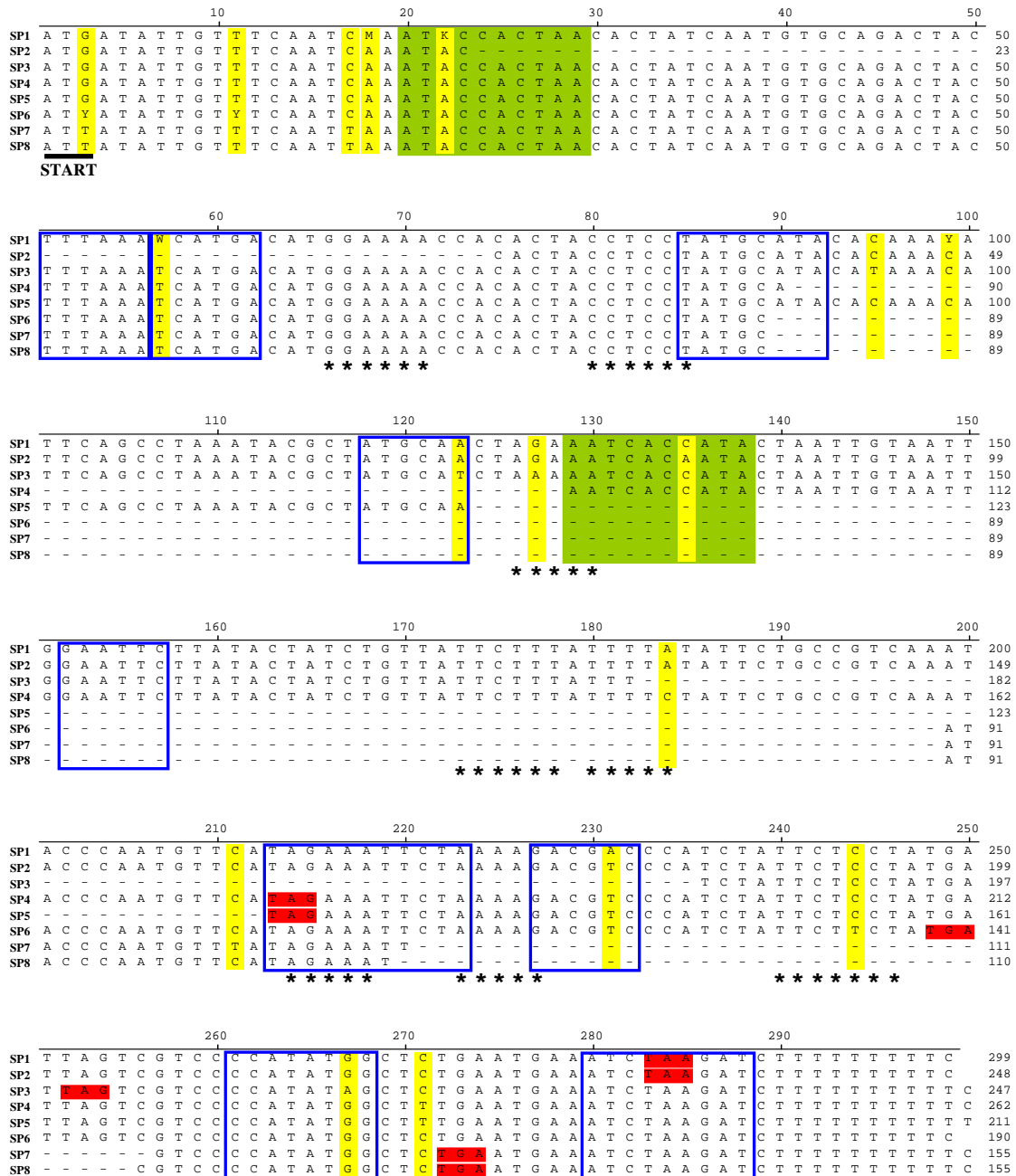
Figure 4. Nucleotide sequence alignment of ORF E3-10.9K sequence profiles (SP1-8). Start codon (black underline), stop codons (red highlight), single base mutations (yellow highlight), palindromic motifs (blue box), inverted repeats (green highlight), and polypurine/polypyrimidine runs (*) are indicated. Adapted from Kajon et al., 2005.

Palindromic sequence motifs, inverted repeats, polypurine/polypyrimidine runs, single base mutations in close proximity to deletion junctions, and loss of one of two short direct repeat sequences at or near deletion junctions are observed in ORF E3-10.9K polymorphism and are consistent with the slippage/misalignment model (Kajon et al., 2005) (Fig. 4).

Viroporins

The term viroporin describes a class of viral proteins encoded by diverse virus families. These proteins are small, highly hydrophobic, involved in the efficient release of progeny virions from infected cells, and are capable of permeabilizing membranes to small molecules and ions (Carrasco, 1995; Gonzalez and Carrasco, 2003). Viroporins encoded by different virus families have similar functions and features, but share little sequence similarity. The term viroporin arose from the initial observation that, during infection of host cells by viruses, there were specific times during which infected cells became permeable to translation inhibitors (Carrasco, 1978). The search for viral products involved in this process led to the discovery that the poliovirus 2B protein is capable of inducing membrane permeability in an *E. coli* expression system (Aldabe et al., 1996). Many virus families encode proteins similar to poliovirus 2B in both features and functions (Antoine et al., 2007; Bodelon et al., 2002; Daniels et al., 2006; Han and Harty, 2004; Madan et al., 2005; Madan et al., 2007; Nieva et al., 2003). Most of the studies of viroporins investigate the biochemical basis of their permeabilizing ability. Aromatic amino acids in or near a hydrophobic domain, stretches of basic amino acids,

32

and the formation of homo-oligomers can all contribute to the permeabilizing activity of the viroporins (Agirre et al., 2002; Sanz et al., 2003).

Non-enveloped DNA virus progeny egress

Non-enveloped DNA viruses replicate and assemble in the host cell nucleus. Therefore, progeny virions must pass the nuclear envelope as well as the plasma membrane to exit cells. A long-held assumption is that non-enveloped DNA viruses exit host cells through a non-specific lytic mechanism. However, recent studies have revealed a more controlled process of non-enveloped DNA virus egress. Besides species C HAdV E3-11.6K/ADP, several other proteins expressed by non-enveloped DNA viruses play a role in progeny virus egress. Two members of the Family *Polyomaviridae* (circular double-stranded DNA genome), JC virus and simian virus 40 (SV40), encode proteins that promote virion release. For JC virus, a small hydrophobic protein called agnoprotein contributes to virion release, and is proposed as a viroporin (Suzuki et al., 2010). Agnoprotein promotes virion release, possibly through changes in membrane permeability and alterations of intracellular Ca^{2+} homeostasis (Suzuki et al., 2010). In the closely related SV40, a viral structural protein, VP3, is implicated in progeny virion release and is also proposed as a viroporin (Daniels et al., 2006). Further studies are necessary to fully elucidate the mechanism of action of these proteins. But these limited investigations suggest a dynamic and controlled process for non-enveloped DNA virus progeny release.

Most of what is known about the molecular biology of HAdV is based on extensive studies of species C HAdV serotypes 2 and 5. Although subspecies B1 HAdVs are important causes of severe respiratory disease in pediatric and military populations, studies of their molecular biology have been neglected. Fundamental features of the viral replication cycle are likely conserved among the HAdVs, but unique features of the subspecies B1 HAdV genomes could contribute to their distinct pathogenesis. For this reason, targeted studies of unique subspecies B1 HAdV genes and molecular biology are justified. Because of its proposed role in virus-host interactions and its extensive diversity among HAdV, the E3 transcription unit is a logical choice for initial examination of changes in this region and the impact of these changes on viral pathogenesis.

Questions also remain regarding the genome type shifts that occur over time. Beyond observations that these genome type shifts occur, little work has been done to understand the basis of the apparent increased severity of disease associated with these shifts. A viral genomic basis for this phenomenon is likely, so understanding subspecies B1 HAdV genetic diversity and its implications for viral fitness and virulence is important. The unique genomic features of subspecies B1 HAdV that emerge as predominant circulating genome types must be investigated to begin to understand how genetic changes impact viral virulence and fitness.

Gaps also remain in our understanding of the late stages of non-enveloped DNA virus replication cycles. My work addresses this in Chapter 6. Enveloped virus budding is relatively well characterized, but a similar effort has not been put forth to understand the mechanisms by which non-enveloped viruses egress from infected cells. This lack of

attention is likely to the result of the well-accepted assumption that most non-enveloped viruses, including adenoviruses, simply lyse cells at the end of infection through an uncontrolled mechanism. However, studies of species C HAdV E3-11.6K/ADP and putative viroporins expressed by polyomaviruses suggest a more controlled mechanism for non-enveloped virus egress. The late stage of the non-enveloped virus replication cycle is a relatively unexplored area of virology. A better understanding of non-enveloped virus egress could lead to new strategies for the development of antivirals.

Finally, the ORF E3-10.9K polymorphism appears to represent a unique case of extensive intraserotypic diversity of an E3 ORF. Questions remain such as: What is the function of ORF E3-10.9K-encoded polypeptides? What is the impact of the polymorphism for the virus life-cycle? What selective pressures might be driving the evolution of this ORF? What is the impact of the polymorphism for virus fitness and virulence? The work described hereafter was undertaken to begin to answer these questions, to drive the field of adenovirology beyond a focus on species C HAdVs, and to uncover important information regarding the impact of genetic variation among subspecies B1 HAdVs for virus fitness and virulence.

Chapter 3: Materials and Methods

<u>Cells, media, and growth conditions</u>

A549 cells (ATCC #CCL-185) were grown in 8% (v/v) newborn calf serum-supplemented Eagle Minimum Essential Medium (EMEM) (A549 Growth Medium). Infected cells were maintained in 2% (v/v) newborn calf serum-supplemented EMEM (A549 Infection Medium). HeLa T-REx™ cells (Invitrogen, Carlsbad, CA) were grown according to manufacturer's instructions in 10% (v/v) fetal bovine serum-supplemented EMEM and 5 μg/mL blasticidin (HeLa T-REx™ Growth Medium). HeLa T-REx™ cells stably transfected with 4/TO enhanced green fluorescent protein (EGFP) expression plasmids were maintained in HeLa T-REx™ Growth Medium supplemented with 100 μg/mL zeocin (HeLa T-REx™ Selection Medium), and expression of fusion proteins was induced with HeLa T-REx™ Selection Medium supplemented with 1 μg/mL tetracycline (HeLa T-REx™ Induction Medium). Cells were grown at 37°C with 5% CO_2.

<u>Viruses, stocks, infections, and viral DNA</u>

Viruses used for this study included the prototype strains of serotypes 3, (strain GB; Rowe et al., 1953), 7 (strain Gomen; Berge et al, 1955), and 16, (strain Ch.79; Murray et al., 1957), and HAdV-7 field strains KCH4 (Wadell et al., 1980), Argentina 87-922 (Kajon et al., 1996), and NHRC 611 (courtesy of Department of Respiratory Diseases Research, Naval Health Research Center). These viruses represent genome types 3p, 7p, 16p 7b, 7h and 7d2, respectively, which encode orthologs of ORF E3-10.9K

36

(Kajon et al., 2005). Virus stocks were grown in A549 cells, harvested by three freeze-thaw cycles and clarified of cell debris by centrifugation at 300 x G. Infectious virus titers were determined by standard plaque assay on A549 cell monolayers under an agarose/medium overlay. AdV infections of A549 cell monolayers were carried out at a multiplicity of infection (MOI) of 1, 5 or 10 plaque forming units (PFU) per cell. Cell medium was aspirated, viral inoculum was added, and flasks were incubated at 37°C with 5% CO_2 for 1 hour with periodic rocking. For experiments requiring the inhibition of viral DNA replication, medium was replenished with A549 Infection Medium containing 40 μg/mL Cytosine β-D-arabinofuranoside hydrochloride (Ara-C) (Sigma, St. Louis, MO). Inhibition of viral DNA replication was maintained by supplementing infection medium with an additional 40 μg/mL of Ara-C at 8, 24, and 36 h pi.

Intracellular viral DNA was isolated from infected cell monolayers by an established method (Kajon and Erdman, 2007).

Bacterial strains

Bacterial strains JM109 (Promega, Madison, WI) and TOP10 (Invitrogen, Carlsbad, CA) were used for routine molecular cloning. ECOS-21 cells (Yeastern Biotech Co., Taiwan) were used for expression of GST-tagged fusion proteins. BW25113 (Datsenko and Wanner, 2000) and SW105 (Warming et al., 2005) strains were obtained from Dr. Katherine Spindler (University of Michigan) and were used for recombination-based mutagenesis of the HAdV-3p genome.

Antibodies

Antibodies used in immunofluorescence microscopy, Western blot analysis, and immunoprecipitations included mouse anti-HA (MMS-101R, Covance, Princeton, NJ), mouse anti-EGFP (JL-8, Clontech, Mountain View, CA), mouse anti-calnexin (Ab2798, Abcam, Cambridge, MA), mouse anti-Golgin97 (A21270, Molecular Probes, Carlsbad, CA), mouse anti-58K Golgi protein (Ab6284, Abcam, Cambridge, MA), rabbit anti-HA conjugated agarose beads (Ab27029, Abcam, Cambridge, MA), goat anti-GST (27457701, GE Healthcare Biosciences, Pittsburgh, PA), HRP-conjugated rabbit anti-goat (305-035-003, Jackson ImmunoResearch, West Grove, PA) and HRP-conjugated goat anti-mouse (115-035-003, Jackson ImmunoResearch, West Grove, PA).

DNA sequencing and alignment software

DNA sequences were generated at the DNA Research Services core facility, University of New Mexico. Sequences were analyzed using Lasergene version 7.0.0 (DNASTAR, Inc., Madison, WI).

Protein structural predictions

Hydrophobicity plots were generated using the Kyte-Doolittle algorithm implemented in Protean software (Lasergene version 7.0.0, DNASTAR, Inc., Madison, WI). N-glycosylation and O-glycosylation sites were predicted using the web-based NetNGlyc 1.0 (http://www.cbs.dtu.dk/services/NetNGlyc/) and NetOGlyc 3.1 (http://www.cbs.dtu.dk/services/NetOGlyc/) (Julenius et al., 2005). Protein topology was

predicted using the web-based TopPred prediction program (http://mobyle.pasteur.fr/cgi-bin/portal.py?form=toppred) (Claros and von Heijne, 1994; von Heijne, 1992).

Molecular cloning of ORF E3-10.9K orthologs for mammalian and bacterial expression

Viral DNA was used as template for PCR-based mutagenesis of ORF E3-10.9K. Primers used are listed in Table 3. For the the ORF E3-10.9K orthologs encoding the 7.7 kDa, 9 kDa, and 10.9 kDa proteins, first round PCR to amplify ORF E3-10.9K was conducted using Hashido forward and Hashido reverse primers (Hashido et al., 1999) (Table 3). A second round of PCR was conducted to add a Kozak consensus sequence,

Table 3. Molecular cloning primers

Mammalian Expression Plasmid Cloning Primers	
Hashido forward	5'-CAAAAAGGTGATGCATTACC-3'
Hashido reverse	5'-TGTTCACCATACTGTAAGA-3'
10.9K up Kozak HindIII	5'-TTATAAGCTTGCCGCCACCATGATATTGTTTC-3'
7.7K down BamHI EGFP	5'-CGGACGGATCCTCATAGGAG-3'
10.9K/9K BamHI EGFP	5'-CATGAGGATCCTTGATTTCATTCAG-3'
4.8K up	5'-TTATAAGCTTATGATATTGTTTC-3'
4.8K down	5'- TTATAAGCTTATGATATTGTTTC-3'

Bacterial Expression Plasmid Cloning Primers	
HAdV-16p/7p/7b up	5'-TTATAAGCTTATGATATTGTTTC-3'
HAdV-16p/3p down	5'-AGGATCCTTGATTTCATTCAG-3'
HAdV-7p down	5'-GGACGGATCCTCATAGG-3'
HAdV-7b down	5'- TTATAAGCTTATGATATTGTTTC-3'

upstream *Hind*III and downstream *Bam*HI restriction endonuclease recognition sequences, and to mutate the stop codon using the following primers: 10.9K up Kozak *Hind*III, 7.7K down *Bam*HI EGFP, and 10.9K/9K BamHI EGFP (Table 3). High fidelity PCR was carried out using iProof High Fidelity DNA Polymerase (Promega, Madison, WI) following the manufacturer's recommended cycling conditions. Second round PCR products were purified using Micropure EZ columns (Millipore, Bedford, MA) and Microcon columns (Millipore, Bedford, MA) following the manufacturer's recommended protocol, digested with *Bam*HI and *Hind*III, and cloned into pEGFP-NI vector (Clontech, Mountain View, CA).

For cloning of the ORF E3-10.9K ortholog encoding the 4.8 kDa protein, first round PCR was performed using the primers 4.8K up and 4.8K down to mutate the stop codon and generate downstream *Bam*HI and upstream *Hind*III restriction endonuclease recognition sites (Table 3). High fidelity PCR was carried out using iProof High Fidelity DNA Polymerase (Promega, Madison, WI) following the manufacturer's recommended cycling procedure. The PCR product was purified using Micropure EZ columns (Millipore, Bedford, MA) and Microcon columns (Millipore, Bedford, MA), and cloned into intermediate cloning vector pCR2.1 TOPO TA (Invitrogen, Carlsbad, CA) according to the manufacturer's recommendations. Positive bacteria colonies were identified by colony-based PCR and plasmid DNA was isolated using GenElute Plasmid Prep kit (Sigma, St. Louis, MO). The ORF encoding 4.8 kDa was then subcloned into pEGFP-N1 vector (Clontech, Mountain View, CA) using *Bam*HI and *Hind*III sites.

Finally, EGFP-tagged ORF E3-10.9K orthologous genes were cloned into pCDNA 4/TO vector (Invitrogen, Carlsbad, CA) using convenient *Hind*III and *Not*I

restriction endonuclease recognition sequences. Plasmids generated were referred to as pCDNA 4/TO 4.8 kDa-EGFP, pCDNA 4/TO 7.7 kDa-EGFP, pCDNA 4/TO 9 kDa-EGFP, and pCDNA 4/TO 10.9 kDa-EGFP.

For generation of bacterial expression constructs, the above procedures were carried out with the following changes. The primers used included HAdV-16p/7p/7b up, HAdV-16p/3p down, HAdV-7p down, and HAdV-7b down (Table 3). Primers introduced mutations to eliminate the start codon and add upstream *Bam*HI and downstream *Sal*I restriction endonuclease sites for subsequent cloning. Subcloning of the mutated inserts into pGEX-5X-1 (Amersham Biosciences, Piscataway, NJ) bacterial expression vector was accomplished by digestion with *Bam*HI and *Sal*I. Bacterial expression constructs were maintained in JM109 *E. coli* (Promega, Madison, WI) and transformed into ECOS-21 *E. coli* (Yeastern Biotech Co., Taiwan) for inducible expression experiments. Plasmids generated were referred to as pGEX-4.8K, pGEX-7.7K, pGEX-9K, and pGEX-10.9K.

All constructs were confirmed by sequencing at the DNA Research Services core facility, University of New Mexico.

RNA isolation

A549 cells were infected with subspecies B1 HAdVs encoding various ORF E3-10.9K orthologs (Table 4) at a MOI of 5 PFU/cell. At 8 and 24 h pi, total RNA was extracted using the RNaqueous kit (Ambion, Austin, TX) following manufacturer's instructions. RNA was treated with TURBO DNA-free kit (Ambion, Austin, TX) to

remove contaminating DNA. Elimination of DNA was confirmed by absence of visible

bands by PCR using total RNA as template (data not shown).

Table 4. Subspecies B1 HAdVs and the size of the protein encoded by their associated ORF E3-10.9K orthologs

Virus	Size of protein encoded by ORF E3-10.9K ortholog
HAdV-16p strain Ch. 79	10.9 kDa
HAdV-3p strain GB	9 kDa
HAdV-7p strain Gomen	7.7 kDa
HAdV-7d2 strain NHRC 611	4.8 kDa
HAdV-7b strain KCH4	4.8 kDa
HAdV-7h strain Argentina 87-922	NULL

RT-PCR

RNA (1 µg) and random decamers were used to generate cDNA using the

RETROscript kit (Ambion, Austin, TX) in a 20 µL total volume following the

manufacturer's recommended protocol. The cDNA product (1 µL) was amplified by

PCR in a total volume of 50 µL of PCR mix including 1X GoTaq Buffer, 1 unit of GoTaq

polymerase, 0.2 mM dNTPs, 1.5 mM $MgCl_2$, and 25 pmol of each primer (Promega,

Madison, WI). The primers used for RT-PCR are described in Table 5. The reactions

were heated to 95˚C for 5 min for the initial denaturation step followed by 34 cycles of

the following: 94˚C for 30 sec, annealing temperature for 30 sec, and 72˚C for 30 sec.

Annealing temperature used for each primer pair was 2˚C lower than the lowest Tm for

the primer pair (Table 5). Cycling was followed by a final extension at 72˚C for 7 min at

the end of which the reaction was kept at 4˚C until analysis. PCR products were analyzed by agarose gel electrophoresis in Tris-Borate-EDTA buffer. PCR products were visualized after ethidium bromide staining with a Universal Hood II/Gel Doc XR Camera and Quantity One software (Bio-Rad, Hercules, CA).

Cloning and sequencing of RT-PCR MLP products

RT-PCR products of interest were gel purified and cloned using the pCR2.1 TOPO TA cloning kit (Invitrogen, Carlsbad, CA). Products were sequenced at the DNA Research Services core facility, University of New Mexico. Consensus sequences for each product were deposited in Genbank (Accession numbers: GU951413-GU951425).

Membrane fractionation

A549 cells were infected at a MOI of 10 PFU/cell. At 48 h pi, cells were washed twice in 1X PBS and 1 mL hypotonic buffer (40 mM HEPES, 4 mM EDTA, 4 mM EGTA, 10 mM DTT, 1 mM sodium vanadate, 1 mM PMSF, complete mini protease inhibitor cocktail (Roche, Basel, Switzerland)) was added. Cells were scraped from the dish, transferred to 1.5 mL tube and incubated on ice for 30 min. After incubation, samples were sonicated 3 times for 2 sec pulses and centrifuged at 100,000 x G for 1 hour at 4°C in a swinging bucket rotor ultracentrifuge. After centrifugation, the supernatant (cytosolic fraction) was collected, the pellet was resuspended in 1 mL of 1 X lysis buffer

Table 5. Primers for RT-PCR

Primer name	Sequence (5'-3')	Tm (°C)	Nucleotide position[1]	Corresponding gene/coding region
E3-10.9K forward	GTTTCAATCAAATACC	43.9	29796-29811	E3-9 kDa glycoprotein
E3-10.9K reverse	CTAATCATAGGAGAATAG	42.5	29973-29990	E3-9 kDa glycoprotein
E3-10.9K reverse Tm60	GGGACGACTAATCATAGGAGAATAG	61.8	29973-29997	E3-9 kDa glycoprotein
TPL3 forward	CAGTCGCAATCGCAAG	60.3	9548-9563	Tripartite leader 3
Hexon reverse	GGTCTGTTAGGCATGGC	59.1	19353-19369	L3/Hexon protein
RIG/s15 forward	TTCCGCAAGTTCACCTACC	62.6	N/A	Small ribosomal subunit rig/S15[2]
RIG/s15 reverse	CGGGCCGGCCATGCTTTACG	76.9	N/A	Small ribosomal subunit rig/S15[2]

[1]with reference to HAdV-3p strain GB full genome sequence (Genbank accession #AY599834)

[2]see reference (Kitagawa, 1991)

(20 mM Tris-HCl [pH 8], 137 mM NaCl, 1 mM EGTA, 1% TritonX-100, 10% glycerol, 1.5 mM MgCl$_2$, 1 mM sodium vanadate, 50 mM NaF, complete mini protease inhibitor cocktail (Roche, Basel, Switzerland)), and the debris was removed by centrifugation for 15 min at 16,000 x G. The supernatant (membrane fraction) was collected. Samples were analyzed for total protein content by a standard Bradford assay (Bradford, 1976).

Protein extraction and glycosidase treatment

At the time of harvest, cells in 100 mm culture dishes were washed twice with ice-cold PBS and incubated on ice with RIPA buffer (50 mM Tris-HCl [pH 8], 150 mM NaCl, 1% NP-40, 0.5% sodium deoxycholate) containing protease inhibitor cocktail (complete Mini, Roche, Basel, Switzerland) for 5 min. Cell lysates were collected and clarified by centrifugation at 16,000 x G for 15 min to remove cellular debris. The supernatants were analyzed for total protein content by a standard Bradford assay (Bradford, 1976).

Aliquots of transfected cell lysates containing 40 μg of total protein or the digestion control fetuin were digested using reagents included in the Enzymatic Protein Deglycosylation Kit (Sigma, St. Louis, MO). All digestions were carried out at 37°C. For digestion with PNGase, 1 μL of enzyme was added to the reaction mixture as indicated in the manufacturer's instructions and incubated for 3 h. For digestion with O-glycosidase and neuraminidase, 1 μL of neuraminidase was first added to the reaction mixture and incubated for 3 h, and then O-glycosidase was added and incubated for an additional 3 h. For digestion with all three glycosidases, the sequence of enzyme addition was PNGase, neuraminidase, and O-glycosidase. After addition of each enzyme, reaction

45

mixtures were incubated for 3 h. Samples (10.4 µL) were separated under reducing conditions in MOPS running buffer using NuPAGE 12% polyacrylamide Bis-Tris gels (Invitrogen, Carlsbad, CA) following the manufacturer's instructions and electrophoretically transferred to PVDF membranes as described below (Invitrogen, Carlsbad, CA).

Immunoprecipitations

Rabbit anti-HA conjugated beads (15 µL) (Abcam, Cambridge, MA) were added to an aliquot of cell lysate containing 1 mg of total protein, further diluted to 500 µL with RIPA buffer containing protease inhibitor cocktail (Roche, Basel, Switzerland), and incubated overnight at 4˚C with rotation. Beads were collected at 500 X G for 30 sec and washed 3 times for 5 min in cold RIPA buffer with protease inhibitor cocktail (Roche, Basel, Switzerland). Bound protein was then eluted in 60 µL of sample buffer with reducing agent by heating at 70˚C for 10 min. Samples (15 µL) were separated under reducing conditions in MES running buffer using NuPAGE 12% polyacrylamide Bis-Tris gels (Invitrogen, Carlsbad, CA) following manufacturer's instructions and electrophoretically transferred onto PVDF membranes for analysis as described below.

Western blot

Protein samples were transferred from polyacrylamide gels to PVDF membranes (Bio-Rad, Hercules, CA) for 35 min at 100 volts in transfer buffer containing 50 mM Tris-base, 380 mM glycine, 0.1% SDS, and 20% methanol. The membrane was blocked with 5% (w/v) non-fat dry milk in 0.1% (v/v) Tween-20 TBS (blocking buffer) for 1 h at

room temperature. The primary antibody was diluted 1:1000 in blocking buffer and incubated with the membrane overnight at 4˚C with rocking. After washing in 0.1% (v/v) Tween-20 TBS (TBS-T), the membrane was incubated with peroxidase-conjugated AffiniPure goat anti-mouse IgG (H+L) (Jackson ImmunoResearch) diluted 1:100,000 in blocking buffer for 1 h at room temperature. After washing, the membrane was treated with Western Lightning Chemiluminescence Reagent Plus (PerkinElmer Life Sciences, Waltham, MA) according to manufacturer's instructions and exposed to blue X-ray film. For Western blot analysis of membrane fractionation experiments, the PVDF membrane was treated with SuperSignal West Femto Maximum Sensitivity Substrate (Thermo Scientific, Rockford, IL).

Immunofluorescence microscopy

Transfected cells grown on coverslips were washed three times in PBS and fixed in 4% (w/v) paraformaldehyde in PBS for 15 min at room temperature at 24 h post-induction with tetracycline. Fixation was quenched by washing with 100 mM glycine PBS 3 times for 5 min. Cells were permeabilized by treatment with 0.2% (v/v) Triton X-100 in PBS for 2 min at room temperature. Coverslips were washed 3 times in PBS and blocked for 1 h with 10% (v/v) goat or donkey serum in 0.1% (v/v) Tween-20 PBS (PBS-T) at room temperature with rocking. Between blocking, primary, and secondary incubations, coverslips were washed three times in PBS-T. After secondary antibody incubation in the dark, coverslips were washed three times in PBS-T and three times in PBS. Coverslips were briefly submerged in ddH$_2$O to remove excess salt and mounted in Slowfade Gold with DAPI (Molecular Probes, Carlsbad, CA) on glass slides. For

staining with wheat germ agglutinin Alexa Fluor 647 conjugate (WGA-647) (Molecular Probes, Carlsbad, CA), transfected cells on coverslips were rinsed 3 times in PBS and incubated for 10 min at 37˚C with 200 µL of 5 µg/mL of WGA-647 in PBS. Cells were then fixed, quenched, and mounted as indicated above.

Images were generated with a Zeiss epifluorescence Axioskop with Hamamatsu Digital camera controlled with SlideBook Image Analysis software version 4.0 (Intelligent Imaging Innovations, Denver, CO). Images were deconvolved using the nearest neighbor algorithm contained within the SlideBook software and figures were prepared using Adobe Photoshop CS3, version 10.0.1 (Adobe Systems Inc., San Jose, CA).

Propidium iodide permeability of *E. coli*

ECOS-21 bacteria transformed with pGEX-5x-1 plasmid constructs were grown overnight at 37ºC with moderate shaking in 2xYT broth (Amresco, Solon, Ohio) supplemented with 100 μg/ml ampicillin and 1% (w/v) glucose (2xYTAG). Cultures were diluted 1:20 into 2xYTAG and incubated at 37ºC with moderate shaking. When the OD600 reading reached 0.5, cultures were induced with 1.0 mM IPTG. Samples for Western blot analysis and propidium iodide staining were taken at 0 and 3 h post induction.

Samples of induced cultures (80 µL) were pelleted at max speed for 1 minute and washed once in PBS. Propidium iodide in PBS (500 µL of 10 μg/ml) was added to bacteria and incubated at 37ºC in the dark for 10 min. Cells were subsequently washed 2 times in PBS and suspended in an appropriate volume of PBS for analysis on a

FACScalibur flow cytometer (Becton Dickenson Biosciences, San Jose, CA). The bacterial cell population was gated and signals from 10,000 events were collected.

Samples of induced cultures (750 μL) were pelleted at max speed for 1 min, supernatant was aspirated, and pellets were frozen at -20ºC. Pellets were resuspended in 200 μL B-PER reagent (Pierce, Rockford, IL) and vortexed for 1 min to lyse cells. Lysates (10 μL) were boiled for 5 min with 20 μL Laemmli buffer, loaded in 10% Tris-Glycine SDS-PAGE gels and transferred to PVDF membranes as indicated above.

Permeability of HeLa T-REx^{TM} cells to trypan blue

HeLa T-REx^{TM} cells were plated at approximately 50% confluency in 6-well culture plates. One day post-plating, medium was aspirated and replaced with either HeLa T-REx^{TM} Induction Medium (induced) or HeLa T-REx^{TM} Selection Medium (uninduced). At 48 h post induction, medium was collected and cells were trypsinized. Medium and cells were pooled and stained with an equal volume of 0.4% Trypan Blue solution (Sigma, St. Louis, MO). Cells (~200) were counted with a light microscope and a hemocytometer. Percent cell viability was determined by dividing the number of unstained cells by the total number of cells counted and multiplying by 100.

Construction of HAdV-3p mutant viruses

A schematic of the strategy to generate HAdV-3p mutant viruses is presented in Figure 5. The highly efficient bacteriophage λ *Red* recombination system (Poteete, 2001) was used to generate HAdV-3p clones encoding a C-terminus HA epitope-tagged version of ORF E3-10.9K (HAdV-3p-9K-HA), ORF E3-10.9K from HAdV-7h strain Argentina

49

87-922 (HAdV-3p-NULL), ORF E3-10.9K with all in-frame ATG codons mutated to TAG stop codons (HAdV-3p-KO), and a recombination control (HAdV-3p-9K).

The bacmid pKSB2Ad3wt, harboring the full-length genome of HAdV-3 prototype strain GB, was a kind gift of Dr. Silvio Hemmi (Sirena et al., 2005). Dr. Samuel Campos (University of Arizona) generated a shuttle plasmid, pE3-9K, to facilitate modification of ORF E3-10.9K within pKSB2Ad3wt. The pE3-9K shuttle (Fig. 5A) was constructed by PCR cloning a C-terminal fragment of ORF E3-20.5K into the *Hind*III/*Bam*HI sites of plasmid pFZF (Campos and Barry, 2004), just upstream of the zeocin resistance gene flanked by <u>F</u>lp <u>r</u>ecognition <u>t</u>arget (FRT) sites. A *Sal*I site was included just upstream of the *Bam*HI site in the primer design. Next, the region just downstream of ORF E3-10.9K, containing ORFs E3-10.2K, E3-15.2K, and a fragment of ORF E3-15.3K was PCR-amplified from pKSB2Ad3wt and cloned into pFZF with *Nhe*I and *Not*I. The pE3-9K shuttle was designed in such a way that any gene of interest could be cloned into the *Sal*I/*Bam*HI sites to replace ORF E3-10.9K of pKSB2Ad3wt upon recombination.

ORF E3-10.9K was either replaced with a C-terminus HA-tagged version of ORF E3-10.9K or the ORF E3-10.9K ortholog encoded by HAdV-7h strain Argentina 87-922, designated E3-NULL, by cloning into pE3-9K shuttle using the *Sal*I/*Bam*HI sites. Alternatively, the pE3-9K shuttle plasmid was subjected to site-directed mutagenesis to mutate all ORF E3-10.9K's in-frame ATG codons to TAG stop codons. The altered pE3-9K shuttle plasmids were then linearized with *Hind*III and *Pvu*I. The purified linear fragment was then transformed by electroporation into *E. coli* strain BW25113, harboring the pKSB2Ad3wt bacmid and the temperature sensitive replicon pKD46, which

expressed the λ *Red* genes under the arabinose-inducible pBAD promoter (Datsenko and

Wanner, 2000). Electroporation was performed in a 0.2 cm gap cuvette with a

micropulser (Biorad) set to 2500 V. Electroporated cells were resuspended in SOC +

0.5% L-arabinose and incubated overnight at room temperature. Induction of the λ *Red*

genes resulted in recombination between the linear pE3-9K fragment and the HAdV-3p
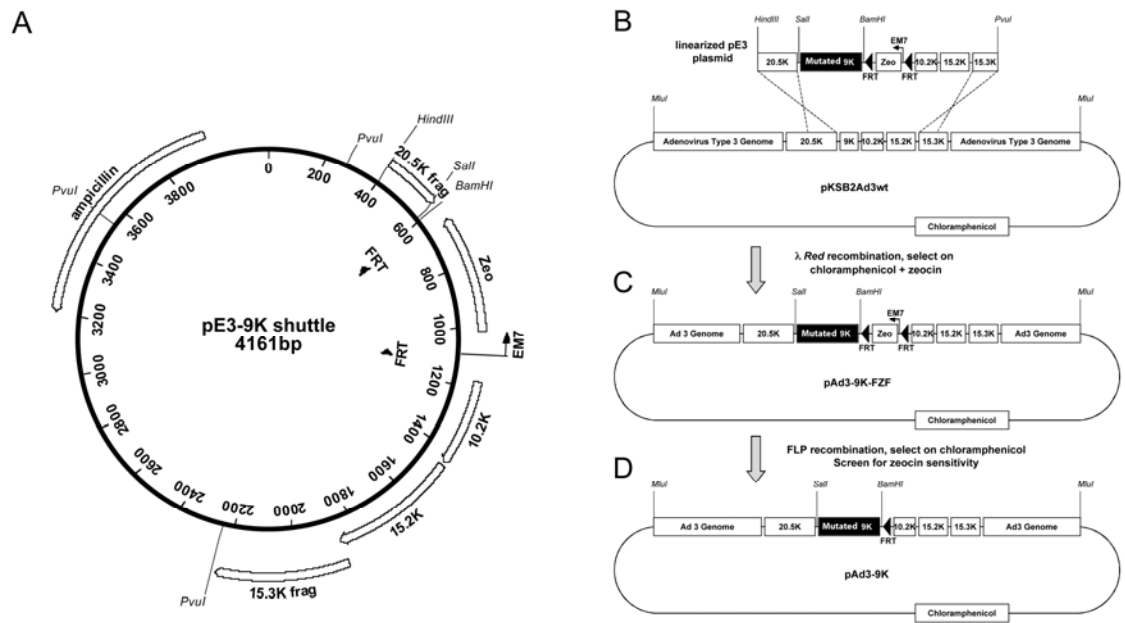
Figure 5. ORF E3-9K shuttle plasmid and recombination strategy. (A) Map of the pE3-9K shuttle plasmid with unique restriction sites. Sequences cloned into the *Sal*I and *Bam*HI sites replace ORF E3-9K of the HAdV-3p genomic bacmid upon recombination. (B) Transformation of the linearized shuttle plasmid containing the desired ORF E3-10.9K mutations into λ *Red* recombination *E. coli* strain BW25113, containing the HAdV-3p genomic bacmid results in recombination across homologous regions. (C) Recombinant bacmids are selected by growth under chloramphenicol and zeocin selection. (D) Transformation of this recombinant into *E. coli* strain SW105 causes collapse across the FRT sites and deletion of the zeocin resistance cassette to generate final pAd3-9K bacmids.

bacmid. Recombinant pAd3-9K- FZF clones were selected by plating at 37°C on 15 μg/mL chloramphenicol and 25 μg/mL zeocin (Fig. 5B, C). Recombinant pAd3-9K-FZF bacmids were then purified and electroporated into *E. coli* strain SW105 (Warming et al., 2005), which expressed *Flp* recombinase under arabinose control. Incubation overnight at room temperature in SOC + 0.5% L-arabinose induced *Flp* recombinase expression, which collapsed the FZF cassette into a single 34 bp FRT site. Transformed cells were plated at 30°C on chloramphenicol (15 μg/mL). Several colonies were picked and screened for sensitivity to zeocin, as proper *Flp* recombination resulted in loss of zeocin resistance (Fig. 5D). Final pAd3-9K clones were screened by restriction digestion and sequenced to confirm the presence of the desired mutations to ORF E3-10.9K. The recombination described above ultimately resulted in a new *Sal*I site between ORF E3-20.5K and ORF E3-9K as well as a *Bam*HI site, the 34 bp FRT scar site, and an *Nhe*I site between ORF E3-10.9K and ORF E3-10.2K in the E3 transcription unit (Fig. 5D). A recombinant pAd3-9Kwt containing the unmodified wild type ORF E3-9K was also constructed to control for the introduction of these additional elements into the HAdV-3p genome.

DNA from pAd3-9K mutant bacmids and pKSB3Ad3wt were digested with *Mlu*I to release the viral genomic DNA. This digest was then transfected into A549 cells using Effectene Reagent (Qiagen, Valencia, CA). Two μg digested bacmid DNA were used per transfection. Transfected cells were incubated for 14 days. For virus recovery, cells were subjected to 3 freeze-thaw cycles at -80˚C and 25˚C, and clarified by centrifugation. The resultant virus was propagated by passage in A549 cells, and presence of virus was confirmed by observation of characteristic AdV cytopathic effect (CPE). Titered stocks

of HAdV-3p mutant viruses and HAdV-3p-WT virus were generated as indicated above. The identities of the mutant viruses were confirmed by sequencing of the E3 transcription unit and restriction enzyme analysis with *Bam*HI and *Sal*I (data not shown).

Ara-C inhibition of viral DNA replication

A549 cells were infected at a MOI of 10 PFU/cell and incubated in Ara-C supplemented A549 Infection Medium as indicated above. At 8 at 48 h pi, cell lysates were harvested in RIPA buffer and protein content was determined by a standard Bradford assay (Bradford, 1976).

Dissemination assay

A549 cells were plated on 24-well culture plates and infected at a MOI of 1, 0.1, or 0.01 PFU/cell for each virus. Infected cells were incubated for 5 days, medium was aspirated, and cells were fixed in 1% formaldehyde and stained with Accustain crystal violet solution (Sigma-Aldrich).

Plaque size assay

A549 cells were plated on 6-well culture plates, infected with approximately 20 PFU per well, and replenished with a semi-solid agarose/medium overlay. Plates were incubated for 13 days and then fixed in 1% formaldehyde and stained with Accustain crystal violet solution (Sigma-Aldrich).

Virus egress assay

A549 cells were infected at a MOI of 10 PFU/cell. After 1 h adsorption at 37˚C, cells were washed 3 times in PBS to remove excess extracellular virus. At 6, 12, 24, 36, 48, 72, 96, and 120 h pi, extracellular and total virus was harvested. For total virus samples, infected cells and supernatant were collected and freeze-thawed 3 times at -80˚C and room temperature. Samples were centrifuged at 300 x G for 5 min to remove cellular debris, and supernatant was collected. For extracellular virus samples, supernatant from infected cells was collected and transferred to a 5 mL round-bottom culture tube. Cells and debris were removed by centrifuging at 300 x G for 5 min, and supernatant was collected. Infectious virus in samples was determined by plaque assay on A549 cells.

Infected cell viability assay

A549 cells were infected at a MOI of 10 PFU/cell. At 24, 48, 72, 96, and 120 h pi, medium was collected from cells and transferred to a tube. Cells were trypsinized and pooled with medium. Pooled samples were mixed with an equal volume of 0.4% Trypan Blue solution (Sigma, St. Louis, MO) and ~200 cells were counted using a light microscope and a hemocytometer. The percent of viable cells was calculated by dividing the number of unstained cells by the total number of cells counted and multiplying by 100.

Live cell microscopy

A reflected fluorescence microscope (CKX41, Olympus) with an attached Infinity 2-3C digital camera (Lumenera) was used to capture images of CPE and live cell fluorescence.

Chapter 4: Results--Biochemical characterization of ORF E3-10.9K

ORF E3-10.9K previously showed a marked genetic polymorphism among subspecies B1 HAdV lab strains and field isolates (Kajon et al., 2005). No biochemical or functional studies of ORF E3-10.9K-encoded protein products have been carried out to date. To elucidate the functional role(s) of ORF E3-10.9K during the HAdV life-cycle, we carried out an initial characterization of several predicted ORF E3-10.9K-encoded protein orthologs using bioinformatics sequence-based protein prediction tools, RT-PCR detection of transcripts during infection with subspecies B1 HAdVs, and fluorescence microscopy to investigate the subcellular localization of ectopically expressed proteins.

Predicted structural features of ORF E3-10.9K-encoded protein orthologs

Kyte-Doolittle hydrophobicity plots were generated and analyzed for several predicted ORF E3-10.9K-encoded protein orthologs encoded by subspecies B1 HAdV field isolates. A 19-amino-acid-long hydrophobic region predicted to be a transmembrane domain was identified in the backbones of the 7.7 kDa, 9 kDa, and 10.9 kDa orthologs (Fig. 6). A smaller protein ortholog, 4.8 kDa, did not contain this hydrophobic domain (Fig. 6). Protein topology predictions showed the C-terminus in a cytoplasmic orientation (C_{cyt}) for 10.9 kDa and 9 kDa protein orthologs and the N-terminus in the cytoplasmic orientation (N_{Cyt}) for the 7.7 kDa protein ortholog.
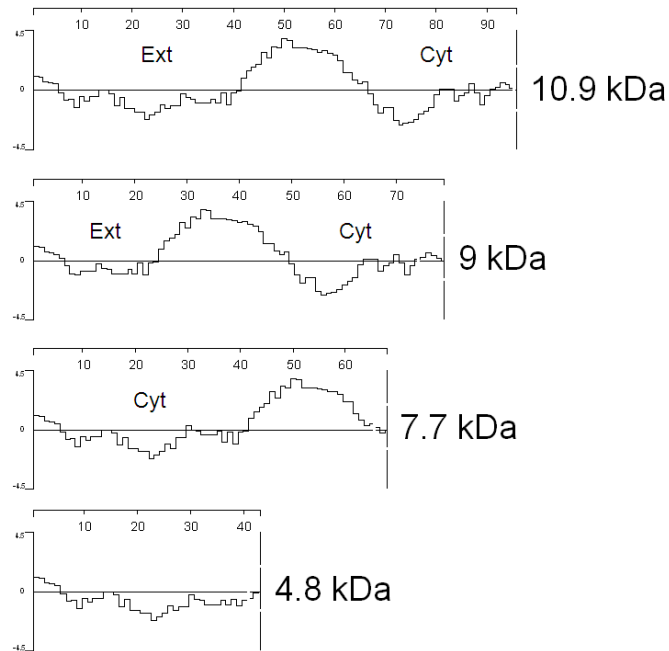
Figure 6. Kyte-Doolittle hydrophobicity plots of selected ORF E3-10.9K-encoded protein orthologs. Amino acid sequences of 4.8 kDa, 7.7 kDa, 9 kDa, and 10.9 kDa ORF E3-10.9K protein orthologs were analyzed using Protean and web-based TopPred software programs (see Chapter 3: Materials and Methods). Predicted protein topology is indicated by Cyt (cytoplasm) or Ext (extracellular/lumen). Positive values (above the center line) denote hydrophobic domains, negative values (below the center line) denote hydrophilic domains.

Species C HAdV E3-11.6K/ADP is post-translationally modified by N- and O-linked glycans (Scaria et al., 1992; Tollefson et al., 2003). In order to investigate if the ORF E3-10.9K protein orthologs were likely to be N- or O-glycosylated as well, we used a web-based glycosylation prediction tool to identify potential N- and O-linked glycosylation sites for the 4.8 kDa, 7.7 kDa, 9 kDa, and 10.9 kDa orthologs. These data suggested that the 4.8 kDa, 7.7 kDa, and 10.9 kDa orthologs contained two potential N-linked glycosylation sites, whereas the 9 kDa ortholog contained one potential N-linked glycosylation site (Fig. 7). No O-glycosylation sites were predicted for the any of the orthologs analyzed.

Another interesting predicted feature of ORF E3-10.9K-encoded protein orthologs was the presence of a region rich in basic amino acids (polybasic region). This polybasic region was present in the 9 kDa and 10.9 kDa orthologs, but was absent in the 7.7 kDa and 4.8 kDa orthologs (Fig. 7). Additionally, the 7.7 kDa, 9 kDa, and 10.9 kDa orthologs had aromatic amino acids in or near their hydrophobic domains (Fig. 7). Taken together, the presence of a polybasic region, aromatic residues in the hydrophobic domain of the ORF E3-10.9K-encoded proteins, and their small size suggest these proteins are membrane-active proteins similar to viroporins.


```
10.9 kDa MILFQSNTTN TINVQTTLNH DMENHTTSYA YTNIQPKYAM QLEITILIVI GILILSVILY FIFCRQIPNV HRNSKRRPIY SPMISRPHMA LNEI*
 9.0 kDa MILFQSNTT~ ~~~~~~~~~~ ~~~~~TSYA YTNIQPKYAM QLEITILIVI GILILSVILY FIFCRQIPNV HRNSKRRPIY SPMISRPHMA LNEI*
 7.7 kDa MILFQSNTTN TINVQTTLNH DMENHTTSYA YTNIQPKYAM HLKITILIVI GILILSVILY FLFSYD*
 4.8 kDa MILFQSNTTN TINVQTTLNH DMENHTTSYA YTNIQPKYAM Q*
   Null IILFQSNTTN TINVQTTLNH DMENHTTSYA YPMFIEILKD VPSILL*
```

— Hydrophobic domain
--- Polybasic region
* Predicted N-glycosylation sites

Figure 7. Predicted amino acid sequences of selected ORF E3-10.9K-encoded protein orthologs. Hydrophobic domain, polybasic region, and predicted N-glycosylation sites are indicated. Aromatic amino acids are indicated in bold. Adapted from Kajon et al., 2005.

Detection of ORF E3-10.9K-encoded protein in infected cells

Two independent attempts to raise anti-E3-10.9K rabbit antisera by immunizing with KLH-conjugated 15-mers representing the regions with the highest antigenic index for the detection of ORF E3-10.9K-encoded protein orthologs were unsuccessful. Rabbit antisera had high levels of cross-reactivity with viral and host proteins, and did not recognize an EGFP-tagged 10.9 kDa fusion protein by Western blot. As an alternative strategy, we generated a HAdV-3p mutant virus encoding the 9 kDa protein ortholog as a C-terminus HA-tagged polypeptide (HAdV-3p-9K-HA). A549 cells were infected at a

MOI of 10 PFU/cell and harvested at 48 h pi. Membrane and cytosolic fractions were isolated and detection of the 9 kDa-HA protein was carried out by immunoblot using an anti-HA antibody (Fig. 8). These data showed that the 9 kDa-HA protein was associated with the membrane fraction, as predicted by Kyte-Doolittle hydrophobicity plots (Fig. 6).
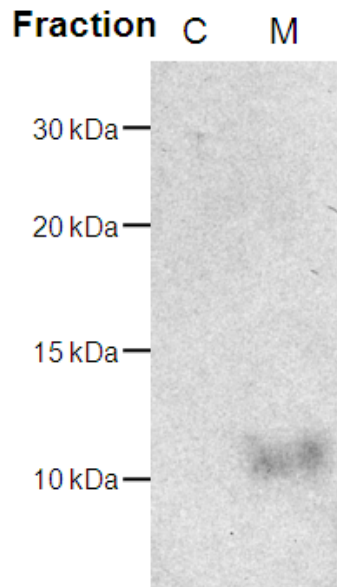
Figure 8. Western blot analysis of HA-tagged 9 kDa protein in cytosolic and membrane fractions of HAdV-3p-9K-HA infected A549 cells. A549 cells were infected at a MOI of 10 PFU/cell with HAdV-3p-9K-HA mutant virus and harvested at 48 h pi for membrane fractionation. Samples (10 μg) were separated under reducing conditions using NuPAGE 12% polyacrylamide Bis-Tris gels in MES running buffer and transferred to a PVDF membrane. The membrane was probed with a monoclonal mouse anti-HA antibody (primary) and a polyclonal HRP-conjugated goat anti-mouse antibody (secondary). C: cytosolic fraction, M: membrane fraction.

Expression from the adenovirus major late promoter

Species C HAdV E3-11.6K/ADP is expressed at late times pi from the AdV MLP (Tollefson et al., 1992). Because ORF E3-10.9K is located in the E3 transcription unit in an analogous region to ORF E3-11.6K/ADP, we hypothesized that ORF E3-10.9K would also be expressed from the MLP. To test this hypothesis, we infected A549 cells with

subspecies B1 HAdVs representing genomic variants encoding different protein orthologs. Total RNA was isolated at 8 and 24 h pi, and RT-PCR was carried out to detect ORF E3-10.9K transcripts (Fig. 9). For all viruses tested, we detected expression
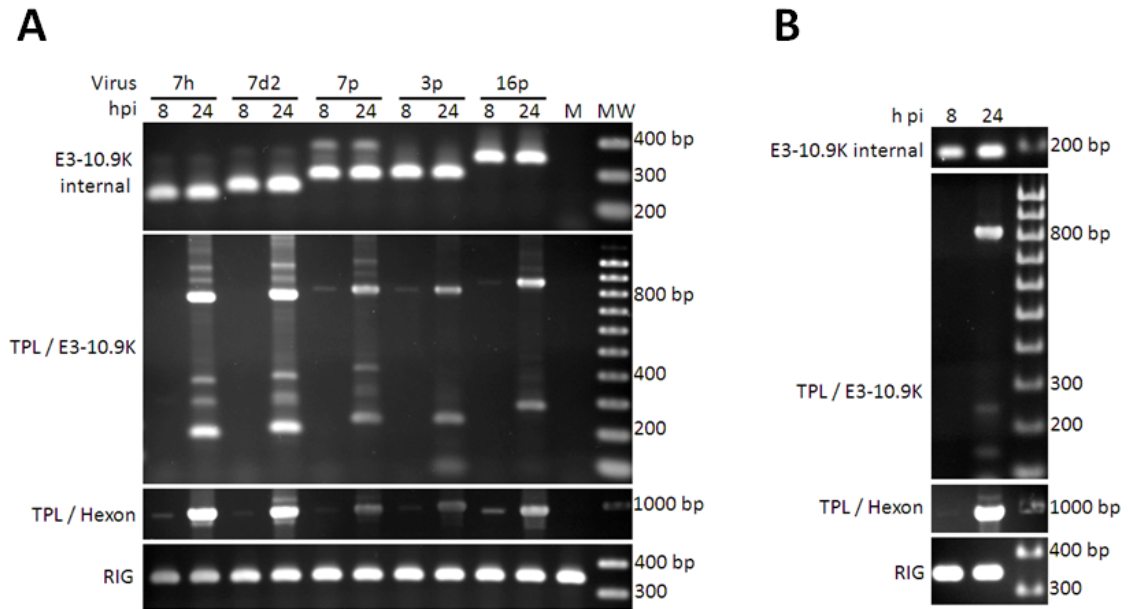
Figure 9. Expression of ORF E3-10.9K from the adenovirus major late promoter. A549 cells were infected at a MOI of 5 PFU/cell with subspecies B1 HAdVs encoding different predicted ORF E3-10.9K orthologs (A) or HAdV-3p-9K-HA mutant virus (B). RNA was harvested at 8 and 24 h pi and analyzed by RT-PCR using primers listed in Table 5. Primer pairs were: E3-10.9K forward and E3-10.9K reverse (E3-10.9K internal), TPL3 forward and E3-10.9K reverse Tm60 (TPL/E3-10.9K), TPL3 forward and Hexon reverse (TPL/Hexon), and RIG/s15 forward and RIG/s15 reverse (RIG). RIG was a positive control for RT and TPL/Hexon was a positive control for viral late gene expression. Mock-infected cells (M) were used as a negative control.

of ORF E3-10.9K at both 8 and 24 h pi using primers internal to ORF E3-10.9K (Fig. 9A). To detect transcripts generated from the MLP, we used an upstream primer specific for leader 3 of the TPL and a downstream primer internal to ORF E3-10.9K (Fig. 2). The TPL sequence is spliced onto all transcripts expressed from the MLP (Berget et al.,

59

1977), making it a useful feature for the detection of MLP transcripts. Using this strategy, strong expression of ORF E3-10.9K from the MLP was detected at 24 h pi, similar to the control PCR detecting the expression of a hexon gene (a known late transcript) from the MLP (Fig. 9A). The same experiment was carried out with the HAdV-3p-9K-HA mutant virus to confirm expression from the MLP (Fig. 9B).

To determine the identity of the RT-PCR products, the approximately 800 bp and 300 bp bands were gel-purified and sequenced. Additionally, a smaller product of approximately 200 bp present only in the HAdV-3p and HAdV-3p-9K-HA samples was purified and sequenced. Sequence data showed that the 800 bp bands contained the TPL sequence immediately preceding ORF E3-20.5K and contained ORF E3-10.9K. The 300 bp bands contained the TPL sequence 6 bp upstream of ORF E3-10.9K (Genbank accession numbers: GU951413-GU951425). The smaller products present only in the HAdV-3p and HAdV-3p-9K-HA samples contained the TPL sequence and a non-coding C-terminus domain of ORF E3-10.9K. These data suggest that ORF E3-10.9K is indeed expressed from the AdV MLP, similar to the species C HAdV E3-11.6K/ADP.

Having found that ORF E3-10.9K was expressed at late times pi from the AdV MLP, similar to species C HAdV E3-11.6K/ADP, we next wanted to determine whether the protein was also expressed at late times pi. We infected A549 cells with the HAdV-3p-9K-HA mutant virus, harvested infected cells at 8 and 48 h pi, and detected the 9 kDa-HA protein by immunoprecipitation and Western blot. The 9 kDa-HA protein was detected at 48 h pi, but we were unable to detect the protein at 8 h pi, suggesting that the protein was primarily expressed at late stages of infection (Fig. 10). To determine
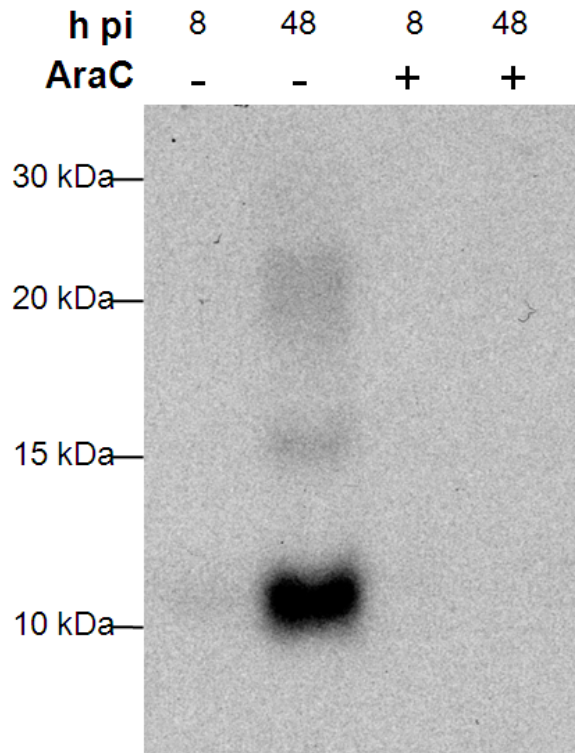
Figure 10. Expression of HA-tagged 9 kDa protein requires viral DNA replication.
A549 cells were infected at a MOI of 10 PFU/cell and either treated with Ara-C to inhibit viral DNA replication and arrest cells at the early stage of infection (+) or mock-treated (-). Cell lysates were collected at 8 and 48 h pi, and 100 µg of total protein were immunoprecipitated with rabbit anti-HA conjugated agarose beads and analyzed by Western blot. Samples were separated under reducing conditions on a NuPAGE 12% polyacrylamide Bis-Tris gel in MES buffer, and transferred to a PVDF membrane. The membrane was probed with a monoclonal mouse anti-HA antibody (primary) and a polyclonal HRP-conjugated goat anti-mouse antibody (secondary).

whether the expression of the 9 kDa-HA protein at late times during infection required viral DNA replication, cells were treated throughout infection with Ara-C to inhibit DNA synthesis. When infected cells were treated with Ara-C, we were unable to detect the 9 kDa-HA protein at 48 h pi, indicating that the expression of the protein required viral DNA replication (Fig. 10). These data support our findings that the ORF E3-10.9K is present on MLP transcripts at late times post infection (Fig. 9), since expression from the MLP requires viral DNA replication.

<u>Glycosylation of proteins</u>

Several products of a higher molecular weight than expected were detected at late times pi in cells infected with HAdV-3p-9K-HA (Fig. 10). These data suggested that the 9 kDa-HA protein was post-translationally modified. Additionally, N-glycosylation sites were predicted for the 7.7 kDa, 9 kDa, and 10.9 kDa protein orthologs (Fig. 7). To investigate whether ORF E3-10.9K-encoded protein orthologs were glycosylated, we generated HeLa T-REx^{TM} cell lines that expressed C-terminal EGFP-tagged ORF E3-10.9K-encoded orthologs under tetracycline regulation. Protein expression was induced with tetracycline and cell lysates were collected at 48 h pi. Total protein samples were incubated with PNGase, neuraminidase, and/or O-glycosidase. Electrophoretic mobility in the observed molecular weight were analyzed by Western blot (Fig. 11). Initially, undigested protein showed higher MW bands for the 7.7 kDa-EGFP, 9 kDa-EGFP, and 10.9 kDa-EGFP proteins (Fig. 11A). Upon digestion with PNGase to remove N-linked glycans, shifts in electrophoretic mobility were observed for 7.7 kDa-EGFP, 9 kDa-EGFP, and 10.9 kDa-EGFP (Fig. 11B). Digestion with neuraminidase and O-glycosidase to remove most O-linked glycans showed slight shifts in electrophoretic mobility for 7.7 kDa-EGFP and 10.9 kDa EGFP, but not 9 kDa-EGFP (Fig. 11B). Digestion with all three glycosidases to remove all N- and most O-linked glycans revealed further shifts in electrophoretic mobility for 7.7 kDa-EGFP and 10.9 kDa-EGFP (Fig. 11B). However, digestion with glycosidases did not return the proteins to their predicted, unmodified size (Fig. 11B). These data suggested that 7.7 kDa-EGFP and 10.9 kDa-EGFP were N- and O-glycosylated, but 9 kDa-EGFP was only N-glycosylated. These data also suggested

that the proteins contained additional post-translational modifications that were not

removed by treatment with PNGase, O-glycosidase, and neuraminidase.

Figure 11. Glycosylation patterns of ORF E3-10.9K protein orthologs. C-terminus EGFP-tagged 4.8 kDa, 7.7 kDa, 9 kDa, and 10.9 kDa were expressed under tetracycline regulation in HeLa-TREx[TM] cells. Total protein was separated under reducing conditions on 12% polyacrylamide NuPAGE gels in MOPS buffer and transferred to PVDF membranes. The membranes were probed with a monoclonal mouse anti-EGFP antibody (primary) and a polycl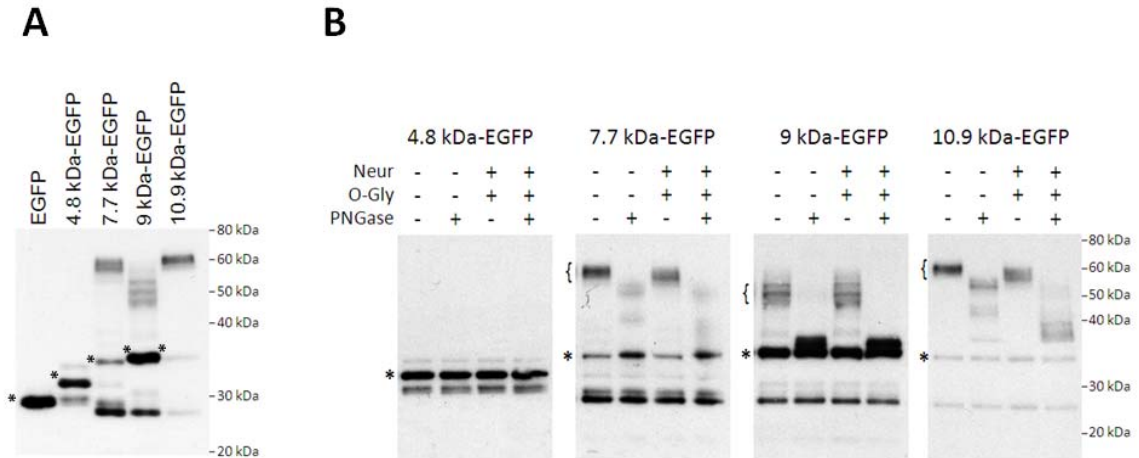onal HRP-conjugated goat anti-mouse antibody (secondary). (A) 10 µg of undigested total protein were analyzed. (B) 40 µg of total protein were digested with PNGase, Neuraminidase, or O-glycosidase to remove N- or O-linked glycans. Approximately 10 µg of protein from digest was analyzed. A fetuin protein digestion control was analyzed in parallel by Coomassie staining to confirm complete digestion with glycosidases (data not shown). *: unmodified EGFP-fusion proteins.

Localization of EGFP-fusions

Having found that the 9 kDa-HA protein was present in the membrane fraction of

infected cells, we next investigated the subcellular localization of ORF E3-10.9K-

encoded protein orthologs. We stained transiently-transfected HeLa T-REx[TM] cells

expressing C-terminal EGFP-tagged ORF E3-10.9K-encoded protein orthologs with

WGA-647, a plasma membrane marker that specifically binds to sialic acid and *N-*

acetylglucosaminyl residues (Fig. 12). Co-localization with WGA-647 was observed for the 9 kDa-EGFP and 10.9 kDa-EGFP proteins but not for the 7.7 kDa-EGFP or 4.8 kDa-EGFP proteins (Fig. 12, merge panels). The 7.7 kDa-EGFP protein appeared to localize primarily to a juxtanuclear compartment, but no co-localization was detected with either calnexin (endoplasmic reticulum marker), Golgin97 (a trans-Golgi marker), or 58K-Golgi protein (a Golgi marker) (Fig. 13, 14, 15, 7.7 kDa panels). The 4.8 kDa-EGFP protein showed diffuse cellular localization similar to that observed for EGFP alone (Fig. 12, 13, 14, 15, 4.8 kDa panels). These data suggest that the C-terminus and hydrophobic domain of the protein are necessary for localization to the plasma membrane, since the 9 kDa and 10.9 kDa proteins contain the C-terminus and the hydrophobic domain while the 4.8 kDa and 7.7 kDa proteins do not.
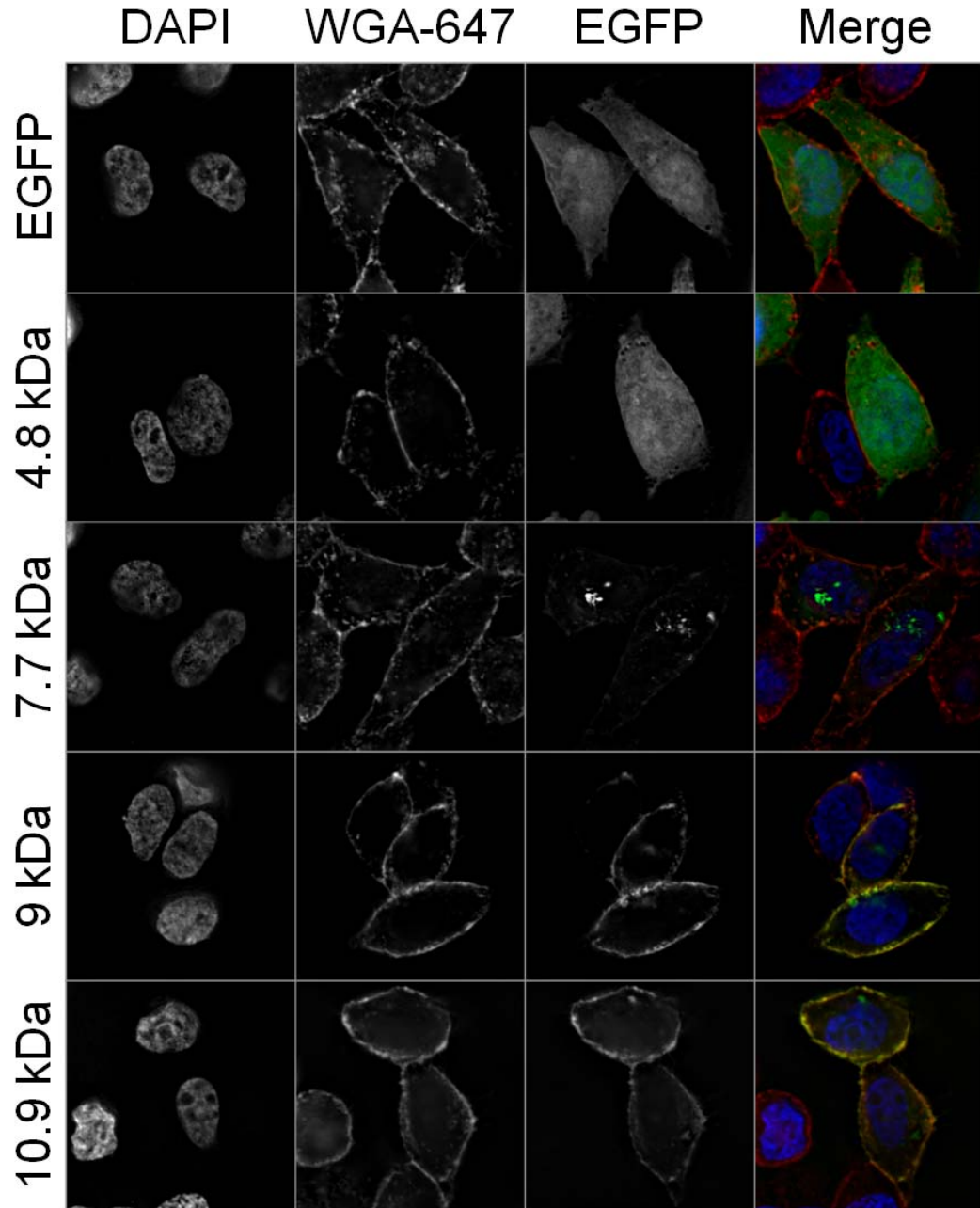
Figure 12. Cellular co-localization of C-terminal EGFP-tagged ORF E3-10.9K-encoded protein orthologs with plasma membrane marker (WGA-647). HeLa-TREx^TM cells were transfected with plasmids expressing EGFP-tagged ORF-E3-10.9K-encoded protein orthologs under a tetracycline inducible promoter. Expression was induced with 1 µg/mL of tetracycline for 24 h. Cells were fixed, stained with WGA-647 (plasma membrane) and DAPI (nucleus), and analyzed by immunofluorescence microscopy. Merge images show pseudo-colored EGFP (green), WGA-647 (red), DAPI (blue) and overlapping EGFP and WGA-647 as yellow.
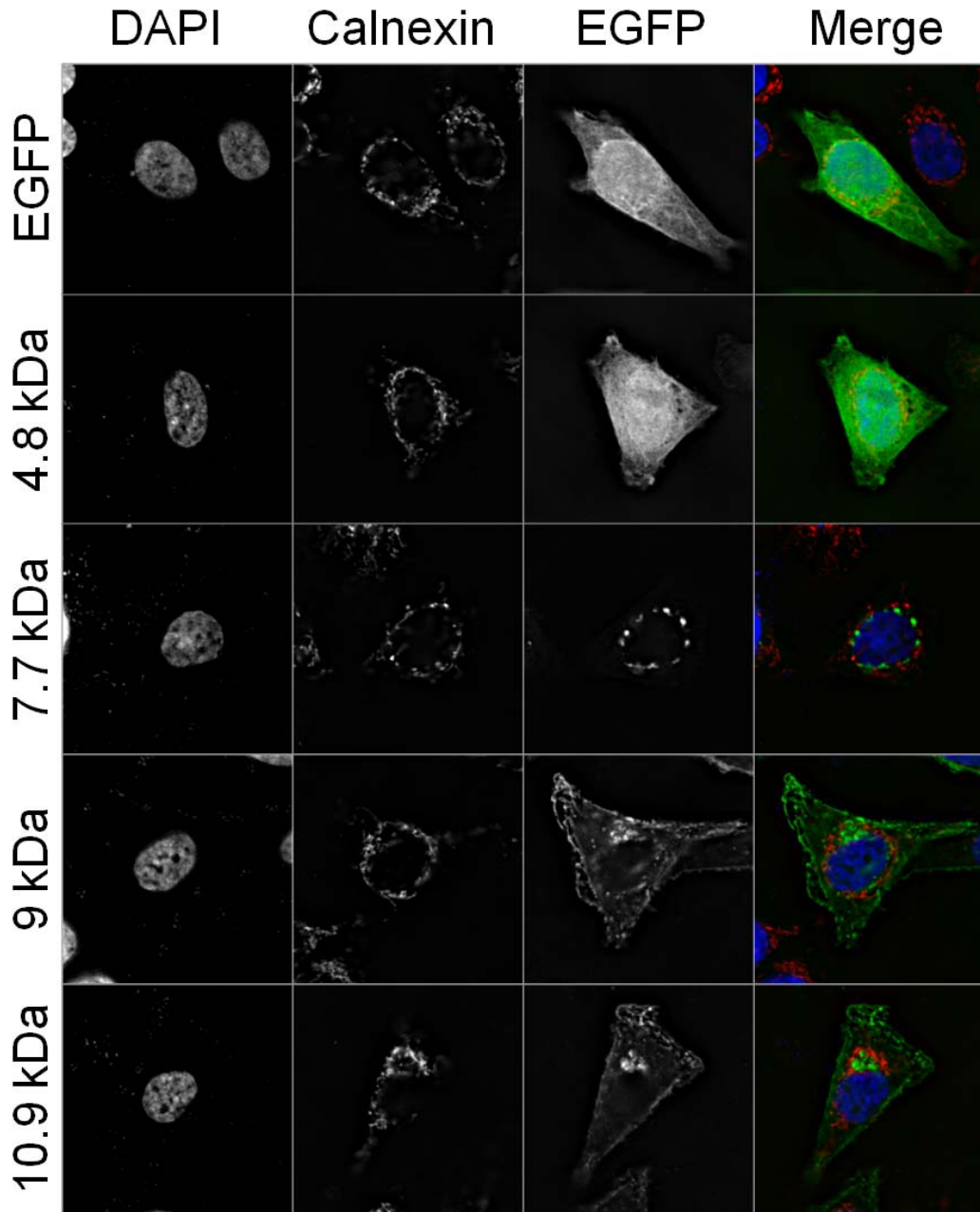
Figure 13. Cellular co-localization of C-terminal EGFP-tagged ORF E3-10.9K-encoded protein orthologs with endoplasmic reticulum marker (Calnexin). HeLa-TREx^TM cells were transfected with plasmids expressing EGFP-tagged ORF-E3-10.9K-encoded protein orthologs under a tetracycline inducible promoter. Expression was induced with 1 μg/mL of tetracycline for 24 h. Cells were fixed, stained with a monoclonal mouse anti-calnexin antibody (primary), a polyclonal Cy5-conjugated donkey anti-mouse antibody (secondary), and DAPI (nucleus) and analyzed by immunofluorescence microscopy. Merge images show pseudo-colored EGFP (green), calnexin (red), DAPI (blue) and overlapping EGFP and calnexin as yellow.

66
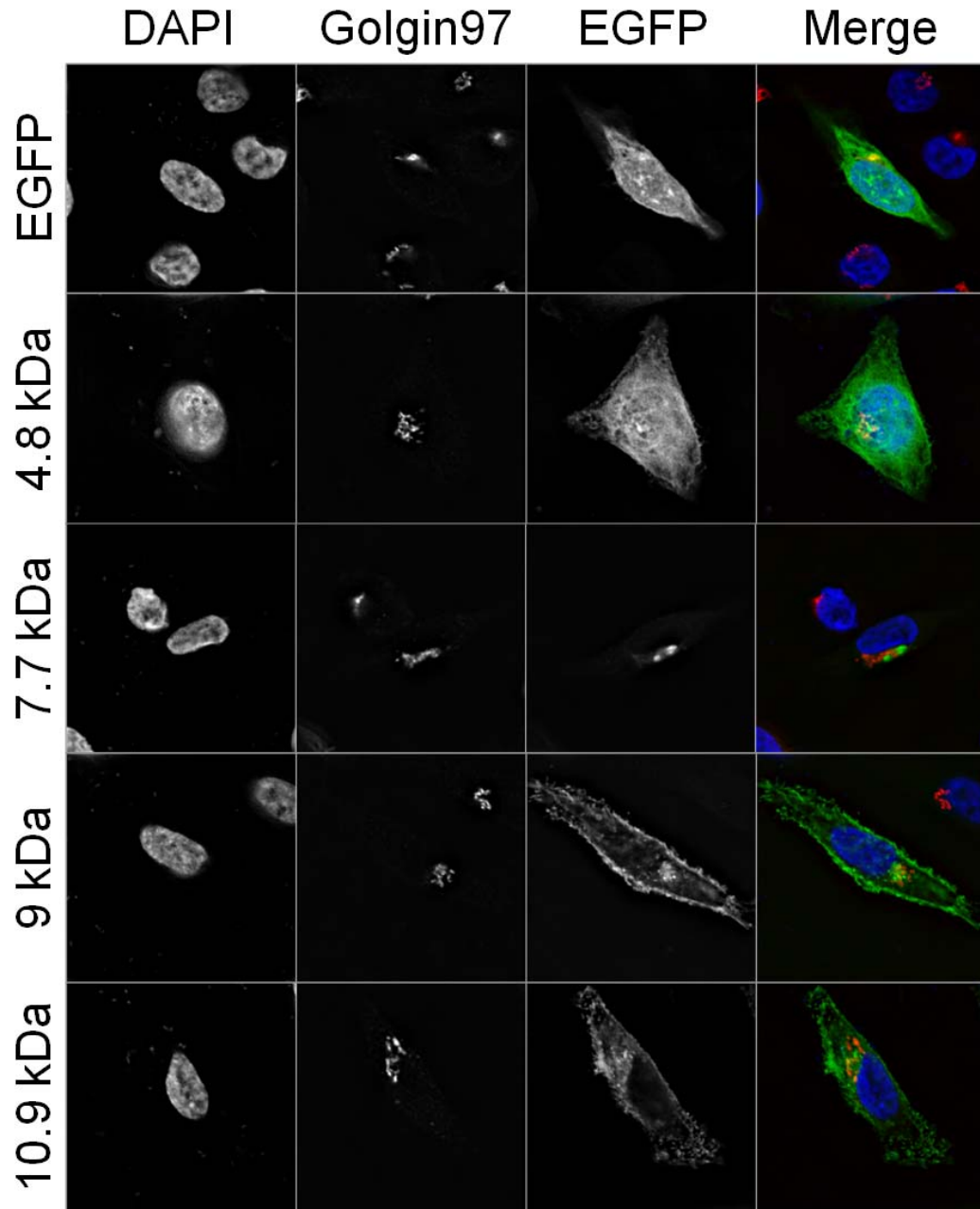
Figure 14. Cellular co-localization of C-terminal EGFP-tagged ORF E3-10.9K-encoded protein orthologs with trans-Golgi marker (Golgin97). HeLa-TREx[TM] cells were transfected with plasmids expressing EGFP-tagged ORF-E3-10.9K-encoded protein orthologs under a tetracycline inducible promoter. Expression was induced with 1 µg/mL of tetracycline for 24 h. Cells were fixed, stained with a monoclonal mouse anti-Golgin97 antibody (primary), a polyclonal Cy5-conjugated donkey anti-mouse antibody (secondary), and DAPI (nucleus) and analyzed by immunofluorescence microscopy. Merge images show pseudo-colored EGFP (green), Golgin97 (red), DAPI (blue) and overlapping EGFP and Golgin97 as yellow.
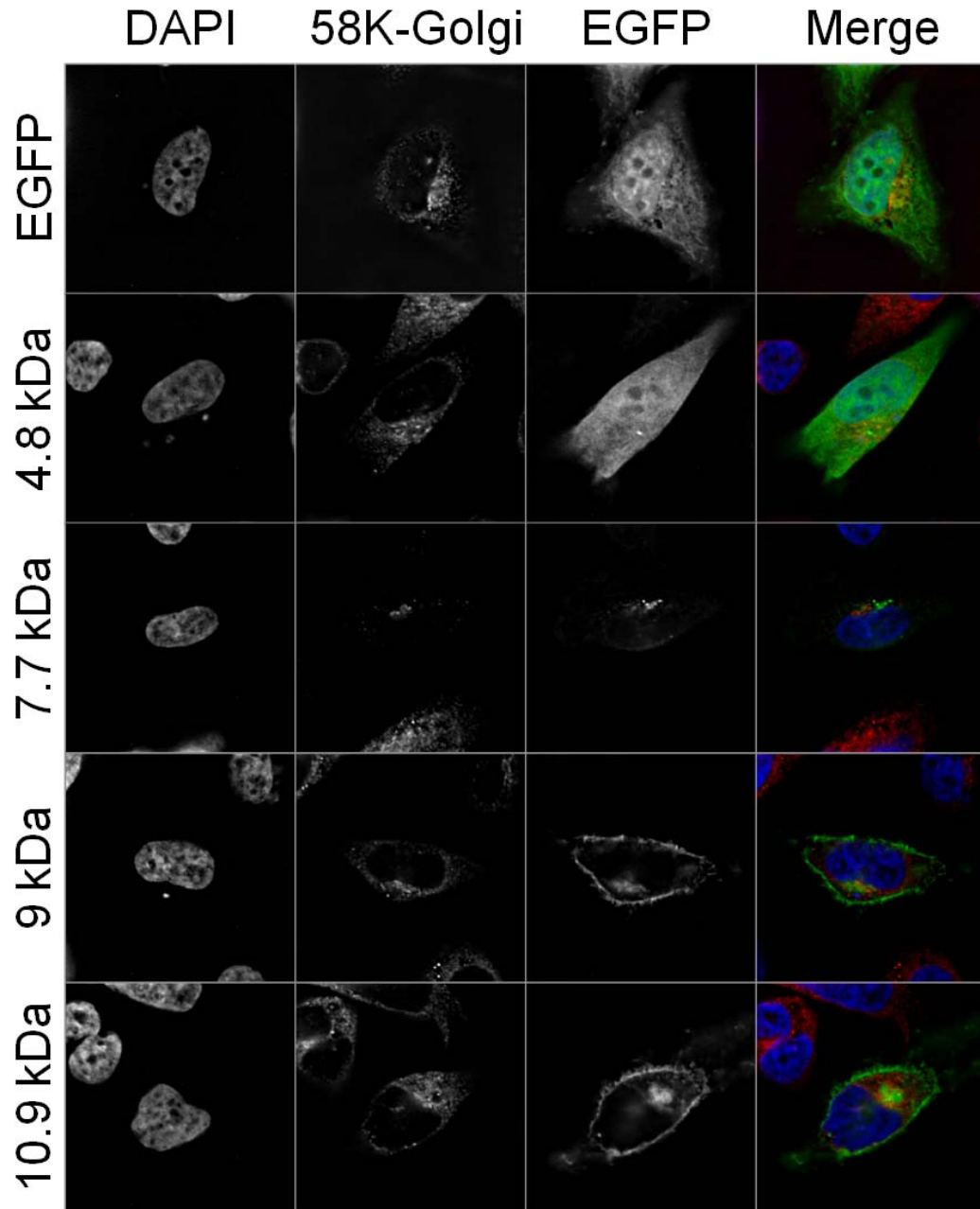
Figure 15. Cellular co-localization of C-terminal EGFP-tagged ORF E3-10.9K-encoded protein orthologs with Golgi marker (58K-Golgi). HeLa-TREx[TM] cells were transfected with plasmids expressing EGFP-tagged ORF-E3-10.9K-encoded protein orthologs under a tetracycline inducible promoter. Expression was induced with 1 μg/mL of tetracycline for 24 h. Cells were fixed, stained with a monoclonal mouse anti-58K-Golgi antibody (primary), a polyclonal Cy5-conjugated donkey anti-mouse antibody (secondary), and DAPI (nucleus) and analyzed by immunofluorescence microscopy. Merge images show pseudo-colored EGFP (green), 58K-Golgi (red), DAPI (blue) and overlapping EGFP and 58K-Golgi as yellow.

Chapter 5: Results--Membrane permeabilizing activity of ORF E3-10.9K-encoded protein orthologs

Results from our initial characterization of ORF E3-10.9K-encoded proteins suggest that the protein orthologs with a hydrophobic domain are likely membrane-active proteins because of their high hydrophobicity, the presence of polybasic regions and aromatic residues in or near the hydrophobic domain, and their localization to cellular membranes. We hypothesized that ORF E3-10.9K-encoded protein orthologs with a hydrophobic domain were membrane-active proteins.

Permeabilization of membranes in *E. coli* expressing N-term GST E3-10.9K fusions

We first investigated the ability of ORF E3-10.9K-encoded protein orthologs to permeabilize membranes using an established *E. coli* expression system. *E. coli* were transformed with plasmids that expressed N-terminus GST-tagged ORF E3-10.9K-encoded orthologs under an inducible *lac* promoter. Cells were collected and stained with propidium iodide at 0 and 3 h post induction of fusion protein expression, and analyzed by flow cytometry. Neither GST alone nor GST-4.8 kDa showed any shift in fluorescence intensity after 3 h of protein expression (Fig. 16A). However, GST-7.7 kDa, GST-9 kDa, and GST-10.9 kDa showed a marked shift in fluorescence intensity after induction of protein expression, suggesting that the presence of a hydrophobic domain is necessary for permeabilizing *E. coli* to propidium iodide (Fig. 16A).

Expression of GST-fusion proteins was confirmed by Western blot with anti-GST antibody (Fig. 16B).
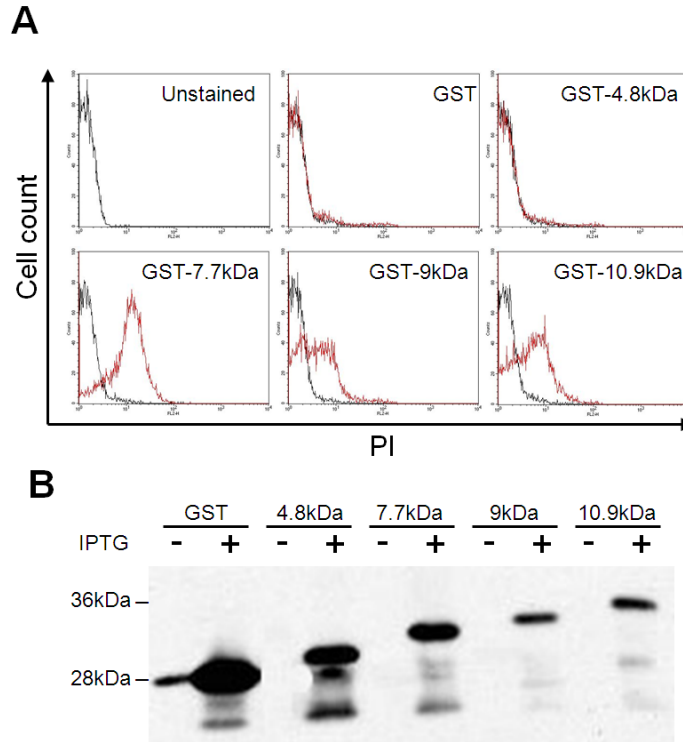
Figure 16. Permeability of *E. coli* expressing GST fusions of ORF E3-10.9K-encoded protein orthologs to propidium iodide. (A) *E. coli* transformed with pGEX bacterial expression constructs expressing ORF E3-10.9K-encoded protein orthologs as N-terminal GST fusions were cultured and fusion-protein expression was induced with 1.0 mM IPTG. Samples (80ul) were removed from the cultures at 0 and 3 h post induction, washed, incubated with propidium iodide in PBS (10 μg/mL), washed, and analyzed by flow cytometry. *E. coli* that were unstained or expressing GST only were used as negative controls. (B) Samples of uninduced (-) and induced (+) cultures were taken at the same time as samples for propidium iodide staining, separated on a 10% Tris-Glycine SDS-PAGE gel, and transferred to a PVDF membrane. The membrane was probed with a polyclonal goat anti-GST antibody (primary) and a polyclonal HRP-conjugated rabbit anti-goat antibody (secondary) to confirm expression of GST-fusion proteins.

<u>Permeabilization of membranes in mammalian cells expressing C-term EGFP E3-10.9K</u>

<u>fusions</u>

Having found that ORF E3-10.9K-encoded protein orthologs with a hydrophobic domain were capable of permeabilizing membranes in an *E. coli* expression system, we next wanted to investigate their ability to permeabilize mammalian cell membranes. For this experiment, stably transfected HeLa T-REx^{TM} cells expressing C-terminal EGFP-tagged ORF E3-10.9K-encoded orthologs under a tetracycline inducible promoter were used. Fusion protein expression was induced at 24 h post plating, and permeability of the cells to trypan blue was assessed by light microscopy. Upon induction of protein expression, no change in permeability of HeLa T-REx^{TM} cells to trypan blue was observed, suggesting that ORF E3-10.9K-encoded protein orthologs were not able to permeabilize mammalian membranes or compromise cell viability (Fig. 17A). Expression of EGFP-fusion proteins in transfected cells after tetracycline induction was confirmed by fluorescence microscopy (Fig. 17B).
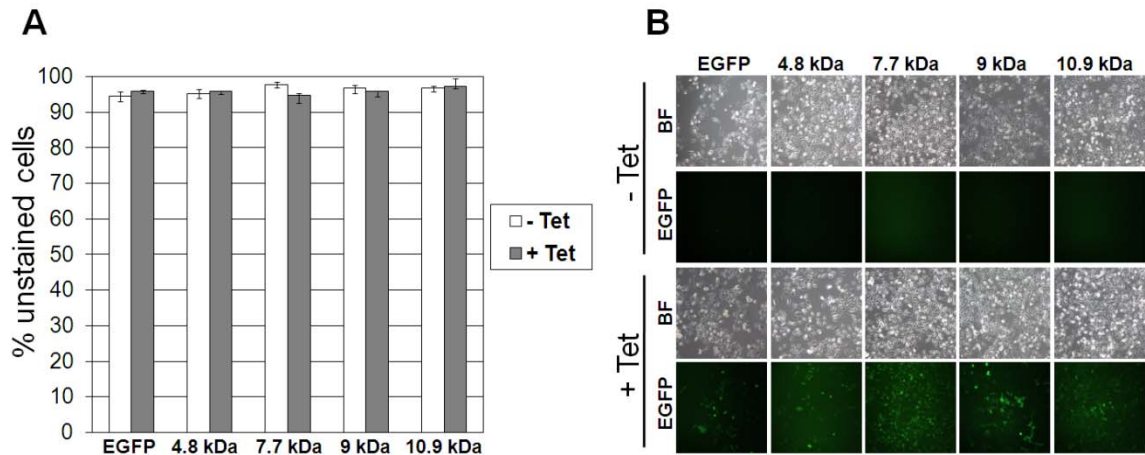
Figure 17. Permeability of HeLa T-REx^TM cells to trypan blue upon expression of EGFP-tagged ORF E3-10.9K-encoded protein orthologs. HeLa T-REx^TM cells stably transfected with pCDNA 4/TO expression plasmids were treated with 1 μg/mL tetracycline (+ Tet) or mock treated (- Tet). (A) At 48 h post treatment, medium was removed and cells were collected by trypsinization. Medium and cells were pooled and stained with an equal volument of 0.4% trypan blue solution. Cells (~200) were counted with a light microscope and a hemocytometer, and the percentage of unstained cells was calculated. Error bars indicate SEM for three independent experiments. (B) Prior to trypan blue staining, expression of EGFP-fusion proteins in tetracycline treated (+ Tet) or untreated (- Tet) live cells was examined by bright field (BF) and fluorescence (EGFP) microscopy. Images are representative of three independent experiments.

Chapter 6: Results--Characterization of HAdV-3p ORF E3-10.9K mutant viruses

The data from our experiments with the HAdV-3p mutant virus expressing a C-terminus HA-tagged 9 kDa protein show that this protein is expressed primarily at late stages of infection (Fig. 10). Additionally, ORF E3-10.9K is located in an analogous region of the E3 transcription unit as species C HAdV E3-11.6K/ADP, which is involved in the efficient release of virus progeny from the host cell at the end of infection (Tollefson et al., 1996b) (Fig. 3). Because of this, we hypothesized that ORF E3-10.9K play a role in the efficient release of progeny virions from infected cells. To test this hypothesis we generated HAdV-3p mutant viruses with mutated ATG codons in the ORF E3-10.9K and investigated their growth characteristics in A549 cells.

Construction of HAdV-3p ORF E3-10.9K mutant viruses

HAdV-3p encodes a 9 kDa protein in ORF E3-10.9K (Fig. 7). Using recombination-based engineering of the HAdV-3p genome (Fig. 5), we generated two control viruses (HAdV-3p-WT and HAdV-3p-9K) and two viruses unable to express a protein from the ORF E3-10.9K (HAdV-3p-KO and HAdV-3p-NULL). Figure 18 is a schematic showing the HAdV-3p mutant viruses generated for these experiments. HAdV-3p-WT was generated from the pKBS2Ad3wt bacmid and had no alterations to the E3 transcription unit. HAdV-3p-9K was a recombination control containing *Sal*I and *Bam*HI restriction sites flanking the ORF E3-10.9K and an FRT scar site. HAdV-3p-KO had an ORF E3-10.9K with all in-frame ATG codons mutated to TAG stop codons.

73

HAdV-3p-NULL contained the non-coding version of ORF E3-10.9K encoded in the genome of HAdV-7h (encoding a null mutation) in place of ORF E3-10.9K encoding the 9 kDa protein (Fig. 18).
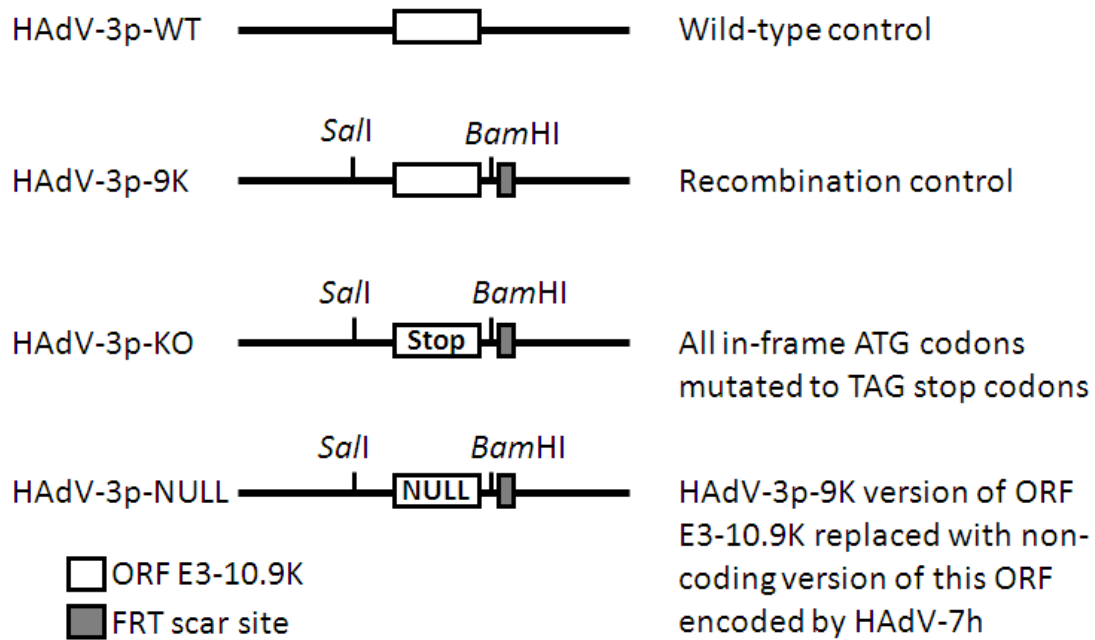
Figure 18. Schematic of HAdV-3p ORF E3-10.9K mutant viruses. Mutant viruses were generated by recombination with pE3-9K shuttle plasmid, digestion of bacmid with *Mlu*I to release the mutated HAdV-3p genome, transfection into A549 cells, and propagation of resultant mutant virus (see Materials and Methods). Recombinants contain *Sal*I and *Bam*HI restriction enzyme sites and an FRT scar site as a result of recombination. HAdV-3p-WT control virus was generated by digestion of pKSB2Ad3wt with *Mlu*I without prior recombination or mutation. HAdV-3p-9K recombination control virus was generated by recombination of pKSB2Ad3wt with unaltered pE3-9K shuttle plasmid in *E. coli* and digestion with *Mlu*I. HAdV-3p-KO mutant virus was generated by recombination of pKSB2Ad3wt with a pE3-9K shuttle plasmid that contained TAG stop codons in place of all ORF E3-10.9K in-frame ATG codons. HAdV-3p-NULL was generated by recombination of pKSB2Ad3wt with a pE3-9K shuttle plasmid that had the HAdV-7h-encoded null version of ORF E3-10.9K (see Fig. 7) in place of the 9 kDa version of ORF E3-10.9K.

Cytopathic effect of HAdV-3p mutant viruses on A549 cell monolayers

A549 cells were infected at a MOI of 1 PFU/cell and analyzed by light microscopy at 4 days pi. Typical AdV CPE was observed for HAdV-3p-WT (control) and HAdV-3p-9K (recombination control). No difference in the progression or appearance of CPE was observed for the HAdV-3p-KO or HAdV-3p-NULL compared to controls (Fig. 19).
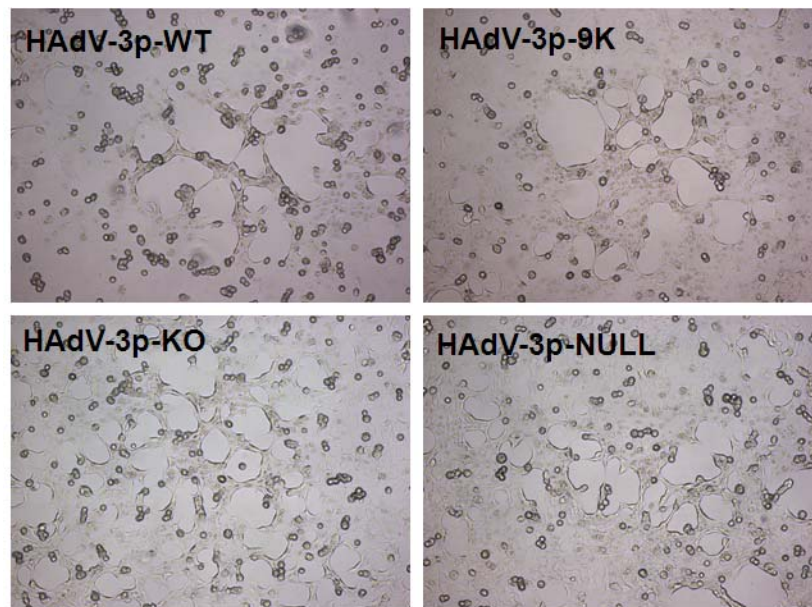
Figure 19. Cytopathic effect of HAdV-3p ORF E3-10.9K mutant viruses on A549 cells. A549 cells were infected with HAdV-3p control (HAdV-3p-WT, HAdV-3p-9K) viruses or HAdV-3p ORF E3-10.9K mutant viruses (HAdV-3p-KO, HAdV-3p-NULL) at a MOI of 1 PFU/cell and analyzed by light microscopy 4 days pi. Classical adenovirus CPE was characterized by rounding and detaching of cells from culture plate surface and "webbing" or "lacy" appearance of cells was observed.

Dissemination of HAdV-3p mutant viruses in A549 cell monolayers

We investigated the ability of HAdV-3p mutant viruses to disseminate in A549 cell monolayers. A549 cells were infected with ten-fold dilutions of HAdV-3p mutant

viruses, replenished with infection medium, and harvested and stained at 5 days pi to visualize the dissemination of virus. No difference was observed among the control HAdV-3p-WT, the recombination control HAdV-3p-9K, HAdV-3p-KO, or HAdV-3p-NULL (Fig. 20).
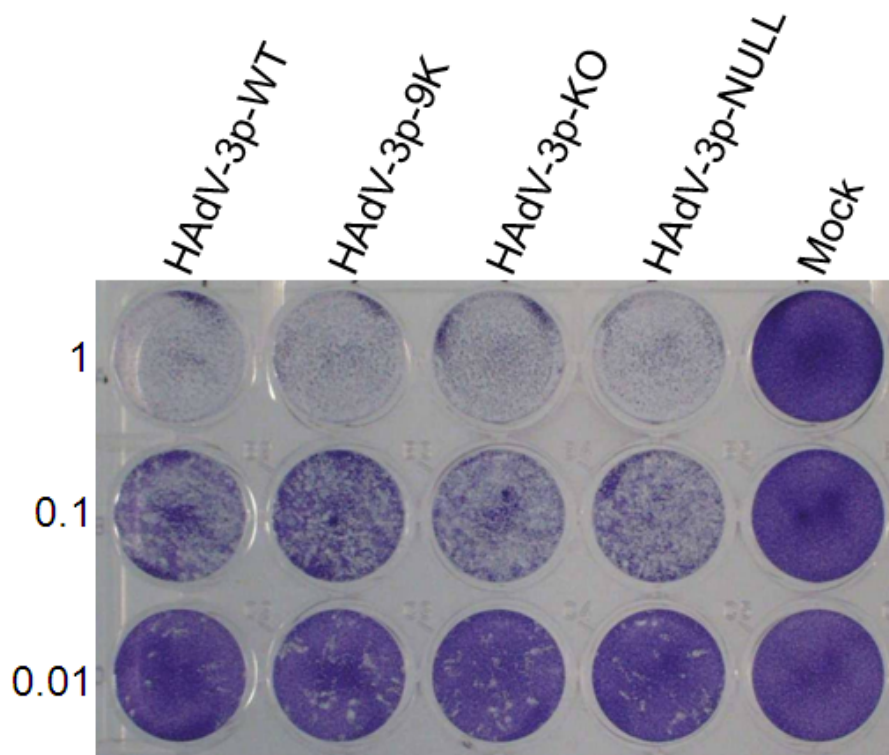
Figure 20. Dissemination of HAdV-3p ORF E3-10.9K mutant viruses in A549 cell monolayers. A549 cells were infected at a MOI of 1, 0.1, or 0.01 PFU/cell, replenished with liquid medium, fixed at 5 days pi, and stained with crystal violet to visualize virus-induced cells monolayer destruction. This image is representative of three independent experiments.

HAdV-3p mutant virus plaque formation in A549 cell monolayers

To investigate the ability of HAdV-3p mutant viruses to form plaques in A549 cell monolayers, cells were infected with ~20 PFU under a semi-solid agarose/medium

overlay and fixed and stained at 13 days pi to visualize plaques. No difference in the

sizes of plaques was observed between control and mutant HAdV-3p viruses (Fig. 21).
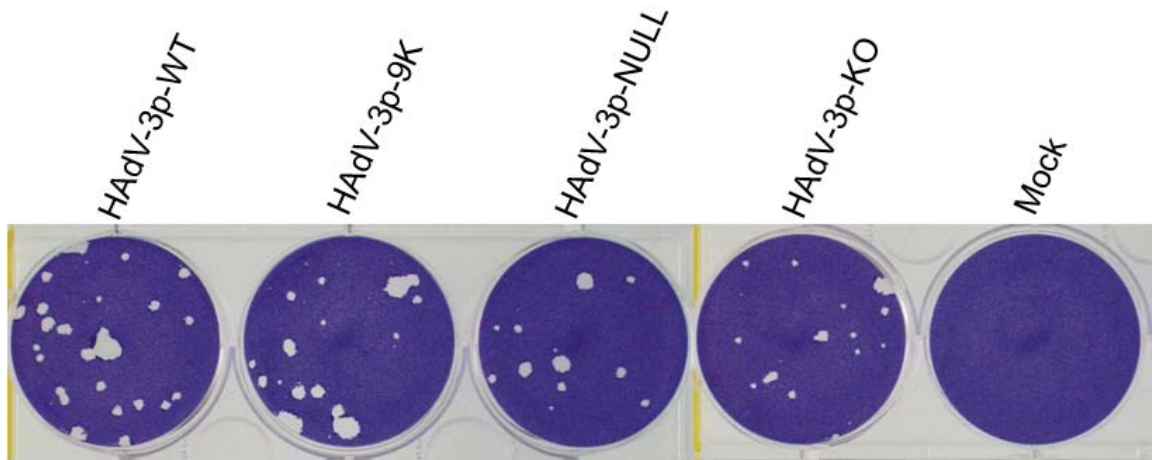
Figure 21. Plaque sizes of HAdV-3p ORF E3-10.9K mutant viruses in A549 cell monolayers. A549 cells in 6-well plates were infected with ~20 PFU/well and overlayed with a semi-solid agarose/medium overlay. At 13 days pi, cells were fixed and stained with crystal violet to visualize plaques. Image is representative of three independent experiments.

HAdV-3p mutant virus egress from infected cells

To test our hypothesis that ORF E3-10.9K-encoded protein orthologs play a role

in the efficient release of virus progeny from infected cells, we carried out virus release

assays in A549 cells. Cells were infected at a MOI of 10 PFU/cell and extracellular

(supernatant) or total (cells and supernatant) infectious virus yields were determined by

plaque assay. In two independent experiments, no difference was observed among the

control and mutant viruses in either total or extracellular virus yields (Fig. 22).
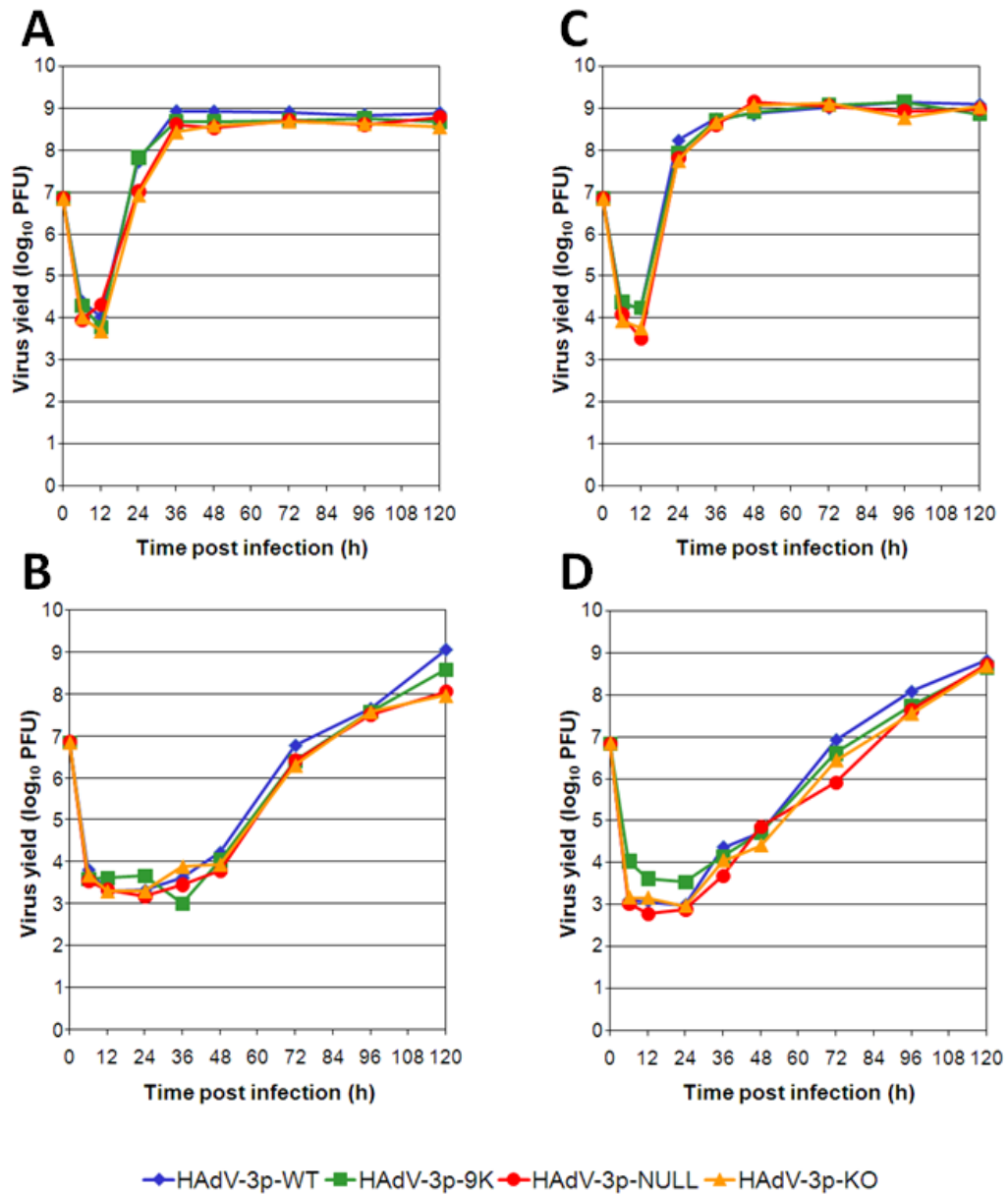
Figure 22. HAdV-3p ORF E3-10.9K mutant virus egress from A549 cells. A549 cells were infected with HAdV-3p ORF E3-10.9K mutant viruses at a MOI of 10 PFU/cell, replenished with liquid medium, and total (A, C) or extracellular (B, D) infectious virus yields were determined by plaque assay at the indicated times pi. Two independent experiments (A,B and C,D) are shown.

Viability of host cells infected with HAdV-3p mutant viruses

To investigate the role of ORF E3-10.9K on the ability of HAdV-3p to kill infected cells, we carried out a trypan blue exclusion assay on A549 cells infected with

HAdV-3p mutant viruses. No difference was observed for the HAdV-3p-NULL or HAdV-3p-KO compared to control HAdV-3p-WT or recombination control HAdV-3p-9K (Fig. 23).
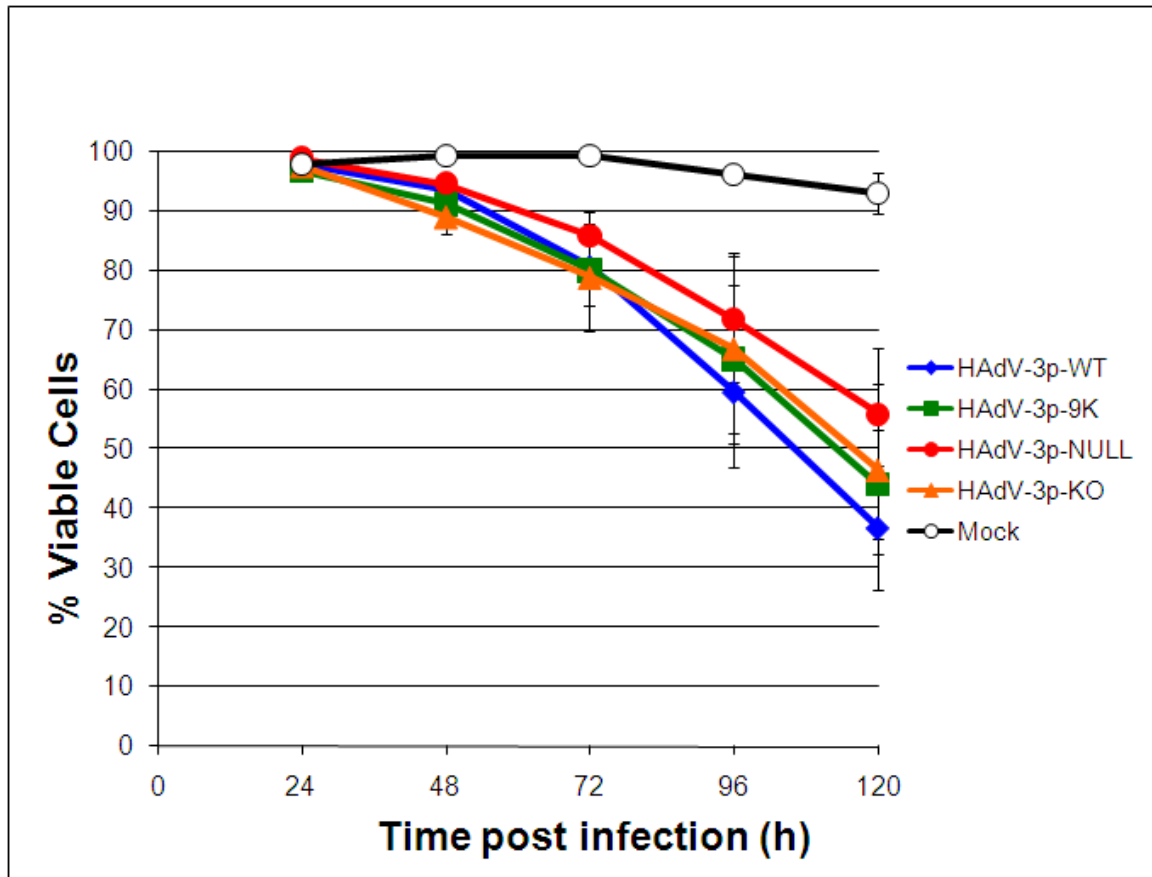
Figure 23. HAdV-3p ORF E3-10.9K mutant virus infected A549 cell viability. A549 cells were infected with HAdV-3p ORF E3-10.9K mutant viruses at a MOI of 10 PFU/cell. Medium and trypsinized cells were pooled at indicated times pi, stained with an equal volume of 0.4% trypan blue solution, and ~200 cells were counted using a light microscope and hemocytometer. The percentage of viable cells was determined by dividing the number of unstained cells by the total number of cells counted. Error bars indicate standard error of the mean for three independent experiments.

Chapter 7: Discussion

Based on the observation that ORF E3-10.9K is encoded in an analogous region of the E3 transcription unit to that of species C HAdV E3-11.6K/ADP and that its predicted protein products display viroporin-like features, we initially hypothesized that ORF E3-10.9K-encoded proteins were implicated in the efficient release of virus progeny at late stages of infection through a mechanism of action that involved the permeabilization or destabilization of host cellular membranes. The results of our experiments using HAdV-3p mutant viruses unable to express ORF E3-10.9K suggest that this hypothesis is incorrect. However, interesting data were obtained to support the likelihood that ORF E3-10.9K plays a role late during the subspecies B1 HAdV life-cycle and that the naturally occurring genetic variability documented for this ORF is likely to impact the function of the encoded products.

Expression of ORF E3-10.9K late during infection

Species C HAdV E3-11.6K/ADP is expressed at late times pi from the MLP (Tollefson et al., 1992). Using RT-PCR, we detected products containing ORF E3-10.9K and the TPL at 24 h pi in cells infected with subspecies B1 HAdVs encoding different orthologs of this ORF (Fig. 9). Additionally, we observed expression of the HA-tagged 9 kDa protein ortholog in infected cells at a late time point by immunoprecipitation and Western blot, but we were unable to detect the protein at an early time point (Fig. 10). The expression of the protein at the late time point was dependent on viral genome replication, as indicated by the results of the Ara-C experiment (Fig. 10). These data

show that, like species C HAdV E3-11.6K/ADP, subspecies B1 HAdV ORF E3-10.9K is expressed at late times from the MLP.

The expression of E3 genes at late times post infection is not unprecedented. Although not as abundant as the ML products, synthesis of all E3 ORFs continues at late stages of infection (Wold et al., 1995). E3-30K encoded by species E HAdV and E3-49K encoded by species D HAdV are of particular interest because they are located in an analogous region of the E3 transcription unit to that of species C HAdV E3-11.6K/ADP and subspecies B1 HAdV ORF E3-10.9K (Fig. 3). ORF E3-30K and ORF E3-49K express products at early and late stages of infection, like other E3 ORFs, but functions have not been determined for these products (Li and Wold, 2000; Windheim et al., 2002). Studies have not been carried out to investigate whether ORF E3-30K and ORF E3-49K are expressed from the MLP like species C HAdV E3-11.6K/ADP and subspecies B1 HAdV ORF E3-10.9K. If expression from the MLP is a conserved feature of ORFs located in this region of the E3 transcription unit, then all these diverse ORFs may encode proteins with a similar function. It would then be reasonable to hypothesize that these proteins may be important for virion progeny egress, but may carry out this fuction by different mechanisms of action.

There are several possible explanations for our inability to detect expression of the HA-tagged 9 kDa protein ortholog at an early time point during infection. First, the protein may not be expressed at early times pi. Although we detected transcripts containing ORF E3-10.9K at early time points during infection by RT-PCR (Fig. 9), these transcripts may not be translated. The presence of the TPL on transcripts greatly enhances translation of the ORFs present on these transcripts (Logan and Shenk, 1984),

and has been discussed previously with regards to species C HAdV E3-11.6K/ADP enhanced protein expression at late times pi (Tollefson et al., 1992). Second, the protein may be expressed at early times pi, but our immunoprecipitation/Western blot method may not be sensitive enough to detect low-level expression. If this was the case, such a low level of expression at early time points may be questionable in its biological relevance. Even upon overexposure of the blot and using the highest sensitivity chemiluminescence reagents available, no product was observed, suggesting that there truly was no expression of the HA-tagged 9 kDa protein at early times pi.

Although numerous studies have been carried out to characterize species C HAdV gene expression, little is known about subspecies B1 HAdV gene expression. One study comparing the E3 transcription unit of HAdV-2 to that of HAdV-3 showed a lack of conservation of splice junctions (Signäs et al., 1986). In contrast with species C HAdV E3-11.6K/ADP (Tollefson et al., 1992), we did not find the presence of the y-leader on the E3 transcripts detected by our method. The y-leader is a 183 bp exon that maps to the 5' end of the E3 transcription unit and is spliced to E3 transcripts in HAdV-2 and HAdV-5 (Wold et al., 1995). This sequence is also found in 25-50% of L5 mRNA coding for the fiber protein (Bhat and Wold, 1986; Chow et al., 1979). The y-leader is proposed to have a role in the regulation of gene expression, but little else is known (Wold et al., 1995). The lack of the y-leader on ORF E3-10.9K transcripts could indicate differences in the regulation of expression for subspecies B1 HAdV compared to species C HAdV, but further experiments are necessary to fully characterize the implications of this observed difference.

In addition to detecting the expression of ORF E3-10.9K from the AdV MLP, we also detected the presence of ORF E3-20.5K on MLP transcripts. This finding was investigated further in our lab and we detected both ORF E3-20.5K and ORF E3-20.1K on transcripts containing the TPL at late times pi. These data led to a new hypothesis that ORF E3-20.5K, ORF E3-20.1K, and ORF E3-10.9K may function in concert. If true, this interaction would not be unprecedented for proteins encoded in the E3 transcription unit. For instance, the RID complex is formed by E3-encoded proteins RIDα and RIDβ, and the E3-6.7K protein interacts with these proteins as well (Benedict et al., 2001).

Future studies will test the new hypothesis by examining expression of the three ORFs E3-20.1K, E3-20.5K, and E3-10.9K during infection. If the products of these three ORFs are indeed acting together, it is likely that they could exhibit some protein-protein interactions detectable using pull-down assays. The generation and examination of HAdV-3p mutant viruses lacking the ability to express proteins from one, two, or all three of these ORFs is currently underway and will provide insight into the potential interactions between these proteins during subspecies B1 HAdV infection.

Subcellular localization of ORF E3-10.9K-encoded proteins

The data presented here show that ORF E3-10.9K predicted proteins containing a C-terminus and a hydrophobic domain (9 kDa and 10.9 kDa) localized primarily to the plasma membrane (Fig. 12). The lack of a C-terminus in the 7.7 kDa ortholog resulted in localization to an intracellular compartment, and the lack of both the hydrophobic domain and the C-terminus in the 4.8 kDa ortholog resulted in diffuse cellular localization (Fig. 12, 13, 14, 15). These data were consistent with the Kyte-Doolittle

hydrophobicity predictions (Fig. 6). Additionally, our data generated from membrane fractionation experiments using a mutant HAdV-3p virus capable of expressing an HA-tagged version of the 9 kDa variant supported the hypothesis that the protein orthologs with a hydrophobic domain localized to membranes during infection (Fig. 8).

Localization to the plasma membrane was clearly observed for the 9 kDa and 10.9 kDa protein orthologs (Fig. 12). However, we were unable to determine the exact localization of the 7.7 kDa protein ortholog. The reason why the 7.7 kDa protein did not localize to the plasma membrane, while the 9 kDa and 10.9 kDa proteins did remains unclear. At this point we are unclear where the 7.7 kDa protein localized, since it did not appear to be in the Golgi apparatus or the endoplasmic reticulum. Future studies will investigate more specifically the localization of 7.7 kDa protein and focus on structural analyses to understand why the 9 kDa and 10.9 kDa proteins localize to the plasma membrane while the 7.7 kDa protein does not. Experiments carried out with species C HAdV E3-11.6K/ADP mutant viruses examined the subcellular localization, glycosylation, and function of targeted mutant versions of E3-11.6K/ADP (Tollefson et al., 2003). Those experiments showed that C-terminus mutants—which would be equivalent to the 7.7 kDa protein ortholog examined in our studies—in general displayed normal glycosylation patterns, but different localization patterns (Tollefson et al., 2003).

The plasma membrane localization of the 9 kDa and 10.9 kDa protein orthologs was unexpected, since we hypothesized that the proteins may have a function similar to species C HAdV E3-11.6K/ADP. E3-11.6K/ADP localizes primarily to the nuclear envelope (Scaria et al., 1992). Numerous laboratory-generated mutants of E3-11.6K/ADP have been examined for subcellular localization and function (Tollefson et

al., 2003). Alterations of the carboxy domain for E3-11.6K/ADP result in non-nuclear membrane cellular localization, including localization to intracellular vesicles or all membranes. Major alterations to remove the hydrophobic domain result in cytoplasmic localization. Changes in the amino domain result in normal localization to the nuclear envelope and Golgi (Tollefson et al., 2003). We made similar observations with our naturally occurring ORF E3-10.9K-encoded protein variants: the loss of the hydrophobic domain resulted in diffuse cellular localization, changes in the carboxy domain altered subcellular localization, and changes in the amino domain had no affect on subcellular localization. E3-11.6K/ADP has not been detected at the plasma membrane (Scaria et al., 1992; Tollefson et al., 2003).

The ORF E3-10.9K-encoded protein orthologs may display a subcellular localization when expressed from the viral genome during infection that is different from what we observed with our ectopically expressed proteins. Any difference would likely be due to the interaction between ORF E3-10.9K-encoded proteins and another virus-encoded protein. To test this possibility, an experiment was carried out using HeLa T-REx^{TM} cells expressing EGFP-tagged ORF E3-10.9K-encoded protein orthologs. These cells were infected with HAdV-16p, and the localization of the EGFP-tagged proteins was examined by immunofluorescence microscopy. Preliminary data showed no difference in subcellular localization of the EGFP-tagged ORF E3-10.9K-encoded protein orthologs in infected versus uninfected cells. These experiments were discontinued because (1) no difference was observed and (2) they were inconclusive because of our inability to determine, and therefore replicate, the normal relative abundance of ORF E3-10.9K-encoded proteins during subspecies B1 HAdV infection. We also unsuccessfully

attempted to determine the localization of the HA-tagged 9 kDa protein ortholog expressed by the HAdV-3p-9K-HA mutant virus by immunofluorescence microscopy using several anti-HA antibodies. All these antibodies showed high cross-reactivity with another unknown HAdV protein (as indicated by staining of cells infected with HAdV-3p-KO mutant virus), and therefore were unsuitable for detecting the localization of the HA-tagged 9 kDa protein in infected cells. In order to further examine subcellular localization of ORF E3-10.9K-encoded protein orthologs in infected cells, HAdV-3p mutants could be generated that express the proteins as fusions with a different epitope tag, such as FLAG.

Although the data presented here was obtained using an artificial system for expression of ORF E3-10.9K-encoded protein orthologs, our findings for experiments using the mutant HAdV-3p expressing the HA-tagged 9 kDa protein showed that this protein localized to host cellular membranes during infection, supporting the observations made with the EGFP-tagged proteins.

Glycosylation patterns of ORF E3-10.9K-encoded proteins

Our data showed differences in glycosylation among ORF E3-10.9K-encoded protein orthologs. Whereas the 4.8 kDa variant showed no evidence of glycosylation, the 7.7 kDa, 9 kDa, and 10.9 kDa variants did (Fig. 11A). The 7.7 kDa and 10.9 kDa showed evidence of both O- and N-linked glycans, while the 9 kDa showed evidence of only N-linked glycans (Fig. 11B). The major difference between the 9 kDa protein ortholog and the 10.9 kDa and 7.7 kDa protein orthologs is a deletion in the N-terminus (Fig. 7). This observation suggested that O-linked glycans were present on the N-terminus of the

protein, or that the O-linked glycosylation required the presence of this N-terminus domain that was missing in the 9 kDa protein ortholog.

Also intriguing was our observation that treatment with glycosidases to remove both N- and O-linked glycans did not result in the complete return of the protein electrophoretic mobility to that of the expected native protein (Fig. 11). This finding could be explained by the lack of complete digestion of the protein, but a control digestion using glycosylated fetuin protein confirmed complete digestion (data not shown). Another, more probable explanation, is that there were other O-linked glycans present on the proteins that were not removed by treatment with O-glycosidase and neuraminidase. Treatment with these two glycosidases removes most, but not all, O-linked glycans. More complicated experiments could be performed using other glycosidases to test this possibility. Another possibility is that a post-translational modification other than glycosylation is present on these proteins.

The implications of the differences in glycosylation patterns for ORF E3-10.9K-encoded protein orthologs are currently unknown. Although the role of glycosylation for protein function varies widely, analysis of E3-11.6K/ADP mutants indicate that glycosylation serves to stabilize the protein (Tollefson et al., 2003). Other roles for glycosylation include protein-protein interactions, proper folding of proteins, and maintenance of protein solubility and conformation (Varki and Lowe, 2009).

Membrane destabilizing activity of ORF E3-10.9K-encoded protein orthologs

Our data showed that, although ORF E3-10.9K-encoded protein orthologs with a hydrophobic domain permeabilized membranes in a bacterial expression system, they did

not appear to permeabilize membranes in a mammalian expression system (Fig. 16, 17). These data suggest that our hypothesis that these proteins may be acting through a membrane destabilizing mechanism is not correct. However, several questions are raised by these experiments.

First, why did the proteins permeabilize bacteria but not mammalian cells? One possible explanation could be our method for assessing permeabilization. For the bacteria expression system, we tested whether the cells became permeable to propidium iodide by flow cytometry. For the mammalian expression system, we tested whether the cells became permeable to trypan blue by light microscopy. Although both propidium iodide and trypan blue are both membrane impermeant dyes, propidium iodide is slightly smaller (668.4 Da) than trypan blue (872.8 Da). Propidium iodide is a DNA/RNA intercalating fluorescent dye that increases in fluorescence 20-30 times upon binding of nucleic acid. We detected this fluorescence using a flow cytometer. Trypan blue is a diazo dye that upon entry into a cell with a non-intact plasma membrane will bind proteins. Stained cells are readily distinguishable from unstained cells by their blue appearance under a light microscope. Although trypan blue and propidium iodide are similar in size, the sensitivity of the propidium iodide assay is likely higher than the trypan blue assay. It is possible that the mammalian cells in our experiments were permeable to trypan blue, but not enough of the dye was able to enter the cells to provide a difference distinguishable by light microscopy. We would expect a higher sensitivity in our flow cytometry experiment detecting propidium iodide stained cells. However, trypan blue has been successfully used to detect the disruption of mammalian cells by membrane-active peptides (Zhang et al., 2009), suggesting that our data reflected a lack

of permeabilizing ability of ORF E3-10.9K-encoded protein orthologs in mammalian cells.

A method potentially more sensitive than trypan blue staining was tested as an alternative: Oregon-green diacetate (OGDA)-release assay. HeLa T-REx™ cells were loaded with OGDA and then expression of ORF E3-10.9K-encoded protein orthologs was induced with tetracycline. Unfortunately, we were unable to obtain results from this experiment because of the quick release of OGDA after loading, which is a common occurrence with cells of epithelial origin (personal communication with Molecular Probes technical support representative). We also carried out a propidium iodide uptake experiment with HeLa T-REx™ cells, but overlap of propidium iodide and EGFP fluorescence signals made the data hard to interpret. The preliminary data we obtained from these experiments showed no permeabilization of the mammalian cells to propidium iodide upon expression of ORF E3-10.9K-encoded protein orthologs. These results should be interpreted with caution because of the unreliable nature of the data and therefore were not included in this dissertation.

Another explanation for the differences in our findings using bacterial and mammalian expression systems is the structural differences between bacterial and mammalian membranes. Bacterial expression systems are used extensively for structure/function studies of viroporins and other membrane-active proteins because of their simplicity and the ease with which experiments can be carried out (Gonzales and Carrasco, 2005). However, our data suggested that results obtained with bacterial expression systems should be interpreted with caution when the protein being examined is normally expressed in a mammalian cell, as most viroporins are.

Both the mammalian and bacterial expression systems were artificial in that we were examining proteins likely overexpressed compared to their native counterparts expressed during the course of infection. However, overexpression of GST alone or GST-4.8 kDa in bacteria did not result in permeabilization of the cells to propidium iodide (Fig. 16), indicating that the permeabilization observed with 7.7 kDa, 9 kDa, and 10.9 kDa was due to some intrinsic membrane activity of these proteins and not to an artifact of overexpression. Additionally, the lack of permeabilization of mammalian cells overexpressing EGFP-tagged ORF E3-10.9K-encoded protein orthologs (Fig. 17) suggested that at lower levels of expression expected in the context of infection, no membrane destabilization would occur.

Alternative approaches to measure membrane permeability include liposome-based assays, hygromycin B inhibition of protein translation, and Merocyanine 540 (MC540) assays. For liposome-based assays, purified proteins are mixed with fluorescent dye-loaded liposomes and the release of dye is measured with a fluorimeter (Agirre et al., 2002; Top et al., 2005). These experiments require the purification or synthetic production of the proteins of interest, which can be difficult for highly hydrophobic, and therefore poorly soluble, proteins such as viroporins and ORF E3-10.9K-encoded protein orthologs. Studies of membrane permeabilizing activity of viroporins often use Hygromycin B assays (Han and Harty, 2004; Lama and Carrasco, 1996; Liao et al., 2006; Madan et al., 2005; Suzuki et al., 2010). Hygromycin B is a protein translation inhibitor that is usually excluded by cellular membranes. Upon expression of a membrane-permeabilizing protein, hygromycin B is able to enter cells (bacterial or mammalian) and inhibit *de novo* protein translation. These studies are

complicated by the fact that the translation of the proteins inducing the cells to become permeable to hygromycin B is also down-regulated as a consequence of the experiment (Lama and Carrasco, 1992). Also, hygromycin B is only excluded from cells at low concentrations, making the experiment difficult to control. MC540 is a lipophilic fluorescent dye that binds to the outer leaflet of plasma membranes and is sensitive to differences in lipid packing (Lelkes et al., 1980; Stillwell et al., 1993; Williamson et al., 1983). When MC540-labelled cells express a membrane-active protein, the fluorescence intensity of the dye decreases and can be measured by flow cytometry (Suzuki et al., 2010). However, the change in fluorescence intensity of the dye only indicates alterations to membrane structures, and does not allow conclusions about the mechanism (Wilson-Ashworth et al., 2006).

The ORF E3-10.9K-encoded protein orthologs with a hydrophobic domain may alter membrane structure in a way that does not result in permeabilization. The alteration of membrane structure could be causing some other effect, as yet to be determined.

Role of ORF E3-10.9K in subspecies B1 HAdV growth and progeny virion egress

Our data does not support the hypothesis that ORF E3-10.9K-encoded protein orthologs are involved in the efficient release of progeny virions from infected cells at the end of infection. We observed no differences between control and ORF E3-10.9K mutant viruses in terms of virus growth, egress, dissemination, or plaque size (Fig. 19, 20, 21, 22). Moreover, no differences were observed in the kinetics of host cell death (Fig. 23). Species C HAdV mutants lacking E3-11.6K/ADP show a marked decrease in the egress of viral progeny from infected cells and slower kinetics of host cell death

(Tollefson et al., 1996b). The data reported herein are in direct opposition to our stated hypothesis, and lead to the conclusion that ORF E3-10.9K-encoded protein orthologs are not the subspecies B1 HAdV equivalent of species C HAdV E3-11.6K/ADP.

The ORF E3-10.9K-encoded protein orthologs may play a role in the release of progeny virions in a way not subject to study by examination of growth phenotypes. Human lung epithelial cells naturally exist in a stratified, differentiated state with distinct apical and basolateral surfaces. The ORF E3-10.9K-encoded protein orthologs may play a role in the release of progeny virions during infection only when cells are polarized. To investigate the role of ORF E3-10.9K on the apical and basolateral egress of progeny virions, human epithelial cells grown in air-liquid interface cultures could be infected with our HAdV-3p mutant viruses and examined for any observable differences in their preferential release of progeny virions. Our choice of A549 cells for the experiments described in this dissertation was based on differences observed using this system for species C HAdV E3-11.6K/ADP mutant viruses (Scaria et al., 1992; Tollefson et al., 1992; Tollefson et al., 1996a; Tollefson et al., 1996b; Tollefson et al., 2003). Even if ORF E3-10.9K-encoded protein orthologs play a role in the efficient release of progeny virions in polarized epithelial cells, we can still conclude that ORF E3-10.9K-encoded protein orthologs are not the subspecies B1 HAdV counterpart of species C HAdV E3-11.6K/ADP since the use of the same experimental system did not yield similar results.

Implications of ORF E3-10.9K polymorphism for subspecies B1 HAdV evolution and fitness

The observed differences in subcellular localization and glycosylation of the products encoded by naturally occurring variants of ORF E3-10.9K suggest functional implications for these mutations. We predict that the 4.8 kDa protein ortholog, and other protein orthologs without a hydrophobic domain, will display a defective function. Additionally, mutations in the carboxy domain will likely impact the protein function as well, since the 7.7 kDa protein shows different subcellular localization.

A trend toward truncation or loss of coding capability for ORF E3-10.9K among circulating strains of HAdV-3 and HAdV-7 was detected in recent molecular epidemiology studies conducted by our lab (L. Dickson, A. Dowling, K. Frietze, A. Kajon, unpublished data). Upon sequencing ORFs E3-10.9K, E3-20.1K, and E3-20.5K for the genomes of geographically and temporally diverse subspecies B1 HAdV field isolates, we observed that currently circulating disease-associated HAdV-7 and HAdV-3 genomic variants encoded versions of ORF E3-10.9K that were either truncation variants without a hydrophobic domain or null variants with mutations of the start codon. However, HAdV-21 and HAdV-16 isolates did not show this same trend. All HAdV-21 and HAdV-16 isolates sequenced were found to retain the ability to encode the 10.9 kDa ortholog. The reason for this difference in the trend toward truncation of ORF E3-10.9K among subspecies B1 HAdVs is unclear. HAdV-7 and HAdV-3 are far more commonly isolated than HAdV-21 and HAdV-16. This difference in isolation frequency could be due to differences in fitness and transmissibility but also to differences in pathogenicity. Data from molecular epidemiological studies are being examined further and will

hopefully yield important information regarding the evolution of ORF E3-10.9K specifically, as well as the evolution of the subspecies B1 HAdV E3 transcription unit.

The apparent trend toward truncation of ORF E3-10.9K for HAdV-7 and HAdV-3 genomic variants can be explained in several ways. First, there may be no selective pressure to maintain ORF E3-10.9K within these genomes, which could lead to truncation or loss since any mutations that occur would have no consequence to the fitness of the virus. In this case, the theoretical original function of ORF E3-10.9K may now be served by another virus-encoded product or the ORF might never have had a function for the virus. Second, there may be a selective pressure against having ORF E3-10.9K. In this case, there would be selection against variants that encode ORF E3-10.9K, leading to a change in the prevalence of the circulating HAdV-7 and HAdV-3 that do not have ORF E3-10.9K. In this case, having ORF E3-10.9K would be detrimental to the virus, so those viruses without ORF E3-10.9K would have a selective advantage. Third, the apparent increase in circulating strains of HAdV-7 and HAdV-3 that do not encode ORF E3-10.9K could be due to sampling bias. In this case, viruses encoding ORF E3-10.9K may not cause severe disease, and so would be poorly represented in a sample of field isolates from symptomatic individuals. This explanation is attractive when taking into account that HAdV-7 and HAdV-3 genomic variants that encode ORF E3-10.9K versions with a hydrophobic domain are infrequently isolated. In order to distinguish between these three possibilities, sampling of asymptomatic individuals would be necessary.

<u>Future directions</u>

If the products of ORF E3-10.9K are not the subspecies B1 HAdV equivalents of species C HAdV E3-11.6K/ADP, several questions must be answered: (1) Is there another protein(s) encoded by subspecies B1 HAdVs serving the function of facilitating viral progeny exit? (2) Do subspecies B1 HAdVs not require an E3-11.6K/ADP-like biological activity to be successful? (3) What is the role of ORF E3-10.9K-encoded proteins if not to facilitate efficient release of virus progeny?

Our revised hypothesis based on the data reported here is that ORF E3-10.9K-encoded protein orthologs serve a function at late stages of infection, possibly by interacting with the products of ORF E3-20.1K and/or ORF E3-20.5K. What that function may be is an open question. At late stages of AdV infection, the primary protein products expressed are structural proteins, which are assembled along with new viral genomes into progeny virions. For species C HAdV, E3-11.6K/ADP is also expressed at late stages of infection and plays a role in the release of progeny virions. Since ORF E3-10.9K-encoded products are expressed late during infection, but are not structural proteins, it is reasonable to hypothesize that this ORF plays a role in the efficient release of progeny virions. However, our data suggest that ORF E3-10.9K-encoded protein products are not the subspecies B1 HAdV equivalent of species C HAdV E3-11.6K/ADP.

What other role might ORF E3-10.9K-encoded protein products be playing late during infection? The E3 transcription unit primarily encodes products that modulate the host response to infection (Burgert and Blusch, 2000). Although the viral products involved in altering the host immune response are primarily important for early stages of infection, ORF E3-10.9K-encoded protein products may be modulators of the host

immune response at late stages. An investigation of our HAdV-3p ORF E3-10.9K mutant viruses in an animal model would be ideal for determining the potential roles of this ORF in viral pathogenesis. However, animal models currently available are only suitable for examination of early stages of infection, since they are not permissive for viral replication and late gene expression (Ginsberg et al., 1989; Sparer et al., 1996). At this point, future experiments are limited to cell culture-based systems. An analysis of the potential role of ORF E3-10.9K in the modulation of the immune response could be carried out by examining the expression of cytokines, chemokines, or other immune-related genes using a cell culture-based experimental system.

There is a suggestion that adenovirus progeny are released via an autophagy-related mechanism rather than the assumed lysis mechanism (Ito et al., 2006; Jiang et al., 2007; Jiang et al., 2008). Studies investigating the mechanism of cell death of AdV-infected cells were carried out using conditionally replicating HAdV-5 with a deletion of the Rb-binding domain of E1A (Fueyo et al., 2000). Although autophagy is implicated as a mechanism of cell death induced by these viruses, the presence or absence of the E3 transcription unit has no effect on the type of cell death resulting from infection (Abou El Hassan et al., 2004), suggesting that the E3-11.6K/ADP is not involved in the proposed autophagic mechanism of cell death. Additionally, an investigation of autophagic modes of cell death in cells infected with non-mutant AdV has not been carried out, but would be essential to establishing the role of autophagy in AdV progeny release and host cell death. If the role of autophagy in natural AdV infection is confirmed, further investigations of subspecies B1 HAdV ORF E3-10.9K function could include examinations of the role of this ORF in autophagic mechanisms of host cell death.

Conclusion

Our data support the conclusion that ORF E3-10.9K is not the subspecies B1 HAdV equivalent of the species species C HAdV E3-11.6K/ADP. This conclusion is based on the observation that, unlike species C HAdV E3-11.6K/ADP, (1) the ORF E3-10.9K-encoded protein orthologs do not localize to the nuclear envelope (Fig. 12-15), and (2) HAdV-3p ORF E3-10.9K mutant viruses unable to express a polypeptide show no difference in virus-induced CPE (Fig. 19), dissemination in cell monolayers (Fig. 20), plaque size (Fig. 21), progeny virus egress (Fig. 22), or host cell killing (Fig. 23). A summary schematic of this conclusion is shown in Figure 24.

Although our data do not support our hypothesis of a role for ORF E3-10.9K-encoded protein products in the efficient release of progeny virions through destabilization or permeabilization of host membranes, we did obtain data to support the conclusion that ORF E3-10.9K-encoded protein orthologs are likely to play a role for subspecies B1 HAdVs during late stages of infection. Additionally, our data support the hypothesis that the naturally observed variation within ORF E3-10.9K is likely to have a functional significance for subspecies B1 HAdV infections. Future experiments should focus on further ascertaining the function of ORF E3-10.9K-encoded protein orthologs, investigating their potential interactions with other viral proteins (including ORF E3-20.1K- and ORF E3-20.5K-encoded protein products), and elucidating the impact of the striking variation present among subspecies B1 HAdVs in ORF E3-10.9K for virus fitness and evolution.
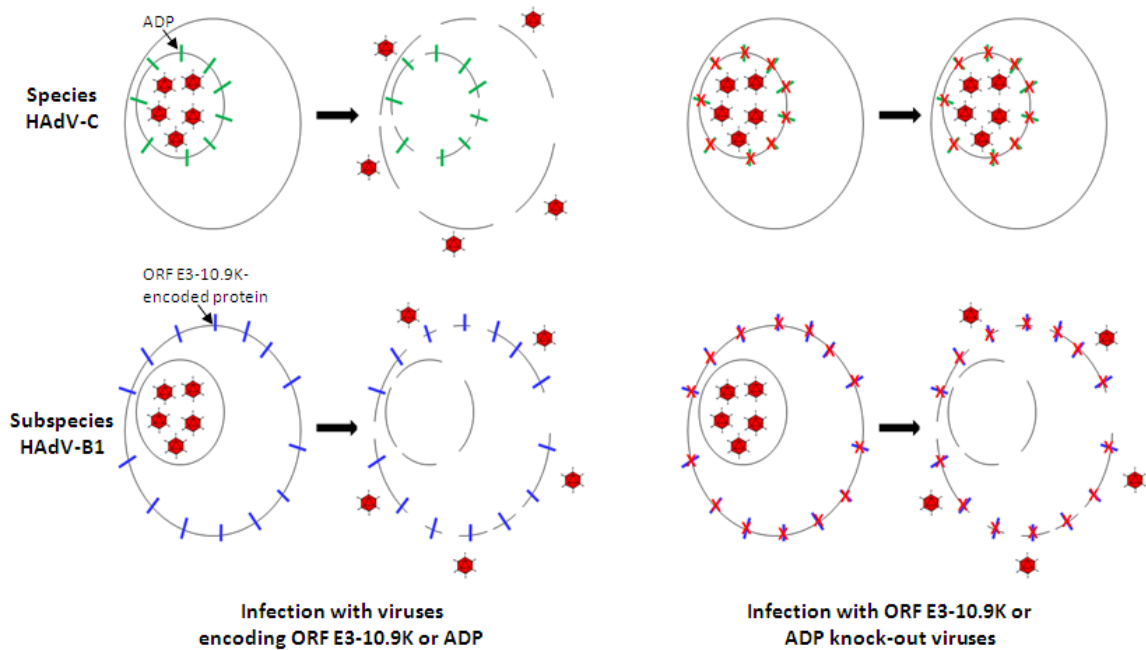
Figure 24. ORF E3-10.9K is not the subspecies B1 HAdV equivalent of the species C HAdV E3-11.6K/adenovirus death protein. The data presented herein support a model for subspecies B1 HAdV egress that is different from that of species C HAdV. In species C HAdV, E3-11.6K/ADP is expressed at late times post infection, localizes to the nuclear envelope, and facilitates efficient progeny virion egress. Species C HAdVs unable to express E3-11.6K/ADP retain progeny virions in the nucleus, resulting in inefficient egress at the end of infection. In subspecies B1 HAdV, ORF E3-10.9K proteins are expressed at late times post infection, but do not localize to the nuclear envelope. Instead the ORF E3-10.9K protein orthologs localize to either the plasma membrane (10.9 kDa and 9 kDa), an intracellular compartment (7.7 kDa), or throughout the cell (4.8 kDa). Subspecies B1 HAdV progeny virions egress efficiently from the host cell regardless of their ability to express an ORF E3-10.9K-encoded protein ortholog.

Appendix A: Acronyms

ADP	Adenovirus death protein
AdPol	Adenovirus DNA polymerase
AdV	Adenovirus
Ara-C	Cytosine β-D-arabinofuranoside hydrochloride
CPE	Cytopathic effect
DBP	DNA binding protein
E3	Early region 3
EGFP	Enhanced green fluorescent protein
EMEM	Eagle Minimum Essential Medium
GST	Glutathione-S-transferase
HAdV	Human adenovirus
HAdV-# (e.g. HAdV-3)	Human adenovirus serotype #
ICTV	International Committee on the Taxonomy of Viruses
ITR	Inverted terminal repeats
ML	Major late transcription unit
MLP	Major late promoter
MOI	Multiplicity of infection
OGDA	Oregon green diacetate
ORF	Open reading frame
pi	Post infection
PFU	Plaque forming units
pTP	Pre-terminal protein
RID	Receptor internalization and degradation
SP	Sequence profile
TNFα	Tumor necrosis factor alpha
TPL	Tripartite leader
VA RNA	Virus associated RNA
WGA-647	Wheat germ agglutinin-647

References

Abou El Hassan, M.A.I., I. van der Meulen-Muileman, S. Abbas, and F.A.E. Kruyt. 2004. Conditionally replicating adenoviruses kill tumor cells via a basic apoptotic machinery-independent mechanism that resembles necrosis-like programmed cell death. J. Virol. **78**:12243-12251.

Adrian, T., and R. Wigand. 1986. Adenovirus 3-7, an intermediate strain of subgenus B. Intervirol. **26**:202-206.

Adrian, T., and R. Wigand. 1989. Genome type analysis of adenovirus 31, a potential causative agent of infants' enteritis. Arch. Virol. **105**:81-7.

Agirre, A., A. Barco, L. Carrasco, and J.L. Nieva. 2002. Viroporin-mediated membrane permeabilization, pore formation by nonstructural poliovirus 2B protein. J. Biol. Chem. **277**:40434-40441.

Aldabe, R., A. Barco, and L. Carrasco. 1996. Membrane permeabilization by poliovirus protein 2B and 2BC. J. Biol. Chem. **271**:23134-7.

Akusjarvi, G. 2008. Temporal regulation of adenovirus major late alternative RNA splicing. Front. Biosci. **13**:5006-15.

Andersson, M., A. McMichael, and P.A. Peterson. 1987. Reduced allorecognition of adenovirus-2 infected cells. J. Immunol. **138**:3960-6.

Andersson, M., S. Pääbo, T. Nilsson, and P.A. Peterson. 1985. Impaired intracellular transport of class I MHC antigens as a possible means for adenoviruses to evade immune surveillance. Cell **43**:215-22.

Antoine, A.F., C. Montpellier, K. Cailliau, E. Prowaeys-Poly, J.P. Vilain, and J. Dubuisson. 2007. The alphavirus 6K protein activates endogenous ionic conductances when expressed in Xenopus oocytes. J. Membr. Biol. **215**:37-48.

Arnberg, N., A.H. Kidd, K. Edlund, J. Nilsson, P. Pring-Akerblom, and G. Wadell. 2002. Adenovirus type 37 binds to cell surface sialic acid through a charge-dependent interaction. Virology **302**:33-43.

Bagchi, S., P. Raychaudhuri, and J.R. Nevins. 1990. Adenovirus E1A proteins can dissociate heteromeric complexes involving the E2F transcription factor: a novel mechanism for E1A trans-activation. Cell **62**:659-69.

Bailey, A., and V. Mautner. 1994. Phylogenetic relationships among adenovirus serotypes. Virology **205**:438-452.

Beard, C.W., A.O. Ball, E.H. Wooley, and K.R. Spindler. 1990. Transcription mapping of mouse adenovirus type 1 early region 3. Virology **175**:81-90.

Beard, C.W., and K.R. Spindler. 1995. Characterization of an 11K protein produced by early region 3 of mouse adenovirus type 1. Virology **208**:457-66.

Beard, C.W., and K.R. Spindler. 1996. Analysis of early region 3 mutants of mouse adenovirus type 1. J. Virol. **70**:5867-74.

Becroft, D.M.O. 1971. Brochiolitis obliterans, brochiectasis, and other sequelae of adenovirus type 21 infection in young children. J. of Clin. Path. **24**:72-82.

Belák, S., A. Virtanen, J. Zabielski, M. Rusvai, G. Berencsi, and U. Pettersson. 1986. Subtypes of bovine adenovirus type 2 exhibit major differences in region E3. Virology **153**:262-71.

Benedict, C., P. Norris, T. Prigozy, J.L. Bodmer, J.A. Mahr, C. Garnett, F. Martinon, J. Tschopp, L.R. Gooding, and C.F. Ware. 2001. Three adenovirus E3 proteins cooperate to evade apoptosis by tumor necrosis factor-related apoptosis-inducing ligand receptor-1 and-2. J. Biol. Chem. **276**: 3270–3278.

Berge, T.O., B. England, C. Mauris, H.E. Shuey, and E.H. Lennette. 1955. Etiology of acute respiratory disease among service personnel at Fort Ord, California. Am. J. Hyg. **62**:283-94.

Berget, S.M., C. Moore, and P.A. Sharp. 1977. Spliced segment at the 5' terminus of adenovirus 2 late mRNA. Proc. Natl. Acad. Sci. USA **74**:3171-5.

Berk, A.J. 1986. Adenovirus promoters and E1A transactivation. Annu. Rev. Genet. **20**:45-79.

Berk, A.J. 2005. Recent lessons in gene expression, cell cycle control, and cell biology from adenovirus. Oncogene **24**:7673-85.

Berk, A.J., F. Lee, T. Harrison, J. Williams, and P.A. Sharp. 1979. Pre-early adenovirus 5 gene product regulates synthesis of early viral messenger RNAs. Cell **17**:935-44.

Bhat, B.M., and W.S. Wold. 1986. Genetic analysis of mRNA sythesis in adenovirus region E3 at different stages of productive infection by RNA-processing mutants. J. Virol. **60**:54-63.

Blusch, J.H., F. Deryckere, M. Windheim, Z. Ruzsics, N. Arnberg, T. Adrian, and H.G. Burgert. 2002. The novel early region 3 protein E3/49K is specifically expressed by adenoviruses of subgenus D: implications for epidemic keratoconjunctivitis and adenovirus evolution. Virology **296**:94-106.

Bodelon, G., L. Labrada, J. Martiniz-Costas, and J. Benavente. 2002. Modification of late membrane permeability in avian reovirus-infected cells, viroporins activity of the S1-encoded nonstructural p10 protein. J. Biol. Chem. **277**:17789-17796.

Bradford, M.M. 1976. A rapid and sensitive method for the quantitation of microgram quantities of protein utilizing the principle of protein-dye binding. Anal. Biochem. **72**:248-54.

Burgert, H.G., and S. Kvist. 1985. An adenovirus type 2 glycoprotein blocks cell surface expression of human histocompatibility class I antigens. Cell **41**:987-97.

Burgert, H.G., and S. Kvist. 1987. The E3/19K protein of adenovirus type 2 binds to the domains of histocompatibility antigens required for CTL recognition. EMBO J. **6**:2019-26.

Burgert, H.G., and J.H. Blusch. 2000. Immunomodulatory functions encoded by the E3 transcription unit of adenoviruses. Virus Genes **21**:13-25.

Campos, S.K. and Barry, M.A. 2004. Rapid construction of capsid-modified adenoviral vectors through bacteriophage λ *Red* recombination. Hum. Gene. Ther. **15**: 1125-1130.

Carballal, G., C. Videla, A. Misirlian, P.V. Requeijo, and M. del C. Aguilar. 2002. Adenovirus type 7 associated with severe and fatal acute lower respiratory infections in Argentine children. BMC Pediatrics **16**:2-6.

Carrasco, L. 1978. Membrane leakiness after viral infection and a new approach to the development of antiviral agent. Nature **272**:694-9.

Carrasco, L. 1995. Modification of membrane permeability by animal viruses. Adv. Virus Res. **45**:61-112.

Cauthen, A.N., C.C. Brown, and K.R. Spindler. 1999. In vitro and in vivo characterization of a mouse adenovirus type 1 early region 3 null mutant. J. Virol. **73**:8640-6.

Cauthen, A.N., and K.R. Spindler. 1999. Novel expression of mouse adenovirus type 1 early region 3 gp11K at late times after infection. Virology **259**:119-28.

Chow, L.T., T.R. Broker, and J.B. Lewis. 1979. Complex splicing patterns of RNAs from the early regions of adenovirus-2. J. Mol. Biol. **134**:265-303.

Chow, L.T., R.E. Gelinas, T.R. Broker, and R.J. Roberts. 1977. An amazing sequence arrangement at the 5' ends of adenovirus 2 messenger RNA. Cell **12**:1-8.

Chroboczek, J., F. Bieber, and B. Jacrot. 1992. The sequence of the genome of adenovirus type 5 and its comparison with the genome of adenovirus type 2. Virology **186**:280-5.

Claros, M.G., and G. von Heijne. 1994. TopPred II: An improved software for membrane protein structure predictions. CABIOS **10**:685-6.

Crawford-Miksza, L., and D.P. Schnurr. 1996. Analysis of 15 adenovirus hexon proteins reveals the location and structure of seven hypervariable regions containing serotype-specific residues. J. Virol. **70**:1836-1844.

Crystal, R.G., N.G. McElvaney, M.A. Rosenfeld, C.S. Chu, A. Mastrangeli, J.G. Hay, S.L. Brody, H.A. Jaffe, N.T. Eissa, and C. Danel. 1994. Administration of an adenovirus containing the human CFTR cDNA to the respiratory tract of individuals with cystic fibrosis. Nat. Genet. **8**:42-51.

Dales, S., and Y. Chardonnet. 1973. Early events in the interaction of adenoviruses with HeLa cells. IV. Association with microtubules and the nuclear pore complex during vectorial movement of the inoculum. Virology **56**:46-83.

Daniels, R., N.M. Rusan, A.K. Wilbuer, L.C. Norkin, P. Wadsworth, and D.N. Hebert. 2006. Simian virus 40 late proteins possess lytic properties that render them capable of permeabilizing cellular membranes. J. Virol. **80**:6575-87.

Datsenko, K.A., and Wanner, B.L. 2000. One-step inactivation of chromosomal genes in *Escherichia coli* K-12 using PCR products. Proc. Natl. Acad. Sci. USA **97**: 6640-6645.

Davison, A.J., M. Benko, and B. Harrach. 2003. Genetic content and evolution of adenoviruses. J. Gen. Virol. **84**:2895-908.

De Jong, J.C., A.G. Wermenbol, M.W. Verweij-Uijeterwaal, K.W. Slaterus, P. Wertheim-Van Dillen, G.J. Van Doornum, S.H. Khoo, and J.C. Hierholzer. 1999. Adenoviruses from human immunodeficiency virus-infected individuals, including two strains that represent new candidate serotypes Ad50 and Ad51 of species B1 and D, respectively. J. Clin. Microbiol. **37**:3940-5.

De Jong, R.N., P.C. van der Vliet, and A.B. Brenkman. 2003. Adenovirus DNA replication: protein priming, jumping back and the role of the DNA binding protein DBP. Curr. Top. Microbiol. Immunol. **272**:187-211.

de Silva, L., P Colditz, and G. Wadell. 1989. Adenovirus type 7 infections in children in New South Wales, Australia. J. Med. Virol. **29**:28-32.

Deryckere, F., and H.G. Burgert. 1996. Tumor necrosis factor alpha induces the adenovirus early 3 promoter by activation of NF-kappaB. J. Biol. Chem. **271**:30249-55.

103

Dickson, L. 2009. Molecular dynamics of adenovirus type 3 and 7 infections in military and civilian populations in the United States. Thesis. University of New Mexico.

Dimitrov, T., P. Krajcsi, T.W. Hermiston, A.E. Tollefson, M. Hannink, and W.S.M. Wold. 1997. Adenovirus E3-10.4K/14.5K protein complex inhibits tumor necrosis factor-induced translocation of cytosolic phospholipase A2 to membranes. J. Virol. **71**:2830–2837.

Dingle, J.H., and A.D. Langmuir. 1968. Epidemiology of acute, respiratory disease in military recruits. Am. Rev. Respir. Dis. **97**:1-65.

Dragulev, B.P., S. Sira, M.G. Abouhaidar, and J.B. Campbell. 1991. Sequence analysis of putative E3 and fiber genomic regions of two strains of canine adenovirus type 1. Virology **183**:298-305.

Dudding, B.A., S.C. Wagner, J.A. Zeller, J.T. Gmelich, G.R. French, and F.H. Top Jr. 1972. Fatal pneumonia associated with adenovirus type 7 in three military trainees. N. Engl. J. Med. **286**:1289-92.

Elsing, A., and H.G. Burgert. 1998. The adenovirus E3/10.4K-14.5K proteins down-modulate the apoptosis receptor Fas/Apo-1 by inducing its internalization. Proc. Natl. Acad. Sci. USA **95**: 10072–10077.

Enders, J.F., J.A. Bell, J.H. Dingle, T. Francis Jr., M.R. Hilleman, R.J. Huebner, and A.M. Payne. 1956. Adenoviruses: group name proposed for new respiratory-tract viruses. Science **124**:119-20.

Erdman, D.D., W. Xu, S.I. Gerber, G.C. Gray, D. Schnurr, A.E. Kajon, and L.J. Anderson. 2002. Molecular epidemiology of adenovirus type 7 in the United States, 1966-2000. Emerg. Infect. Dis. **8**:269-77.

Esford, L.E. and Y. Haj-Ahmad. 1994. Sequence analysis of the putative E3 region of bovine adenovirus type 2. Intervirology **37**:277-86.

Evans, P.S., M. Benkö, B. Harrach, and G.J. Letchworth. 1998. Sequence, transcriptional analysis, and deletion of the bovine adenovirus type 1 E3 region. Virology **244**:173-85.

Evans, R.M., N. Fraser, E. Ziff, J. Weber, M. Wilson, and J.E. Darnell. 1977. The initiation sites for RNA transcription in Ad2 DNA. Cell **12**:733-9.

Flomenberg, F., M. Chen, and M. Horwitz. 1988. Sequence and genetic organization of adenovirus type 35 early region 3. J. Virol. **62**:4431-4437.

Friedman, J.M., and M.S. Horwitz. 2002. Inhibition of tumor necrosis factor alpha-induced NF-κB activation by the adenovirus E3-10.4/14.5K complex. J. Virol. **76**:5515–

5521.

Fueyo, J., C. Gomez-Manzano, R. Alemany, P.S.Y. Lee, T.J. McDonnell, P. Mitlianga, Y.X. Shi, V.A. Levin, W.K.A. Yung, and A.P. Kyritsis. 2000. A mutant oncolytic adenovirus targeting the Rb pathway produces anti-glioma effect in vivo. Oncogene **19**:2-12.

Gerber, S.I., D.D. Erdman, S.L. Pur, P.S. Diaz, J. Segreti, A.E. Kajon, R.P. Belkengren, and R.C. Jones. 2001. Outbreak of adenovirus genome type 7d2 infection in a pediatric chronic-care facility and tertiary-care hospital. Clin. Infect. Dis. **32**:694-700.

Ginsberg, H.S., H.G. Pereira, R.C. Valentine, and W.C. Wilcox. 1966. A proposed terminology for the adenovirus antigens and virion morphological subunits. Virology **28**:782-3.

Ginsberg, H.S., U. Lundholm-Beauchamp, R.L. Horswood, B. Pernis, W.S. Wold, R.M. Chanock, and G.A. Prince. 1989. Role of early region 3 (E3) in pathogenesis of adenovirus disease. Proc. Natl. Acad. Sci. USA **86**:3823-7.

Golovina, G.I., F.N. Zolotaryov, and T.I. Yurlova. 1991. Sensitive analysis of genetic heterogeneity of adenovirus types 3 and 7 in the Soviet Union. J. Clin. Microbiol. **29**:2313-21.

Gonzalez, M.E., and L. Carrasco. 2003. Viroporins. FEBS Lett. **552**:28-34.

Gooding, L.R., I.O. Sofola, A.E. Tollefson, P. Duerksen-Hughes, and W.S.M. Wold. 1990. The adenovirus E3-14.7K protein is a general inhibitor of tumor necrosis factor-mediated cytolysis. J. Immunol. **145**:3080–3086.

Gray, G.C., P.R. Goswami, M.D. Malasig, A.W. Hawksworth, D.H. Trump, M.A. Ryan, and D.P. Schnurr. 2000. Adult adenovirus infections: loss of orphaned vaccines precipitates military respiratory disease epidemics. For the Adenovirus Surveillance Group. Clin. Infect. Dis. **31**:663-70.

Grayston, J.T., R.L. Woolridge, C.G. Loosli, B.F. Gundelfinger, P.B. Johnston, and W.E. Pierce. 1959. Adenovirus infections in naval recruits. J. Infect. Dis. **104**:61-70.

Greber, U.F., M. Suomalainen, R.P. Stidwill, K. Boucke, M.W. Ebersold, and A. Helenius. 1997. The role of the nuclear pore complex in adenovirus DNA entry. EMBO J. **16**:5998-6007.

Greber, U.F., and M. Way. 2006. A superhighway to virus infection. Cell **124**:741-54.

Gustafsson, B., W. Huang, G. Bogdanovic, F. Gauffin, A. Nordgren, G. Talekar, D.A. Ornelles, and L.R. Gooding. 2007. Adenovirus DNA is detected at increased frequency

in Guthrie cards from children who develop acute lymphoblastic leukaemia. Br. J. Cancer **97**:992-4.

Han, Z., and R.N. Harty. 2004. The NS3 protein of bluetongue virus exhibits viroporins-like properties. J. Biol. Chem. **279**:43092-7.

Hashido, M., A. Mukouyama, K. Sakae, H. Tsuzuki, T. Yamashita, T. Inada, and S. Inouye. 1999. Molecular and serological characterization of adenovirus genome type 7h isolated in Japan. Epidemiol. Infect. **122**:281-6.

Hausmann, J., D. Ortmann, E. Witt, M. Veit, and W. Seidel. 1998. Adenovirus death protein, a transmembrane protein encoded in the E3 region, is palmitoylated at the cytoplasmic tail. Virology **244**:343-51.

Hawkins, L.K., and W.S.M. Wold. 1995a. A 20,500-Dalton protein is coded by region E3 of subgroup B but not subgroup C human adenoviruses. Virology **208**:226-233.

Hawkins, L.K., and W.S.M. Wold. 1995b. The E3-20.5K membrane protein of subgroup B human adenoviruses contains O-linked and complex N-linked oligosaccharides. Virology **210**:335-344.

Herbert, F.A., D. Wilkinson, E. Burchak, and O. Morgante. 1977. Adenovirus type 3 pneumonia causing lung damage in childhood. Can. Med. Assoc. J. **116**:274-6.

Hierholzer, J.C., A. Torrence, and P.F. Wright. 1980. Generalized viral illness caused by an intermediate strain of adenovirus (21/H2+35). J. Infect. Dis. **141**:281-8.

Hierholzer, J.C., and F.H. Rodriguez Jr. 1981. Antigenically intermediate human adenovirus strain associated with conjunctivitis. J. Clin. Microbiol. **13**:395-7.

Hilleman, M.R., and J.H. Werner. 1954. Recovery of a new agent from patients with acute respiratory illness. Proc. Soc. Exp. Biol. Med. **85**:183-8.

Hilleman, M.R. 1957. Epidemiology of adenovirus respiratory infections in military recruit populations. Ann. N.Y. Acad. Sci. **67**:262-72.

Hon, K.L., E. Leung, J. Tang, C.M. Chow, T.F. Leung, K.L. Cheung, and P.C. Ng. 2008. Premorbid factors and outcome associated with respiratory virus infections in a pediatric intensive care unit. Pediatr. Pulmonol. **43**:275-80.

Honkaniemi, E., G. Talekar, W. Huang, G. Bogdanovic, E. Forestier, U. von Doblen, M. Engvall, D.A. Ornelles, L.R. Gooding, and B. Gustafsson. 2010. Adenovirus DNA in Guthrie cards from children who develop acute lymphoblastic leukaemia (ALL). Br. J. Cancer **102**:796-8.

Horton, T.M., T.S. Ranheim, L. Aquino, D.I. Kusher, S.K. Saha, C.F. Ware, W.S.M.

Wold, and L.R. Gooding. 1991. Adenovirus E3 14.7K protein functions in the absence of other adenovirus proteins to protect transfected cells from tumor necrosis factor cytolysis. J. Virol. **65**:2629–2639.

ICTVdB – The Universal Virus Database, version 4. 2002. http://www.ncbi.nlm.nih.gov/ICTVdb/ICTVdB.

Idamakanti, N., P.S. Reddy, L.A. Babiuk, and S.K. Tikoo. 1999. Transcription mapping and characterization of 284R and 121R proteins produced from early region 3 of bovine adenovirus type 3. Virology **256**:351-9.

Ito, H., H. Aoki, F. Kühnel, Y. Kondo, S. Kubicka, T. Wirth, E. Iwado, A. Iwamaru, K. Fujiwara, K.R. Hess, F.F. Lang, R. Sawaya, and S. Kondo. 2006. Autophagic cell death of malignant glioma cells induced by a conditionally replicating adenovirus. J. Natl. Cancer Inst. **98**:625-36.

Jiang, H., E.J. White, C. Gomez-Manzano, and J. Fueyo. 2008. Adenovirus's last trick: You say lysis, we say autophagy. Autophagy **4**:118-120.

Jiang, H., C. Gomez-Manzano, H. Aoki, M.M. Alonso, S. Kondo, F. McCormick, J. Xu, Y. Kondo, B.N. Bekele, H. Colman, F.F. Lang, and J. Fueyo. 2007. Examination of the therapeutic potential of Delta-24-RGD in brain tumor stem cells: role of autophagic cell death. J. Natl. Cancer Inst. **99**:1410-4.

Jones, M.S., B. Harrach, R.D. Ganac, M.M. Gozum, W.P. Dela Cruz, B. Riedel, C. Pan, E.L. Delwart, and D.P. Schnurr. 2007. New adenovirus species found in a patient presenting with gastroenteritis. J. Virol. **81**:5978-84.

Julenius, K., A. Molgaard, R. Gupta, and S. Brunak. 2005. Prediction, conservation analysis and structural characterization of mammalian mucin-type O-glycosylation sites. Glycobiology **15**:153-164.

Kajon, A.E., and D.D. Erdman. 2007. Assessment of genetic variability among subspecies B1 human adenoviruses for molecular epidemiology studies. Methods Mol. Med. **131**:335-55.

Kajon, A.E., A.S. Mistchenko, C. Videla, M. Hortal, G. Wadell, and L.F. Avendano. 1996. Molecular epidemiology of adenovirus acute lower respiratory infections of children in the south cone of South America (1991-1994). J. Med. Virol. **48**:151-6.

Kajon, A.E., J.M. Moseley, D. Metzgar, H.S. Huong, A. Wadleigh, M.A. Ryan, and K.L. Russell. 2007. Molecular epidemiology of adenovirus type 4 infections in US military recruits in the postvaccination era (1997-2003). J. Infect. Dis. **196**:67-75.

Kajon, A.E., P. Murtagh, S. Garcia Franco, M.C. Freire, M.C. Weissanbacher, and J. Zorzopulos. 1990. A new genome type of adenovirus 3 associated with severe lower acute respiratory infection in children. J. Med. Virol. **58**:408-12.

Kajon, A., and G. Wadell. 1994. Genome analysis of South American adenovirus strains of serotype 7 collected over a 7-year period. J. Clin. Microbiol. **32**:2321-3.

Kajon, A.E., and G. Wadell. 1996. Sequence analysis of the E3 region and fiber gene of human adenovirus genome type 7h. Virology **215**:190-196.

Kajon, A.E., W. Xu, and D.D. Erdman. 2005. Sequence polymorphism in the E3 7.7K ORF of subspecies B1 human adenoviruses. Virus Res. **107**:11-9.

Kim, Y.J., J.Y. Hong, H.J. Lee, S.H. Shin, Y.K. Kim, T. Inada, M. Hashido, and P.A. Piedra. 2003. Genome type analysis of adenovirus types 3 and 7 isolated during successive outbreaks of lower respiratory tract infections in children. J. Clin. Microbiol. **41**:4595-9.

Kleiboeker, S.B. 1994. Sequence analysis of putative E3, pVIII, and fiber genomic regions of a porcine adenovirus. Virus Res. **31**:17-25.

Körner, H., U. Fritzsche, and H.G. Burgert. 1992. Tumor necrosis factor alpha stimulates expression of adenovirus early region 3 proteins: implications for viral persistence. Proc. Natl. Acad. Sci. USA **89**:11857-61.

Kornuc, M., S. Kliewer, J. Garcia, D. Harrich, C. Li, and R. Gaynor. 1990. Adenovirus early region 3 promoter regulation by E1A/E1B is independent of alterations in DNA binding and gene activation of CREB/ATF and AP1. J. Virol. **64**:2004-13.

Krajcsi, P., T. Dimitrov, T.W. Hermiston, A.E. Tollefson, T.S. Ranheim, S.B. Vande Pol, A.H. Stephenson, and W.S.M. Wold. 1996. The adenovirus E3-14.7K protein and the E3-10.4K/14.5K complex of proteins, which independently inhibit tumor necrosis factor (TNF)-induced apoptosis, also independently inhibit TNF-induced release of arachidonic acid. J. Virol. **70**:4904–4913.

Kunkel, T.A. 1990. Mis-alignment-mediated DNA synthesis errors. Biochemistry **29**:8003-8011.

Lama, J., and L. Carrasco. 1992. Expression of poliovirus nonstructural proteins in Escherichia coli cells. Modification of membrane permeability induced by 2B and 3A. J. Biol. Chem. **267**:15932-7.

Lama, J., and L. Carrasco. 1996. Screening for membrane-permeabilizing mutants of the poliovirus protein 3AB. J. Gen. Virol. **77**:2109-119.

Lang, W.R., C.W. Howden, J. Laws, and J.F. Burton. 1969. Bronchopneumonia with serious sequelae in children with evidence of adenovirus type 21 infection. Br. Med. J. **1**:73-9.

Larranaga, C., A. Kajon, E. Villagra, and L.F. Avendano. 2000. Adenovirus surveillance on children hospitalized for acute lower respiratory infections in Chile (1988-1996). J. Med. Virol. **60**:342-6.

Lechner, R.L., and T.J. Kelly Jr. 1977. The structure of replicating adenovirus 2 DNA molecules. Cell **12**:1007-20.

Lelkes, P.I., D. Bach, and I.R. Miller. 1980. Perturbations of membrane structure by optical probes: II. Differential scanning calorimetry of dipalmitoyllecithin and its analogs interacting with Merocyanine 540. J. Membr. Biol. **54**:141-8.

Lenaerts, L., E. De Clercq, and L. Naesens. 2008. Clinical features and treatment of adenovirus infections. Rev. Med. Virol. **18**:357-74.

Leopold, P.L., G. Kreitzer, N. Miyazawa, S. Rempel, K.K. Pfister, E. Rodriguez-Boulan, and R.G. Crystal. 2000. Dynein- and microtubule-mediated translocation of adenovirus serotype 5 occurs after endosomal lysis. Hum. Gene Ther. **11**:151-65.

Lewis, A.M., A.S. Rabson, and A.S. Levine. 1974. Studies of non-defective adenovirus 2-simian virus 40 hybrid viruses: transformation of hamster kidney cells by adenovirus 2 and the nondefective hybrid viruses. J. Virol. **12**:1291-1301.

Li, E., D. Stupack, G.M. Bokoch, and G.R. Nemerow. 1998a. Adenovirus endocytosis requires actin cytoskeleton reorganization mediated by Rho family GTPases. J. Virol. **72**:8806-12.

Li, E., D. Stupack, R. Klemke, D.A. Cheresh, and G.R. Nemerow. 1998b. Adenovirus endocytosis via alpha(v) integrins requires phosphoinositide-3-OH kinase. J. Virol. **72**:2055-61.

Li, Q.G., and G. Wadell. 1986. Analysis of 15 different genome types of adenovirus type 7 isolated on five continents. J. Virol. **60**:331-5.

Li, Q.G., and G. Wadell. 1988. Comparison of 17 genome types of adenovirus type 3 identified among strains recovered from six continents. J. Clin. Microbiol. **26**:1009-15.

Li, Y., and W.S. Wold. 2000. Identification and characterization of a 30K protein (Ad4E3-30K) encoded by the E3 region of human adenovirus type 4. Virology **273**:127-38.

Liao, Y., J.P. Tam, and D.X. Liu. 2006. Viroporin activity of SARS-CoV E protein. Adv. Exp. Med. Biol. **581**:199-202.

Linné, T. 1992. Differences in the E3 regions of the canine adenovirus type 1 and type 2. Virus Res. **23**:119-33.

Liu, F., and M.R. Green. 1994. Promoter targeting by adenovirus E1A through interaction with different cellular DNA-binding domains. Nature **368**:520-5.

Liu, H., J.H. Naismith, and R.T. Hay. 2003. Adenovirus DNA replication. Curr. Top. Microbiol. Immunol. **272**:131-64.

Logan, J., and T. Shenk. 1984. Adenovirus tripartite leader sequence enhances translation of mRNAs late after infection. Proc. Natl. Acad. Sci. USA **81**:3655-3659.

Lonberg-Holm, K., and L. Philipson. 1969. Early events of virus-cell interaction in an adenovirus system. J. Virol. **4**:323-38.

Louie, J.K., A.E. Kajon, M. Holodniy, L. Guardia-LaBar, B. Lee, A.M. Petru, J.K. Hacker, and D.P. Schnurr. 2008. Severe pneumonia due to adenovirus serotype 14: a new respiratory threat? Clin. Infect. Dis. **46**:421-5.

Mabit, H., M.Y. Nakano, U. Prank, B. Saam, K Dohner, B. Sodeik, and U.F. Greber. 2002. Intact microtubules support adenovirus and herpes simplex virus infections. J. Virol. **76**:9963-71.

Madan, V., M. de J. Garcia, M.A. Sanz, and L. Carrasco. 2005. Viroporin activity of murine hepatitis virus E protein. FEBS Lett. **579**:3607-3612.

Madan, V., S. Sanchez-Martinez, N. Vedovato, G. Rispoli, L. Carrasco, and J.L. Nieva. 2007. Plasma membrane-porating domain in poliovirus 2B protein. A short peptide mimics viroporins activity. J. Mol. Biol. **374**:951-64.

Madan, V., M. de J. García, M.A. Sanz, and L. Carrasco. 2005. Viroporin activity of murine hepatitis virus E protein. FEBS Lett. **579**:3607-12.

Marttila, M., D. Persson, D. Gustafsson, M.K. Liszewski, J.P. Atkinson, G. Wadell, and N. Arnberg. 2005. CD46 is a cellular receptor for all species B adenoviruses except types 3 and 7. J. Virol. **79**:14429-36.

Mathias, P., T. Wickham, M. Moore, and G. Nemerow. 1994. Multiple adenovirus serotypes use alpha v integrins for infection. J. Virol. **68**:6811-4.

McNamara, M.J., W.E. Pierce, Y.E. Crawford, and L.F. Miller. 1962. Patterns of adenovirus infection in the respiratory diseases of naval recruits. A longitudinal study of two companies of naval recruits. Am. Rev. Resp. Dis. **86**:485-97.

Mei, Y.-F., and G. Wadell. 1992. The nucleotide sequence of adenovirus type 11 early 3 region: comparison of genome type Ad11p and Ad11a. Virology **191**:125-133.

Metzgar, D., M. Osuna, A.E. Kajon, A.W. Hawksworth, M. Irvine, and K.L. Russell. 2007. Abrupt emergence of diverse species B adenoviruses at U.S. military recruit training centers. J. Infect. Dis. **196**:1465-73.

Mittal, S.K., L. Prevec, L.A. Babiuk, and F.L. Graham. 1993. Sequence analysis of bovine adenovirus type 3 early region 3 and fibre protein genes. J. Gen. Virol. **74**:2825.

Moise, A.R., J.R. Grant, T.Z. Vitalis, and W.A. Jefferies. 2002. Adenovirus E3-6.7K maintains calcium homeostasis and prevents apoptosis and arachidonic acid release. J. Virol. **76**:1578–1587.

Morin, J.E., M.D. Lubeck, J.E. Barton, A.J. Conley, A.R. Davis, and P.P. Hung. 1987. Recombinant adenovirus induces antibody response to hepatitis B virus surface antigen in hamsters. Proc. Natl. Acad. Sci. USA **84**:4626-30.

Murray, E.S., R.S. Chang, S.D. Bell, M.L. Tarizzo, and J.C. Snyder. 1957. Agents recovered from acute conjunctivitis cases in Saudi Arabia. Am. J. Ophth. **43**:32-5.

Nevins, J.R. 1981. Mechanism of activation of early viral transcription by the adenovirus E1A gene product. Cell **26**:213-20.

Nevins, J.R., and J.E. Darnell Jr. 1978. Groups of adenovirus type 2 mRNA's derived from a large primary transcript: probable nuclear origin and possible common 3' ends. J. Virol. **25**:811-23.

Nevins, J.R., H.S. Ginsberg, J.M. Blanchard, M.C. Wilson, and J.E. Darnell Jr. 1979. Regulation of the primary expression of the early adenovirus transcription units. J. Virol. **32**:727-33.

Nieva, J.L., A. Agirre, S. Nir, and L. Carrasco. 2003. Mechanisms of membrane permeabilization by picornavirus 2B viroporins. FEBS Lett. **552**:68-73.

Pääbo, S., T. Nilsson, and P.A. Peterson. 1986. Adenoviruses of subgenera B, C, D, and E modulate cell-surface expression of major histocompatibility complex class I antigens. Proc. Natl. Acad. Sci. USA **83**:9665-9.

Pardo-Mateos, A., and C.S. Young. 2004. Adenovirus IVa2 protein plays an important role in transcription from the major late promoter in vivo. Virology **237**:50-9.

Parks, C.L., and T. Shenk. 1997. Activation of the adenovirus major late promoter by transcription factors MAZ and Sp1. J. Virol. **71**:9600-7.

Patterson, S., and W.C. Russell. 1983. Ultrastructural and immunofluorescence studies of early events in adenovirus-HeLa cell interactions. J. Gen. Virol. **64**:1091-9.

Persson, H., H. Jörnvall, and J. Zabielski. 1980. Multiple mRNA species for the precursor to an adenovirus-encoded glycoprotein: identification and structure of the signal sequence. Proc. Natl. Acad. Sci. USA **77**:6349-53.

Persson, H., B. Oberg, and L. Philipson. 1978. Purification and characterization of an early protein (E14K) from adenovirus type 2-infected cells. J. Virol. **28**:119-39.

Pettersson, U., and R.J. Roberts. 1986. Adenovirus gene expression and replication: a historical review. Cancer Cells **4**:37-57.

Phelps, W.C., S. Bagchi, J.A. Barnes, P. Raychaudhuri, V. Kraus, K. Münger, P.M. Howley, and J.R. Nevins. 1991. Analysis of trans activation by human papillomavirus type 16 E7 and adenovirus 12S E1A suggests a common mechanism. J. Virol. **65**:6922-30.

Philipson, L., and R.F. Pettersson. 2004. The coxsackie-adenovirus receptor--a new receptor in the immunoglobulin family involved in cell adhesion. Curr. Top. Microbiol. Immunol. **273**:87-111.

Pichla-Gollan, S.L., M. Drinker, X. Zhou, F. Xue, J.J. Rux, G.P. Gao, J.M. Wilson, H.C. Ertl, R.M. Burnett, and J.M. Bergelson. 2006. Structure-based identification of a major neutralizing site in adenovirus hexon. J. Virol. **81**:1680-1689.

Poteete, A.R. 2001. What makes the bacteriophage λ *Red* system useful for genetic engineering: molecular mechanism and biological function. FEMS Microbiol. Lett. **201**:9-14.

Reddy, P.S., E. Nagy, and J.B. Derbyshire. 1995. Sequence analysis of putative pVIII, E3 and fibre regions of porcine adenovirus type 3. Virus Res. **36**:97-106.

Ross, S., and A.J. Levine. 1979. The genomic map position of the adenovirus type 2 glycoprotein. Virology **99**:427-30.

Rowe, W.P., R.J. Huebner, L.K. Gilmore, R.H. Parrott, and T.G. Ward. 1953. Isolation of a cytopathogenic agent from human adenoids undergoing spontaneous degeneration in tissue culture. Proc. Soc. Exp. Biol. Med. **84**:570-3.

Russell, W.C. 2009. Adenoviruses: update on structure and function. J. Gen. Virol. **90**:1-20.

Ryan, M.A., G.C. Gray, B. Smith, J.A. McKeehan, A.W. Hawksworth, and M.D. Malasig. 2002. Large epidemic of respiratory illness due to adenovirus types 7 and 3 in healthy young adults. Clin. Infect. Dis. **34**:577-82.

Sambrook, J., M. Sleigh, J.A. Engler and T.R. Broker. 1980. The evolution of the adenoviral genome. Ann. NY Acad. Sci. **354**:426-452.

Sanz, M.A., V. Madan, L. Carrasco, and J.L. Nieva. 2003. Interfacial domains in Sindbis virus 6K protein. Detection and functional characterization. J. Biol. Chem. **278**:2051-7.

Scaria, A., A.E. Tollefson, S.K. Saha, and W.S. Wold. 1992. The E3-11.6K protein of adenovirus is an Asn-glycosylated integral membrane protein that localizes to the nuclear membrane. Virology **191**:743-53.

Schmitz, H., R. Wigand, and W. Heinrich. 1983. Worldwide epidemiology of human adenovirus infections. Am. J. Epidemiol. **117**:455-66.

Schnurr, D., A. Bollen, L. Crawford-Miksza, M.E. Dondero, and S. Yagi. 1995. Adenovirus mixture isolated from the brain of an AIDS patient with encephalitis. J. Med. Virol. **47**:168-71.

Shaw, A.R., and E.B. Ziff. 1980. Transcripts from the adenovirus-2 major late promoter yield a single early family of 3' coterminal mRNAs and five late families. Cell **22**:905-16.

Shisler, J., C. Yang, B. Walter, C.F. Ware, and L.R. Gooding. 1997. The adenovirus E3-10.4K/14.5K complex mediates loss of cell surface Fas (CD95) and resistance to Fas-induced apoptosis. J. Virol. **71**:8299–8306.

Short, J.J., A.V. Pereboev, Y. Kawakami, C. Vasu, M.J. Holterman, and D.T. Curiel. 2004. Adenovirus serotype 3 utilizes CD80 (B7.1) and CD86 (B7.2) as cellular attachment receptors. Virology **322**:349-59.

Short, J.J., C. Vasu, M.J. Holterman, D.T. Curiel, and A. Pereboev. 2006. Members of adenovirus species B utilize CD80 and CD86 as cellular attachment receptors. Virus Res. **122**:144-53.

Signäs, C., G. Akusjärvi, and U. Pettersson. 1986. Region E3 of human adenoviruses; differences between the oncogenic adenovirus-3 and the non-oncogenic adenovirus-2. Gene **50**:173-84.

Stillwell, W., S.R. Wassall, A.C. Dumaual, W.D. Ehringer, C.W. Browning, and L.J. Jenski. 1993. Use of merocyanine (MC540) in quantifying lipid domains and packing in phospholipid vesicles and tumor cells. Biochim. Biophys. Acta. **1146**:136-44.

Similä, S., O. Linna, P. Lanning, E. Heikkinen, and M. Ala-Houhala. 1981. Chronic lung damage caused by adenovirus type 7: a ten-year follow-up study. Chest **80**:127-131.

Sirena, D., Z. Ruzsics, W. Schaffner, U.F. Greber, and S. Hemmi. 2005. The nucleotide sequence and a first generation gene transfer vector of species B human adenovirus serotype 3. Virology **343**:283-98.

Sparer, T.E., R.A. Tripp, D.L. Dillehay, T.W. Hermiston, W.S. Wold, and L.R. Gooding. 1996. The role of human adenovirus early region 3 proteins (gp19K, 10.4K, 14.5K, and 14.7K) in a murine pneumonia model. J. Virol. **70**:2431-9.

Spigelblatt, L., and R. Rosenfeld. 1983. Hyperlucent lung: long-term complication of adenovirus type 7 pneumonia. Can. Med. Assoc. J. **128**:47-9.

Suomalainen, M., M.Y. Nakano, S. Keller, K. Boucke, R.P. Stidwill, and U.F. Greber. 1999. Microtubule-dependent plus- and minus end-directed motilities are competing processes for nuclear targeting of adenovirus. J. Cell Biol. **144**:657-72.

Suzuki, T., Y. Orba, Y. Okada, Y. Sunden, T. Kimura, S. Tanaka, K. Nagashima, W.W. Hall, and H. Sawa. 2010. The Human Polyoma JC Virus Agnoprotein Acts as a Viroporin. PLoS Pathog. **6**:e1000801.

Tollefson, A.E., T.W. Hermiston, D.L. Lichtenstein, C.F. Colle, R.A. Tripp, T. Dimitrov, K. Toth, C.E. Wells, P.C. Doherty, and W.S.M. Wold. 1998. Forced degradation of Fas inhibits apoptosis in adenovirus-infected cells. Nature **392**:726–730.

Tollefson, A.E., P. Krajcsi, M.H. Pursley, L.R. Gooding, and W.S. Wold. 1990a. A 14,500 MW protein is coded by region E3 of group C human adenoviruses. Virology **175**:19-29.

Tollefson, A.E., P. Krajcsi, S.P. Yei, C.R. Carlin, and W.S. Wold. 1990b. A 10,400-molecular-weight membrane protein is coded by region E3 of adenovirus. J. Virol. **64**:794-801.

Tollefson, A.E., J.S. Ryerse, A. Scaria, T.W. Hermiston, and W.S. Wold. 1996a. The E3-11.6-KDa adenovirus death protein (ADP) is required for efficient cell death: characterization of cells infected with adp mutants. Virology **220**:152-162.

Tollefson, A.E., A. Scaria, T.W. Hermiston, J.S. Ryerse, L.J. Wold, and W.S. Wold. 1996b. The adenovirus death protein (E3-11.6K) is required at very late stages of infection for efficient cell lysis and release of adenovirus from infected cells. J. Virol. **70**:2296-306.

Tollefson, A.E., A. Scaria, S.K. Saha, and W.S.M. Wold. 1992. The 11,600-Mw protein encoded by region E3 of adenovirus is expressed early but is greatly amplified at late stages of infection. J. Virol. **66**:3633-3642.

Tollefson, A.E., A. Scaria, B. Ying, and W.S. Wold. 2003. Mutations within the ADP (E3-11.6K) protein alter processing and localization of ADP and the kinetics of cell lysis of adenovirus-infected cells. J. Virol. **77**:7764-78.

Tollefson, A.E., K. Toth, K. Doronin, M. Kuppuswamy, O.A. Doronina, D.L. Lichtenstein, T.W. Hermiston, C.A. Smith, and W.S.M. Wold. 2001. Inhibition of TRAIL-induced apoptosis and forced internalization of TRAIL receptor 1 by adenovirus proteins. J. Virol. **75**:8875–8887.

Tollefson, A.E., and W.S. Wold. 1988. Identification and gene mapping of a 14,700-molecular-weight protein encoded by region E3 of group C adenoviruses. J. Virol **62**:33-9.

Top, F.H. Jr. 1975. Control of adenovirus acute respiratory disease in U.S. Army trainees. Yale J. Biol. Med. **48**:185-95.

Top, D., R. de Antueno, J. Salsman, J. Corcoran, J. Mader, D. Hoskin, A. Touhami, M.H. Jericho, and R. Duncan. 2005. Liposome reconstitution of a minimal protein-mediated membrane fusion machine. EMBO J. **24**:2980-8.

Toth, M., W. Doerfler, and T. Shenk. 1992. Adenovirus DNA replication facilitates binding of the MLTF/USF transcription factor to the viral major late promoter within infected cells. Nucleic Acids Res. **20**:5143-8.

Tribouley, C., P. Lutz, A. Staub, and C. Kedinger. 1994. The product of the adenovirus intermediate gene IVa2 is a transcriptional activator of the major late promoter. J. Virol. **68**:4450-7.

Tuboly, T. and E. Nagy. 2000. Sequence analysis and deletion of porcine adenovirus serotype 5 E3 region. Virus Res. **68**:109-17.

Varki, A. and J.B. Lowe. 2009. Biological Roles of Glycans. *In* A. Varki, R.D. Cummings, J.D. Esko, H.H. Freeze, P. Stanley, C.R. Bertozzi, G.W. Hart, and M.E. Etzler (ed.), Essentials of Glycobiology, 2nd ed. CSH Press, La Jolla, CA

Videla, C., G. Carballal, and A. Kajon. 1999. Genomic analysis of adenovirus isolated from Argentinian children with acute lower respiratory infections. J. Clin. Virol. **14**:67-71.

Von Heijne, G. 1992. Membrane protein structure prediction: hydrophobicity analysis and the 'positive inside' rule. J. Mol. Biol. **225**:487-94.

Vrati, S., D. Boyle, R. Kocherhans, and G.W. Both. 1995. Sequence of ovine adenovirus homologs for 100K hexon assembly, 33K, pVIII, and fiber genes: early region E3 is not in the expected location. Virology **209**:400-8.

Wadell, G. 1984. Molecular epidemiology of human adenoviruses. Curr. Top. Microbiol. Immunol. **110**:191-120.

Wadell, G., M.K. Cooney, A. da Costa Linhares, L. de Silva, M.L. Kennett, R. Kono, R. Gui-Fang, K. Lindman, J.P. Nascimento, B.D. Schoub, and C.D. Smith. 1985. Molecular epidemiology of adenoviruses: global distribution of adenovirus 7 genome types. J. Clin. Microbiol. **21**:403-8.

Wadell, G., T.M. Varsányi, A. Lord, and R.N.P. Sutton. 1980. Epidemic outbreaks of adenovirus 7 with special reference to the pathogenicity of adenovirus genome type 7b. Am. J. Epidemiol. **112**:619-28.

Walsh, M.P., A. Chintakuntlawar, C.M. Robinson, I. Madisch, B. Harrach, N.R. Hudson, D. Schnurr, A. Heim, J. Chodosh, D. Seto, and M.S. Jones. 2009. Evidence of molecular evolution driven by recombination events influencing tropism in a novel human adenovirus that causes epidemic keratoconjunctivitis. PLoS One **4**:e5635.

Walsh, M.P., J. Seto, M.S. Jones, J. Chodosh, W. Xu, and D. Seto. 2010. Computational analysis identifies human adenovirus type 55 as a re-emergent acute respiratory disease pathogen. J. Clin. Microbiol. **48**:991-3.

Wang, E.W., M.O. Scott, and R.P. Ricciardi. 1988. An adenovirus mRNA which encodes a 14,700-Mr protein that maps to the last open reading frame of region E3 is expressed during infection. J. Virol. **62**:1456-9.

Warming, S., N. Constantino, D.L. Court, N.A. Jenkins, and N.G. Copeland. 2005. Simple and highly efficient BAC recombineerng using *galK* selection. Nucleic Acids Res. **33**: e36.

Weinmann, R., T.G. Brendler, H.J. Raskas, and R.G. Roeder. 1976. Low molecular weight viral RNAs transcribed by RNA polymerase III during adenovirus 2 infection. Cell **7**:557-66.

Wigand, R. and T. Adrian. 1989. Intermediate adenovirus strains of subgenus D occur in extensive variety. Med. Microbiol. Immunol. **178**:37-44.

Williamson, P., K. Mattocks, and R.A. Schlegel. 1983. Merocyanine 540, a fluorescent probe sensitive to lipid packing. Biochim. Biophys. Acta. **732**:387-93.

Windheim, M., and H.G. Burgert. 2002. Characterization of E3/49K, a novel, highly glycosylated E3 protein of the epidemic keratoconjunctivitis-causing adenovirus type 19a. J. Virol. **76**:755-66.

Wilson-Ashworth, H.A., Q. Bahm, J. Erickson, A. Shinkle, M.P. Vu, D. Woodbury, and J.D. Bell. 2006. Differential detection of phospholipid fluidity, order, and spacing by

fluorescence spectroscopy of bis-pyrene, prodan, nystatin, and merocyanine 540. Biophys. J. **91**:4091-101.

Wold, W.S., A.E. Tollefson, and T.W. Hermiston. 1995. E3 transcription unit of adenovirus. Curr. Top. Microbiol. Immunol. **199**:237-74.

Xia, D., L.J. Henry, R.D. Gerard, and J. Deisenhofer. 1994. Crystal structure of the receptor-binding domain of adenovirus type 5 fiber protein at 1.7Å resolution. Structure **2**:1259-1270.

Ying, B. and W.S. Wold. 2003. Adenovirus ADP protein (E3-11.6K), which is required for efficient cell lysis and virus release, interacts with human MAD2B. Virology **313**:224-34.

Zhang, L., M.A. Agosto, T. Ivanovic, D.S. King, M.L. Nibert, and S.C. Harrison. 2009. Requirements for the formation of membrane pores by the reovirus myristoylated µ1N peptide. J. Virol. **83**:7004-7014.